Title

The Synthesis and Reactivity of Organoiridium Complexes Containing Metal-Heteroatom Bonds

Author

Klein, D.P.

Publication Date

1989-11-01

LBL-28353

Lawrence Berkeley Laboratory
UNIVERSITY OF CALIFORNIA

Materials & Chemical Sciences Division

The Synthesis and Reactvity of Organoiridium Complexes Containing Metal-Heteroatom Bonds

D.P. Klein
(Ph.D. Thesis)

November 1989

Prepared for the U.S. Department of Energy under Contract Number DE-AC03-76SF00098.

DISCLAIMER

LBL-28353

The Synthesis and Reactivity of Organoiridium Complexes Containing Metal-Heteroatom Bonds

Darryl Patrick Klein

Ph.D. Thesis

November 1989

Lawrence Berkeley Laboratory

and

Department of Chemistry

University of California

Berkeley, California 94720

This work was supported by the Director, Office of Energy Research, Office of Basic Energy Sciences, Chemical Sciences Division, of the U.S. Department of Energy under contract no. DE-AC03-76SF00098.

The Synthesis and Reactivity of Organoiridium Complexes Containing Metal-Heteroatom Bonds

Darryl Patrick Klein

Abstract

Chapter 1 Irradiation of $Cp^*(PMe_3)IrH_2$(**1**) in *tert*-butylamine and *tert*-butanol gives exclusively the products of C-H, rather than N-H or O-H, insertion $Cp^*(PMe_3)Ir(CH_2CMe_2XH)H$ (**2**, X = NH; **3**, X= O). These oxidative addition products can be converted to the 2-aza- and 2-oxametallacyclobutane complexes **7** and **8** by replacement of iridium-bound hydride by chloride using $CHCl_3$, followed by treatment with the hindered base $KN(TMS)_2$. Both **7** and **8** react with a variety of electrophilic organic compounds (t-BuNC, CO_2, t-BuNCO) to give new metallacycles as products.

Chapter 2. The monomeric methylene complex $Cp^*(PMe_3)Ir(CH_2)$ (**2**) is produced upon photolysis of the 2-oxametallacycle $Cp^*(PMe_3)Ir(CH_2CMe_2O)$ (**1**) in toluene solution at low temperature, and is found to be indefinitely stable in solution below -40 °C. The methylene carbon in **2** is quite basic; the reaction of **2** with a variety of organic acids is described. Complex **2** also reacts with non-protic reagents. Treatment with dihydrogen gives the (methyl)hydride **8**, while carbon dioxide reacts in a [2+2] fashion to give the addition product **11**.

Chapter 3. The synthesis of a variety of iridium and rhodium mono- and bis-thiolate complexes is described. These molecules can be prepared by exchange reactions of organic thiols with $Cp^*(PMe_3)Ir(OEt)H$ (**6**) or by nucleophilic displacement of metal-bound chloride by sodium alkyl thiolates. Several of these complexes have been characterized by X-ray crystallography. A preliminary study on the chemistry of these compounds is presented which shows that reaction can take place at either the sulfur atom or the metal center.

Acknowledgements

There are so many people to thank that it is difficult to know where to begin. First, I would like to thank Dr. Colin Francis, my undergraduate research advisor, and the entire Francis group at USC for introducing me to chemical research. Their patience and friendship is gratefully acknowledged.

I am deeply indebted to my research advisor here at Berkeley, Bob Bergman. His ideas and suggestions have been invaluable. His enthusiasm for my work and the financial support behind it have been more than generous. I would also like to thank him for encouragement to talk about my work at the Toronto ACS meeting. Other professors I need to thank are Peter Vollhardt for encouragement and many letters of reference, and Steve Pedersen and Leonard Bjeldanes for agreeing to read this thesis.

A benefit I have enjoyed while working in the Bergman group has been the interaction with many talented students and postdocs. I would like to first thank Mary Trost, whose sector was next to mine in 210 Lewis. She helped me immensely when I was a first-year, has been a close friend, and even taught me how to win at Hack. Jeff Chang deserves special mention for sharing with me the trials and tribulations of dissecting Oscar and building Jennifer from the ground up. Stuart McCallum was helpful with NMR questions (if you weren't in a hurry) and was full of amusing stories, practical jokes, and general weirdness. The recently departed Tom Foo and I went through classes, GRC's, and prelims together. His friendship during those trying times was great.

Of the current group members, Bob Simpson deserves special thanks. He has been a great colleague and an even better friend. Grant Kloster, a fair second baseman, always kept the computers running. This was no small feat considering the heavy use and abuse we put them through. Grant also worked hard on the thiolate project despite the smell. A collective thank you to all of the members past and present in the Bergman and Pedersen groups for chemistry discussions, softball and basketball games, Roma trips, etc.

Karen Wong has been great to work with. She has taught me everything I know about ChemDraw and Microsoft Word, made sure I got paid, expedited my purchase orders, and generally kept me out of trouble. Besides all this, she has been a wonderful friend. I will miss her greatly.

My family has always been there for me and without them I wouldn't be where I am now. My grandmother, brothers, and in-laws are all fantastic. My wife Robin has been truly wonderful. I don't know how she put up with everything (myself included) during four long years of graduate school. I love her very much. Last of all, I must thank my parents. They sacrificed a lot to put me through college, but there was never one complaint. I can never repay them for all they have done. I love them both and it is to to them that I dedicate this thesis.

Table of Contents

Chapter 1

Synthesis and Reactivity of the 2-Oxa- and 2-Azametallacyclobutane Complexes $Cp^*(PMe_3)Ir(CH_2CMe_2O)$ and $Cp^*(PMe_3)Ir(CH_2CMe_2NH)$: Potential Models for Olefin Oxidation Intermediates

Introduction

Several important transition-metal-based systems are known that are capable of oxidizing alkenes to epoxides and aldehydes.[1] One of the most important is cytochrome P-450,[2] and model systems involving porphyrins and other chelating ligands have been used to probe the mechanism of these biological oxidations.[3] Several mechanisms have been postulated for such transformations,[4] but one of the most intriguing and often invoked[5] involves 2-oxametallacyclobutane complexes as crucial intermediates (Scheme I).

The 2-oxa- and related 2-azametallacyclobutanes have also been invoked as intermediates in a number of other chemical transformations. For example, Schrock has reported an organometallic analogue of the Wittig reaction, in which a tantalum alkylidene complex reacts with organic carbonyl compounds to give a tantalum oxide polymer and an alkene (Scheme II).[6] Miyashita and coworkers have shown that thermal decomposition of $(PPh_3)_2Ni(OC(CH_3)_3)(CH_3)$ produces methane and 2,2-dimethyloxirane, and they proposed a 2-oxametallacyclobutane complex as an intermediate (Scheme III).[7] Alper and coworkers have described the catalytic formation of β-lactams by the reaction of aziridines with carbon monoxide in the presence of $[Rh(CO)_2Cl]_2$.[8] They believe the first step in this reaction is formation of a 2-azametallacyclobutane complex (Scheme IV). However, despite the potential relevance of these types of structures to the mechanism of these and other reactions, very few such metallacycles have been prepared and characterized.[9]

In our laboratories, it has been shown that the dihydride complex $Cp^*(PMe_3)IrH_2$ (1) loses H_2 upon photolysis to generate an intermediate that oxidatively adds C-H bonds of the solvent.[10] Thus, stable alkyl hydride complexes of the formula $Cp^*(PMe_3)Ir(R)H$ are formed (Scheme V). Initial studies employed hydrocarbons such as benzene or cyclohexane as solvent. Presented in this chapter are the results of photochemical studies on the dihydride **1** with *tert*-butanol and *tert*-butylamine as solvent, as well as the conversion of the products of these reactions into 2-oxa- and 2-azametallacyclobutane complexes. Also presented is the reactivity of these metallacycles with a variety of electrophilic organic compounds.

Scheme I. Possible mechanism for epoxidation of olefins by cytochrome P-450 and model systems.

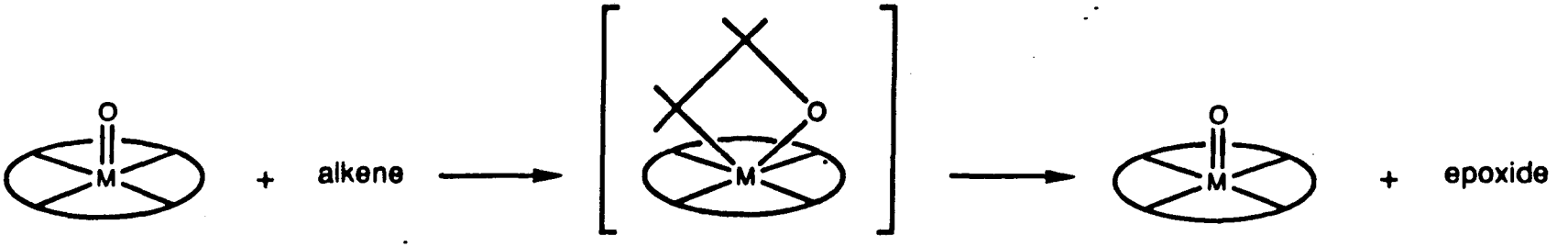

Scheme II

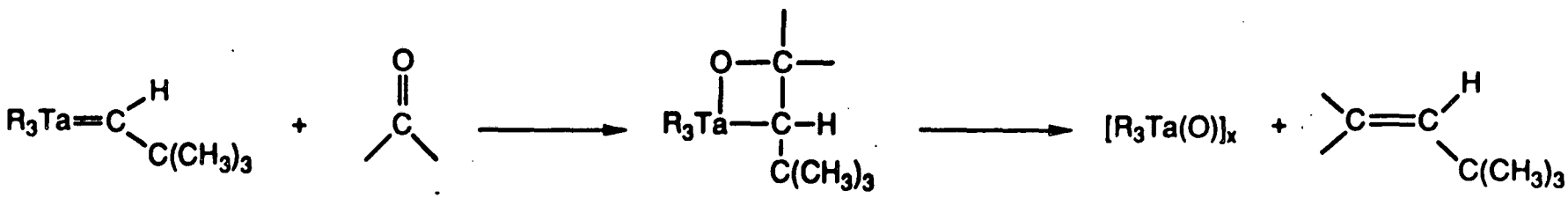

R = $(CH_3)_3CCH_2$

Scheme III

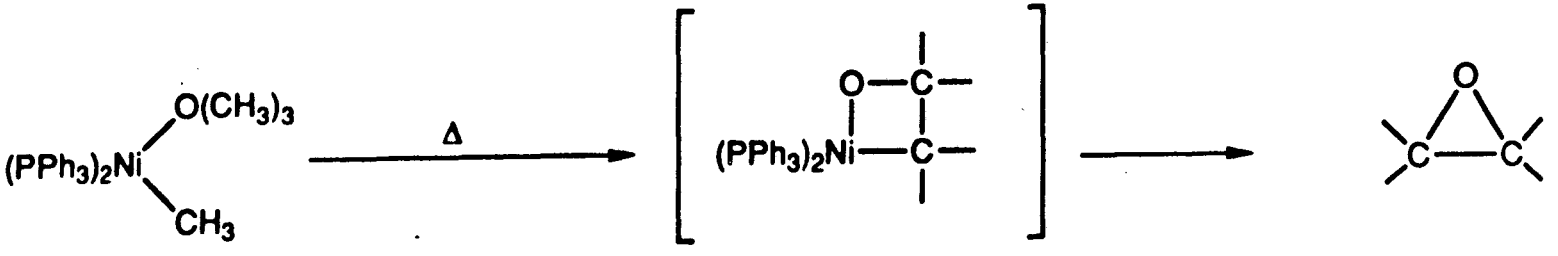

Scheme IV

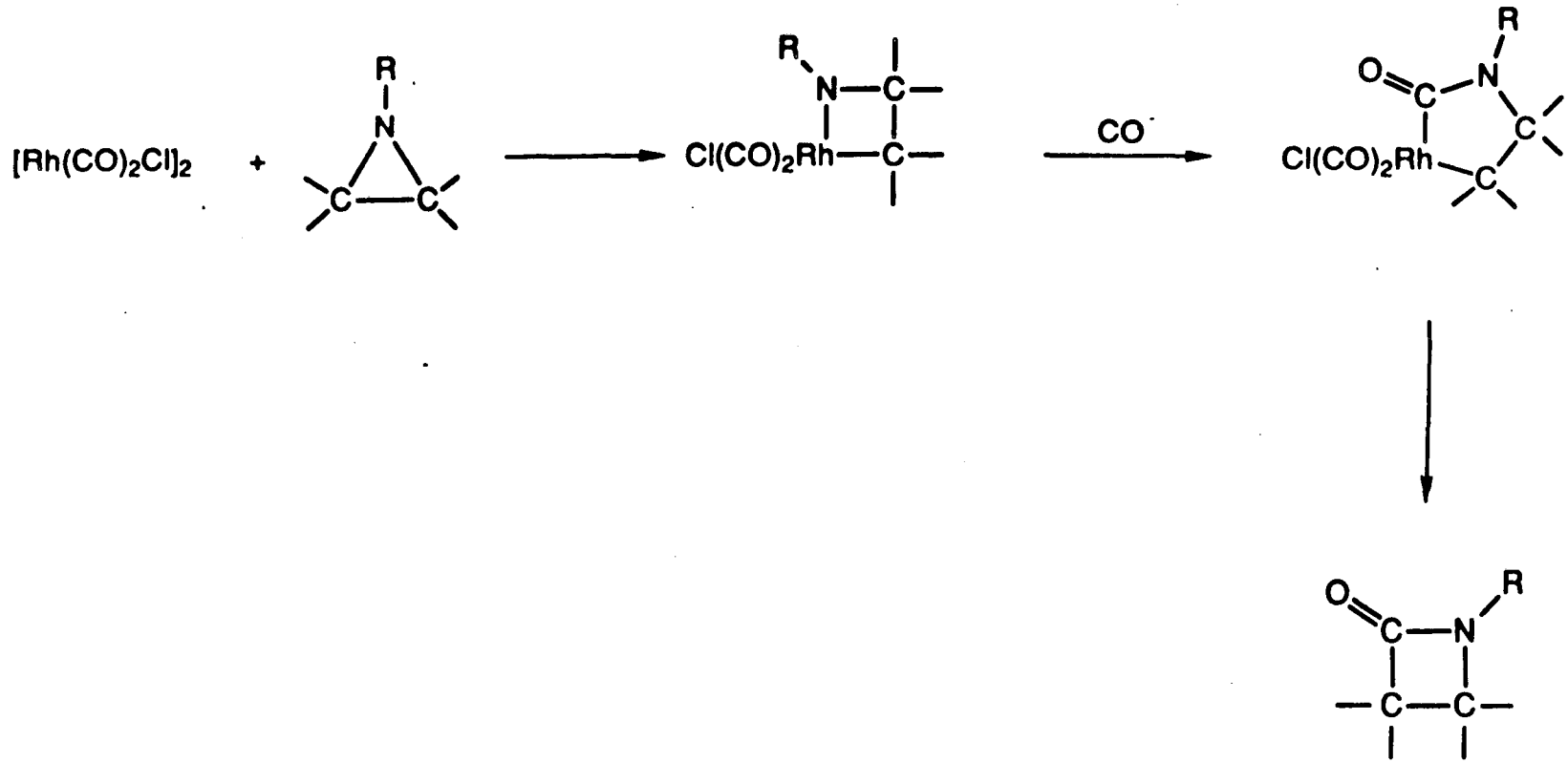

Scheme V

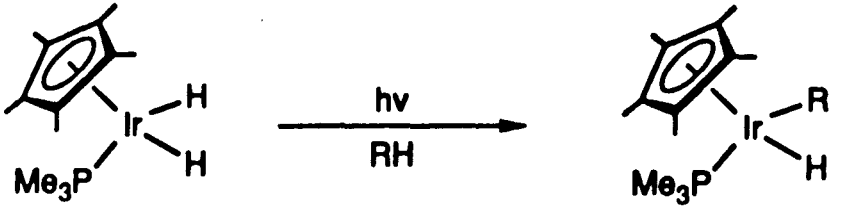

1

Results

Photolysis of $Cp^*(PMe_3)IrH_2$ (1) in *tert*-butylamine and *tert*-butanol. Irradiation of a sample of the dihydride **1** in neat *tert*-butylamine (t-$BuNH_2$) for six hours at 5 °C gave a single new organometallic product as determined by ^1H NMR spectroscopy. This material is identified as the C-H activation product of t-$BuNH_2$, $Cp^*(PMe_3)Ir(CH_2CMe_2NH_2)H$ (**2**) (Scheme VI). The resonance for the NH_2 group in the ^1H NMR spectrum is obscured, but a characteristic high field doublet (δ -17.81, J = 35.4 Hz) is seen for the iridium-hydride ligand. No trace of the amido hydride $Cp^*(PMe_3)Ir(NH\text{-}tBu)H$, the product of N-H activation of t-$BuNH_2$, could be detected.

Because of similar solubility properties, we were unable to separate **2** from residual dihydride remaining in the reaction mixture. Fortunately, the consistently high conversion of the dihydride to the alkyl hydride **2** (typically 90%) allowed this crude material to be used in subsequent reactions.

Similar results were obtained upon photolysis of the dihydride **1** in *tert*-butanol (t-BuOH). Irradiation of **1** in neat t-BuOH[11] at 25 °C for six hours also led to a single new organometallic product as determined ^1H NMR spectroscopy. This material is identified as the C-H activation product of t-BuOH, $Cp^*(PMe_3)Ir(CH_2CMe_2OH)H$ (**3**) (Scheme VII). The ^1H NMR spectrum of **3** exhibits a singlet (δ 2.79) for the OH proton and a characteristic high field doublet (δ -17.76, J = 34.8 Hz) for the iridium-hydride ligand. No trace of the alkoxy hydride $Cp^*(PMe_3)Ir(O\text{-}tBu)H$, the O-H activation product of t-BuOH, could be detected.

Up to 95% conversion of the dihydride **1** to the alkyl hydrides **2** and **3** can be achieved if dilute (5-10 mM) solutions of **1** are irradiated in appropriate photoreactors. Descriptions of the two photoreactors used in these studies are given in the experimental section of this chapter. Photolysis of solutions of **1** in sealed NMR tubes required much longer reaction times (24-36 hours) to approach 90% conversion.[12]

Reaction of $Cp^*(PMe_3)Ir(CH_2CMe_2NH_2)H$ (2) and $Cp^*(PMe_3)Ir(CH_2CMe_2OH)H$ (3) with Chloroform. Treatment of a benzene solution of the alkyl hydride **2** with one equivalent of chloroform led to a slow reaction (Scheme VIII). The pale yellow product, isolated in

Scheme VI

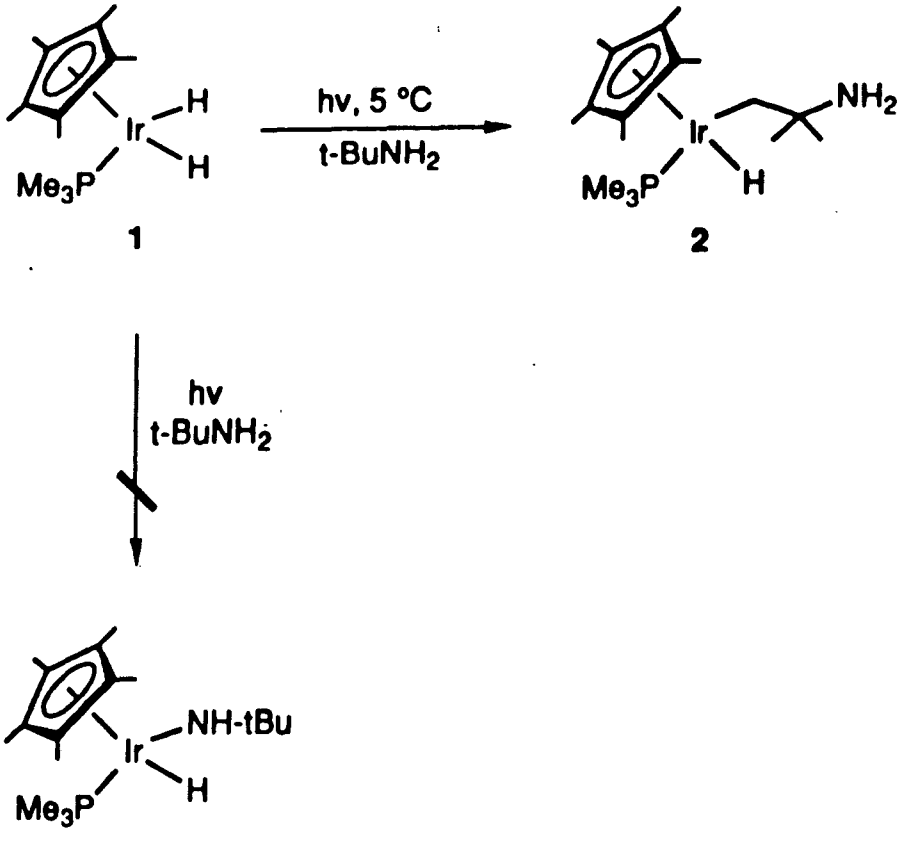

Scheme VII

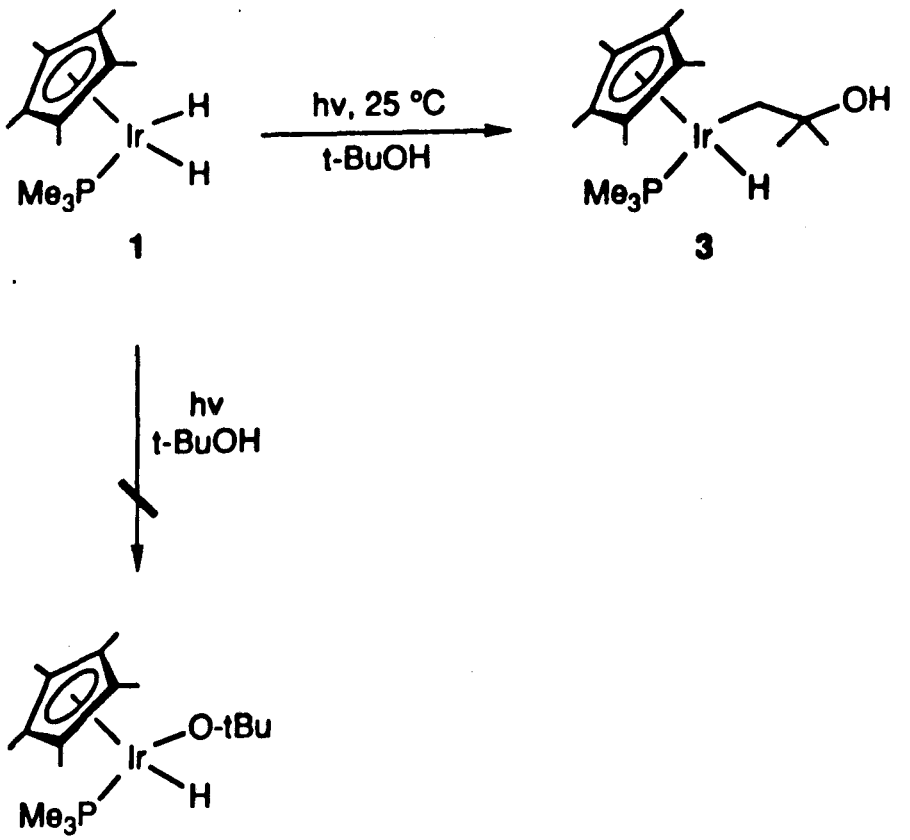

1 3

Scheme VIII

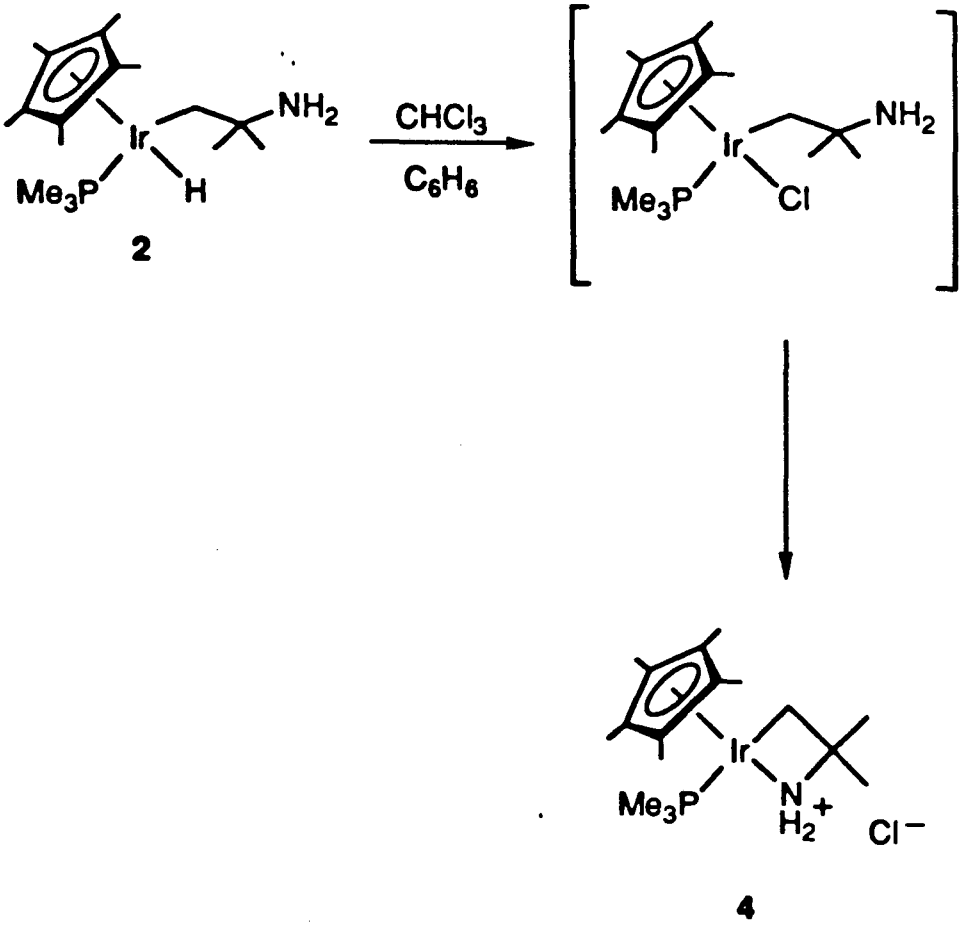

2

4

64% yield, is only sparingly soluble in benzene or toluene and is completely insoluble in pentane. The amine protons are observed as a multiplet at unusually low field (δ 6.04) in the ^1H NMR spectrum. A fast atom bombardment (FAB) mass spectrum gives a peak corresponding to the cation $[Cp^*(PMe_3)Ir(CH_2CMe_2NH_2)]^+$. On this basis, we assign the structure of this material as the cyclic ammonium salt $[Cp^*(PMe_3)Ir(CH_2CMe_2NH_2)]^+(Cl^-)$ (**4**). Presumably, the open-chained alkyl chloride is formed first, but this material rapidly cyclizes to give the observed product **4**.

Crystals of **4** suitable for an X-ray diffraction study were grown from a toluene/hexamethyldisiloxane solution. Complex **4** is extremely hygroscopic, and the crystals used for the X-ray determination, grown outside of the drybox, incorporate two molecules of water per iridium center. The diffraction study was performed by Dr. F. J. Hollander of the U.C. Berkeley College of Chemistry X-ray Diffraction Facility, and this confirmed the proposed structure. Details are given in the experimental section. An ORTEP diagram of the iridium cation is shown in Figure I. Two additional ORTEP diagrams illustrating the packing of the water molecules, chloride anions, and iridium cations are shown in Figures II and III, while selected bond distances and angles are given in Table I. The four-membered ring is essentially planar, having a dihedral angle of 16.1(6) °. The iridium-carbon (2.113(3) Å) and iridium-nitrogen bond lengths (2.119(2) Å) are nearly identical.

The chloride anion in **4** can be efficiently exchanged for hexafluorophosphate anion (PF_6^-) by reaction of **4** with potassium hexafluorophosphate (KPF_6^-) in isopropanol (Scheme IX). This new material, $[Cp^*(PMe_3)Ir(CH_2CMe_2NH_2)]^+(PF_6^-)$ (**5**), was isolated in 76% yield. The ^1H and $^{13}C\{^1H\}$ NMR spectra of **5** are very similar to those recorded for **4**. The $^{31}P\{^1H\}$ NMR spectrum of **5** exhibits a singlet for the PMe_3 ligand (δ -34.5 ppm) and a septet for the PF_6^- anion (δ -142.5, J_{P-F} = 711.5 Hz).

Treatment of a benzene solution of the alkyl hydride **3** with one equivalent of chloroform led to the slow conversion of this material to the uncyclized alkyl chloride complex $Cp^*(PMe_3)Ir(CH_2CMe_2OH)Cl$ (**6**) in 85% isolated yield (Scheme X). This air-stable material was fully characterized by standard analytical and spectroscopic techniques. The ^1H NMR spectrum of

Figure I. ORTEP diagram and labelling scheme for complex **4** showing the iridium cation only.

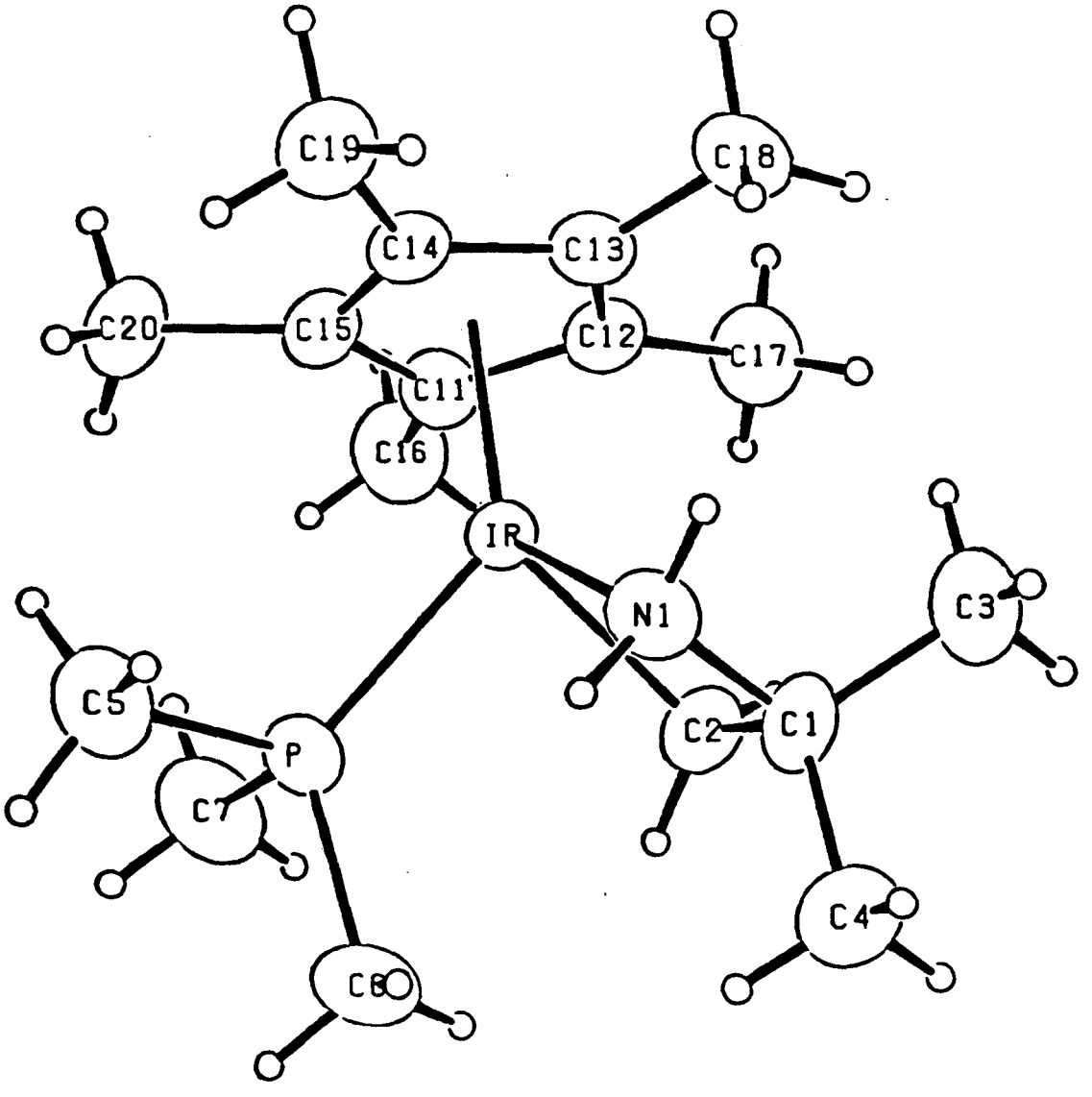

Figure II. ORTEP diagram for complex **4** showing one iridium cation and the packing of chloride anions and water molecules.

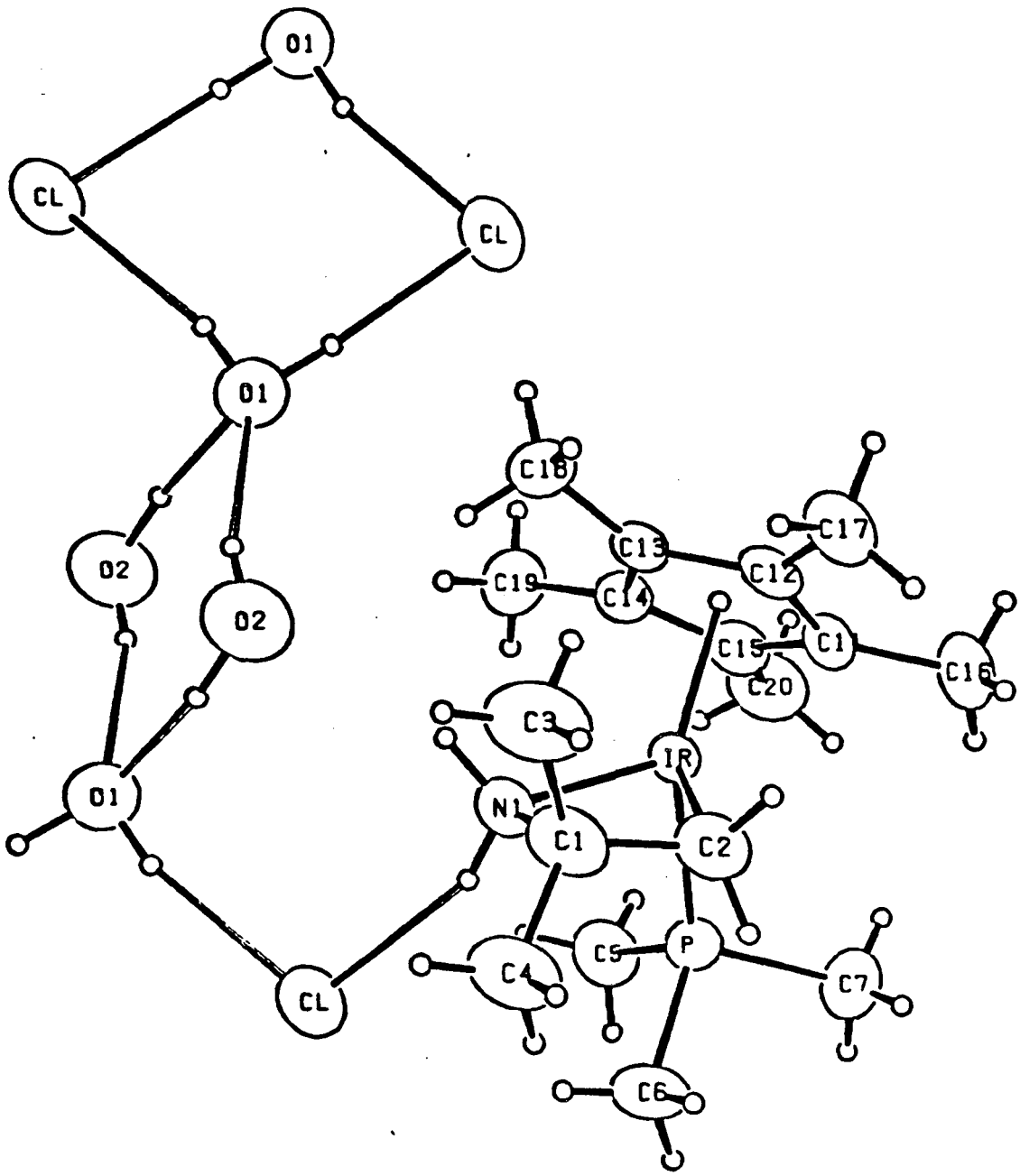

Figure III. ORTEP diagram for complex **4** showing the hydrogen bonding network.

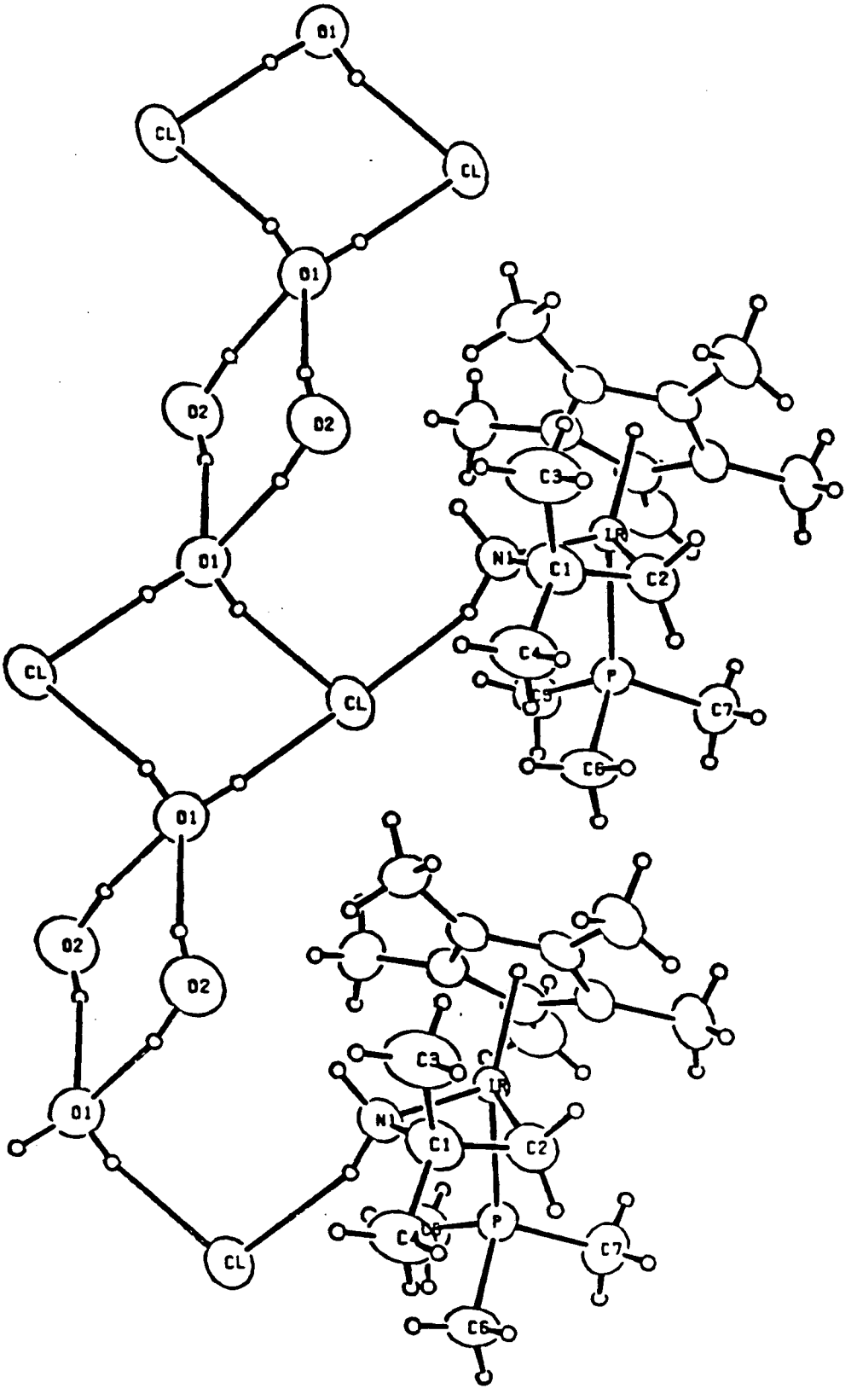

Table I. Selected bond distances and angles for complex **4**.

Intramolecular Distances

ATOM 1	ATOM 2	DISTANCE
IR	P	2.268(1)
IR	N1	2.119(2)
IR	C2	2.113(3)
IR	C11	2.177(3)
IR	C12	2.228(3)
IR	C13	2.246(3)
IR	C14	2.239(3)
IR	C15	2.247(3)
IR	CP1	1.867
C1	N1	1.508(4)
C1	C2	1.525(5)
C1	C3	1.541(5)
C1	C4	1.532(5)
P	C5	1.801(3)
P	C6	1.828(3)
P	C7	1.814(3)
C11	C12	1.437(4)
C12	C13	1.426(4)
C13	C14	1.427(4)
C14	C15	1.415(4)
C15	C11	1.433(4)
C16	C11	1.506(4)
C17	C12	1.483(4)
C18	C13	1.488(4)
C19	C14	1.511(4)
C20	C15	1.515(4)

Hydrogen Bond Distances

ATOM 1	ATOM 2	DISTANCE
N1	H1A	0.95
H1A	CL	2.35
N1	CL	3.251(3)
O1	H(O1)A	0.90
H(O1)A	CL	2.26
O1	CL	3.143(3)
O1	H(O1)B	1.02
H(O1)B	CL	2.28
O1	CL	3.283(3)
O2	H(O2)A	1.06
H(O2)A	O1	1.92
O2	O1	2.942(4)
O2	H(O2)B	0.86
H(O2)B	O1	2.21
O2	O1	3.018(4)
O2	N1	3.317(4)

Intramolecular Angles

ATOM 1	ATOM 2	ATOM 3	ANGLE
CP1	IR	P	128.57
CP1	IR	N1	128.33
CP1	IR	C2	130.23
P	IR	N1	93.08(7)
P	IR	C2	90.42(9)
N1	IR	C2	66.85(11)
IR	N1	C1	95.3(2)
N1	C1	C2	100.5(2)
C1	C2	IR	95.0(2)
N1	C1	C3	108.1(3)
N1	C1	C4	110.9(3)
C2	C1	C3	111.6(3)
C2	C1	C4	115.6(3)
C3	C1	C4	109.7(3)
IR	P	C5	114.68(11)
IR	P	C6	120.34(11)
IR	P	C7	113.95(12)
C5	P	C6	99.9(2)
C5	P	C7	105.1(2)
C6	P	C7	100.6(2)
C12	C11	C15	107.3(2)
C12	C11	C16	125.3(3)
C15	C11	C16	125.8(3)
C11	C12	C13	107.6(2)
C11	C12	C17	125.0(3)
C13	C12	C17	127.3(3)
C12	C13	C14	108.5(2)
C12	C13	C18	126.6(3)
C14	C13	C18	124.8(3)
C13	C14	C15	107.8(2)
C13	C14	C19	125.4(3)
C15	C14	C19	126.4(3)
C11	C15	C14	108.6(2)
C11	C15	C20	124.3(3)
C14	C15	C20	126.7(3)

Scheme XVIII

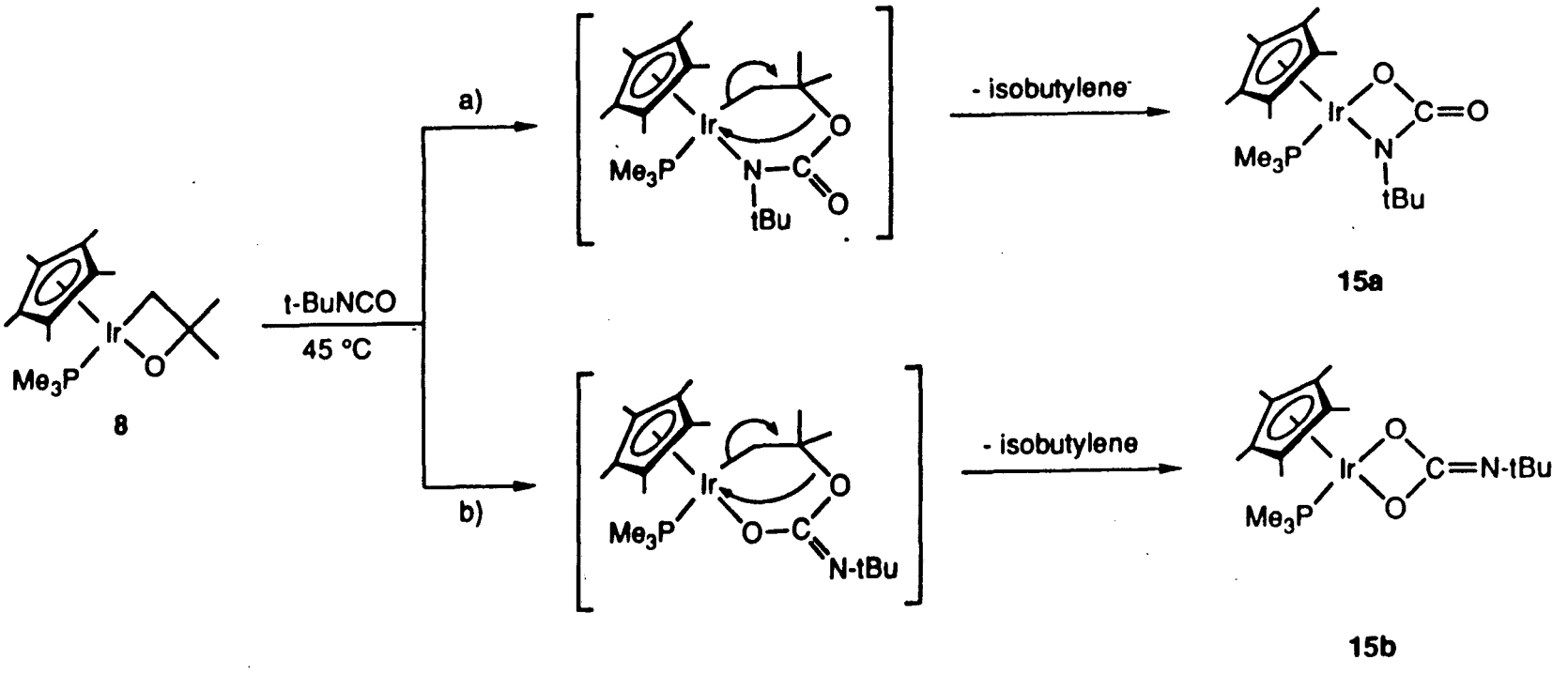

Scheme IX

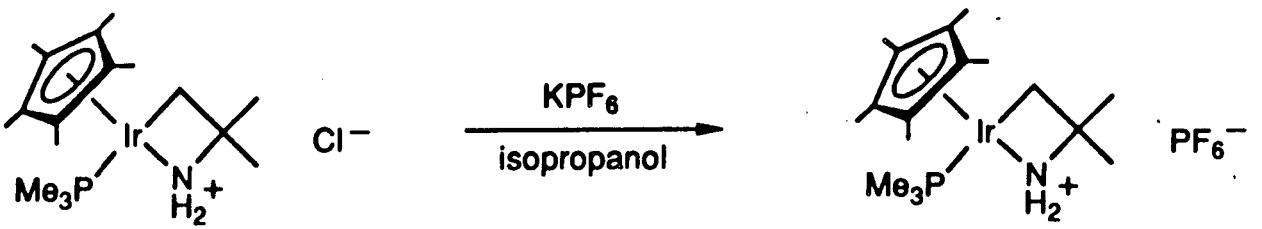

4 **5**

Scheme X

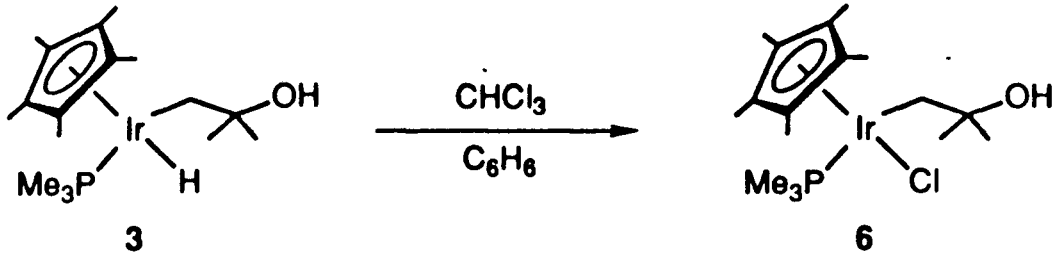

3 6

6 exhibits a singlet (δ 4.12) for the OH proton, while the infrared (IR) spectrum shows an O-H stretch at 3421 cm^{-1}. Evidence that this material remains uncyclized is found in the $^{13}C\{^1H\}$ NMR spectrum. The methylene carbon is observed at δ +12.8 ppm (J_{P-C} = 10.0 Hz), typical for an uncyclized alkyl group in this series. The methylene carbon attached to iridium in a metallacyclobutane complex would resonate at higher field (δ -10 to -45 ppm) (*vide infra*).

Deprotonation of $[Cp^*(PMe_3)Ir(CH_2CMe_2NH_2)]^+(Cl^-)$ (4) and $Cp^*(PMe_3)Ir(CH_2CMe_2OH)Cl$ (6). The ammonium salt $[Cp^*(PMe_3)Ir(CH_2CMe_2NH_2)]^+(Cl^-)$ (**4**) is the conjugate acid of the target neutral 2-azametallacyclobutane complex $Cp^*(PMe_3)Ir(CH_2CMe_2NH)$. Attempted deprotonation of this material with several bases (lithium *tert*-butoxide, lithium di-*iso*-propylamide) gave only intractable materials, but ultimately it was discovered that the strong, hindered base potassium hexamethyldisilazide [$KN(SiMe_3)_2$] reacted with **4** at -40 °C in toluene to give a single new complex as determined by ^1H NMR spectroscopy (Scheme XI). This material, isolated in 95% yield, was too sensitive for elemental analysis. It was, however, characterized by NMR and IR spectroscopy, as well as high resolution mass spectrometry. A broad singlet (δ -0.35 ppm) integrating to one proton is observed in the ^1H NMR spectrum and an N-H stretch is seen at 3415 cm^{-1} in the IR spectrum. The methylene carbon appears as a doublet at relatively high field (δ -21.7 ppm, J_{P-C} = 6.6 Hz) in the $^{13}C\{^1H\}$ NMR spectrum. This leads us to identify the product of this reaction as the neutral 2-azametallacyclobutane complex $Cp^*(PMe_3)Ir(CH_2CMe_2NH)$ (**7**).

Likewise, treatment of the uncyclized alkyl chloride $Cp^*(PMe_3)Ir(CH_2CMe_2OH)Cl$ (**6**) with $KN(SiMe_3)_2$ in benzene at room temperature also led to the formation of a single new complex as determined by ^1H NMR spectroscopy (Scheme XII). Based on analytical and spectroscopic data, we assign the structure of this material as the analogous oxygen-containing metallacycle $Cp^*(PMe_3)Ir(CH_2CMe_2O)$ (**8**). Complex **8** was isolated in 95% yield as yellow crystals, and like its nitrogen-containing analogue, is extremely air-sensitive both in solution and in the solid state. Again, the methylene carbon for this four-membered metallacycle is seen at characteristically high field (δ -16.8 ppm, J_{P-C} = 6.1 Hz) in the $^{13}C\{^1H\}$ NMR spectrum.

Scheme XI

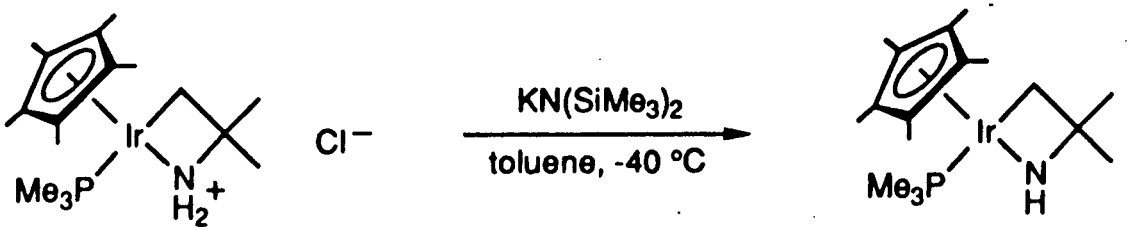

4 **7**

Scheme XII

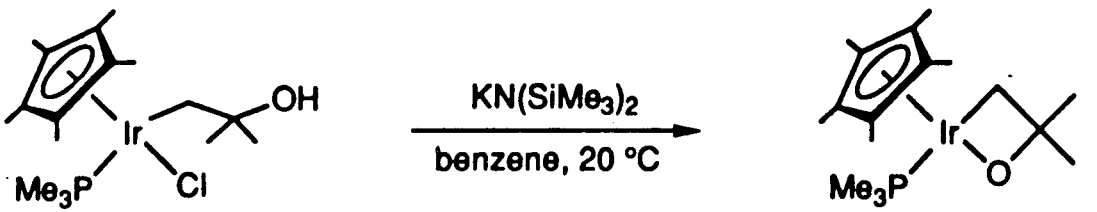

6 **8**

Chemistry of the 2-aza- and 2-oxametallacyclobutane Complexes. Treatment of the 2-azametallacyclobutane complex **7** with with *tert*-butylisocyanide (t-BuNC) resulted in rapid insertion of the isonitrile into the iridium-nitrogen bond of **7** to give the new metallacycle $Cp^*(PMe_3)Ir[CH_2CMe_2N(H)C(N\text{-}tBu)]$ (**9**) in 91% isolated yield (Scheme XIII). Evidence that insertion has taken place into the iridium-nitrogen bond rather than the iridium-carbon bond is provided by the $^{13}C\{^1H\}$ NMR spectrum. The methylene carbon (δ 25.2 ppm) retains a phosphorus-carbon coupling of 7.3 Hz, typical for a P-Ir-C linkage in this system. The imine carbon resonance appears as a doublet at δ 155.6 ppm ($J_{P\text{-}C}$ = 14.4 Hz). Also, a characteristic C=N stretching absorption is observed at 1563 cm^{-1} in the IR spectrum.

The reaction of t-BuNC with the 2-oxametallacyclobutane complex **8** was more sluggish, reaching completion only after heating for several days at 45 °C (Scheme XIV). Again, insertion was found to occur into the iridium-heteroatom bond, giving the new metallacycle $Cp^*(PMe_3)Ir[CH_2CMe_2OC(N\text{-}tBu)]$ (**10**) in 60% yield. Analogous to the results presented above, the methylene carbon (δ 15.9 ppm in the $^{13}C\{^1H\}$ NMR spectrum) retains a phosphorus-carbon coupling ($J_{P\text{-}C}$ = 7.1 Hz). The imine carbon resonance appears at δ 160.5 ppm ($J_{P\text{-}C}$ = 20.0 Hz) in the $^{13}C\{^1H\}$ NMR spectrum and the C=N stretch is seen at 1586 cm^{-1} in the IR spectrum.

The 2-azametallacyclobutane complex **7** reacted with carbon dioxide (CO_2) over several days at room temperature to give the metallaurethane $[Cp^*(PMe_3)Ir[CH_2CMe_2N(H)C(O)O]$ (**11**) (Scheme XV).We have been unable to crystallize pure **11**, but lyophilization of the crude product from benzene allowed its isolation as a white powder that was greater than 90% pure (NMR). A C=O stretching absorption at 1626 cm^{-1} is seen in the IR spectrum, while the carbonyl carbon resonance appears at δ 162.6 ppm in the $^{13}C\{^1H\}$ NMR spectrum. This resonance does not show coupling to phosphorus, suggesting that the regioisomer shown in Scheme XV is correct. Interestingly, an intermediate was observed when the reaction was monitored by ^1H NMR spectroscopy. This material formed immediately on mixing of **7** with CO_2 and was slowly converted to **11** on standing in solution. Due to the reactivity of this material we have been unable to isolate it. It exhibits a broad resonance at δ 12.71 ppm in the ^1H NMR spectrum and a

Scheme XIII

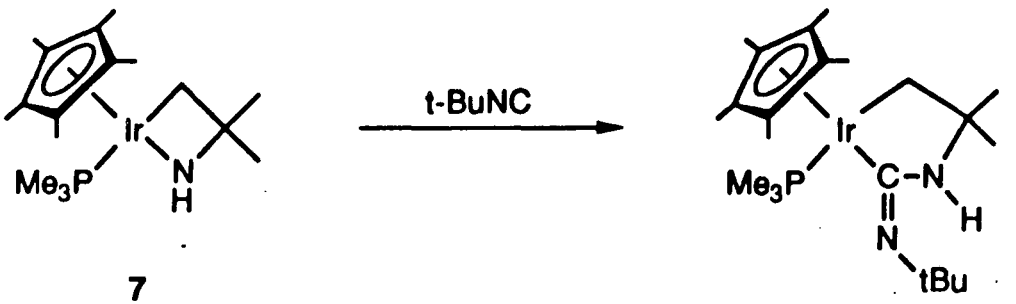

7 9

Scheme XVI

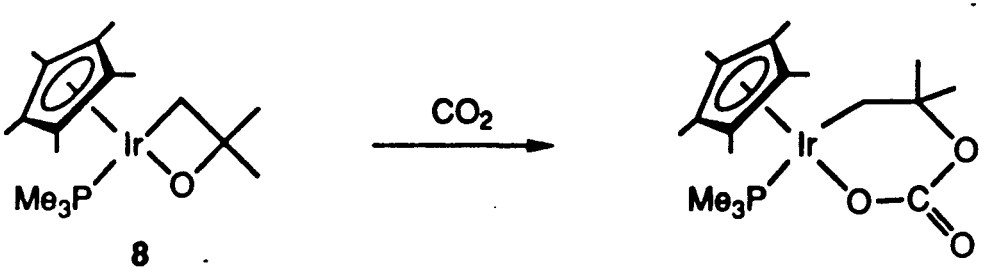

8 **13**

Scheme XV

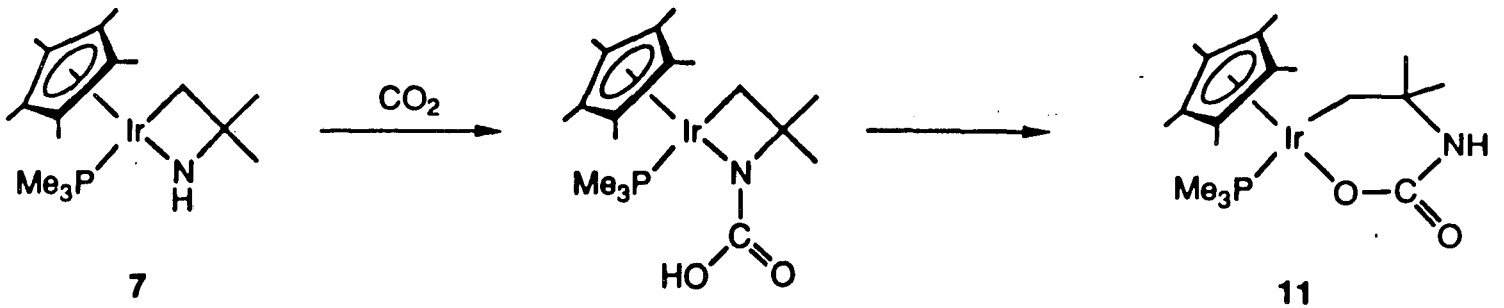

7

12

11

carbonyl stretch at 1605 cm^{-1} in the IR spectrum. We suggest that this initially formed product is the carbamic acid derivative $[Cp^*(PMe_3)Ir[CH_2CMe_2NC(O)OH)]$ (**12**), which slowly rearranges to the metallaurethane **11**.

The oxygen-substituted metallacycle **8** also reacted with CO_2, once again giving insertion of the unsaturated molecule into the iridium-heteroatom bond (Scheme XVI). The resulting metallacarbonate $[Cp^*(PMe_3)Ir[CH_2CMe_2OC(O)O]$ (**13**) was isolated in 80% yield as a yellow powder. A carbonyl stretch at 1644 cm^{-1} is seen in the IR spectrum, while the carbonyl carbon is observed as a singlet at 157.0 ppm in the $^{13}C\{^1H\}$ NMR spectrum. No intermediate analogous to that observed on reaction of **7** with CO_2 was detected.

Both metallacycles **7** and **8** were treated with the heterocumulene *tert*-butylisocyanate (t-BuNCO) to see if the reactivity of this small molecule would mimic that of the isoelectronic CO_2. Treatment of the 2-azametallacyclobutane complex **7** with t-BuNCO led to the immediate formation of a new, yellow air-stable material in nearly quantitative yield (Scheme XVII). Spectral and analytical data are consistent with its assignment as the substituted urea $Cp^*(PMe_3)Ir[CH_2CMe_2NC(O)NH(tBu)]$ (**14**). Evidence that metallacycle **7** acts as an organic amine toward isocyanate rather than giving the product of insertion of isocyanate into the iridium-nitrogen bond is found in the $^{13}C\{^1H\}$ NMR spectrum. The methylene carbon resonance appears at δ -10.3 ppm, typical for a metallacyclobutane complex (*vide infra*). Complex **14** is isostructural with the proposed intermediate **12** formed upon reaction of **7** with CO_2. Once formed, however, complex **14** shows no proclivity to rearrange to the analogous insertion product isolated in the CO_2 reaction.

Treatment of the 2-oxametallacyclobutane complex **8** with t-BuNCO gave more complicated results. No reaction was observed at room temperature, but after heating at 45 °C for several days the initially yellow solution became bright green. Analysis of the crude product by NMR spectroscopy showed several organometallic complexes and free isobutylene. Two of the organometallic products retained coordinated PMe_3 [$^{31}P\{^1H\}$ NMR: δ -18.4 ppm (s) and -20.5 ppm (s)]. Crystallization of this crude material from pentane in the drybox gave yellow crystals of the

Scheme XVI

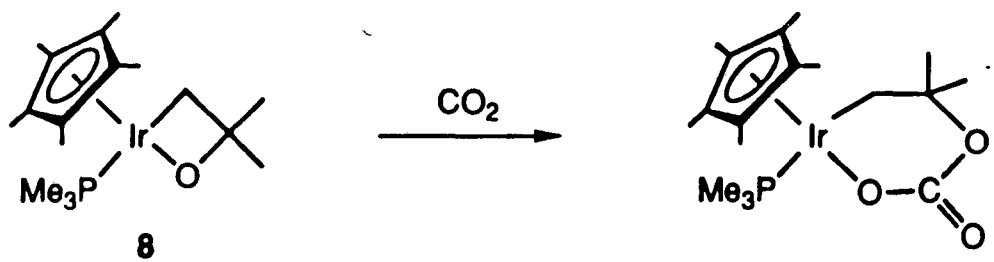

8 **13**

Scheme XVII

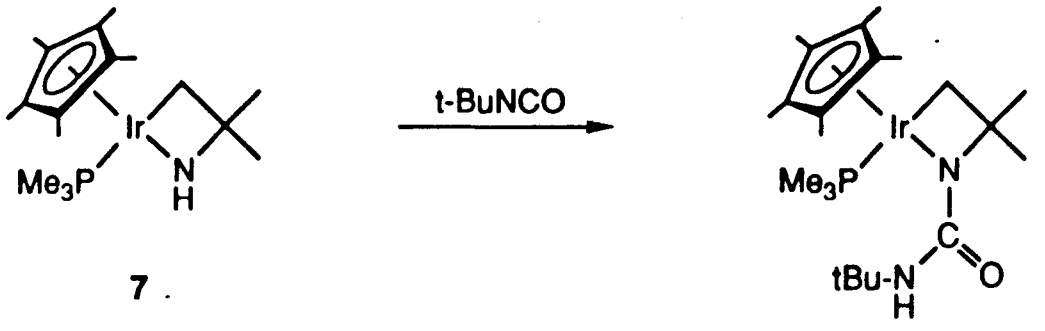

7

14

metallacarbamate **15a** (or its regioisomer **15b**) in 72% yield. A possible mechanism for the formation of **15** is given in Scheme XVIII. Insertion of t-BuNCO into the iridium-oxygen bond of **8** followed by loss of isobutylene would lead to the observed product. It was found that complex **15** is extremely sensitive, reacting with minute traces of water to give the metallacarbonate **16** (Scheme XIX),[13] the other phosphine-containing species in the crude product mixture. The green material formed in this reaction could not be isolated in pure form and its identity remains unknown.

Discussion

The photolysis of the dihydride $Cp^*(PMe_3)IrH_2$ (**1**) in neat t-$BuNH_2$ or t-BuOH gave high yields (80 - 95%) of the alkyl hydride complexes **2** and **3**, respectively. No product corresponding to N-H or O-H activation was detected in these reactions. It is possible that the amido hydride $Cp^*(PMe_3)Ir(NH\text{-}tBu)H$ and the alkoxy hydride $Cp^*(PMe_3)Ir(O\text{-}tBu)H$ are being produced and that their formation is reversible (either thermally or photochemically), giving alkyl hydrides **2** and **3** as the thermodynamic rather than kinetic products of these reactions. Unfortunately, we have been unable to prepare these compounds independently so that we might test their stability to the reaction conditions. It is known, however, that the related alkoxy hydride $Cp^*(PPh_3)Ir(OEt)H$ reductively eliminates ethanol under similar photochemical conditions to give the presumed C-H activating intermediate generated upon irradiation of$Cp^*(PPh_3)IrH_2$.[14]

The 2-aza- and 2-oxametallacyclobutane complexes **7** and **8** described in this chapter represent the first simply-substituted members of this class of compounds to be isolated and characterized. Prior to this work, the only isolable 2-oxametallacyclobutane complexes were those obtained by reaction of tetracyanoethylene oxide with several platinum, rhodium, and iridium precursors.[15] The resulting tetracyano-substituted 2-oxametallacycles are unreactive.

Shortly after the publication of our results,[16] Grubbs and coworkers reported the synthesis of stable 2-oxametallacyclobutane complexes of the form $Cp_2Ti[CH_2C(=CR_2)O]$ (R = H, Ph),[9a] by the addition of a ketene to a titanium methylene complex (Scheme XX, Path a) and by addition of a

Scheme XVIII

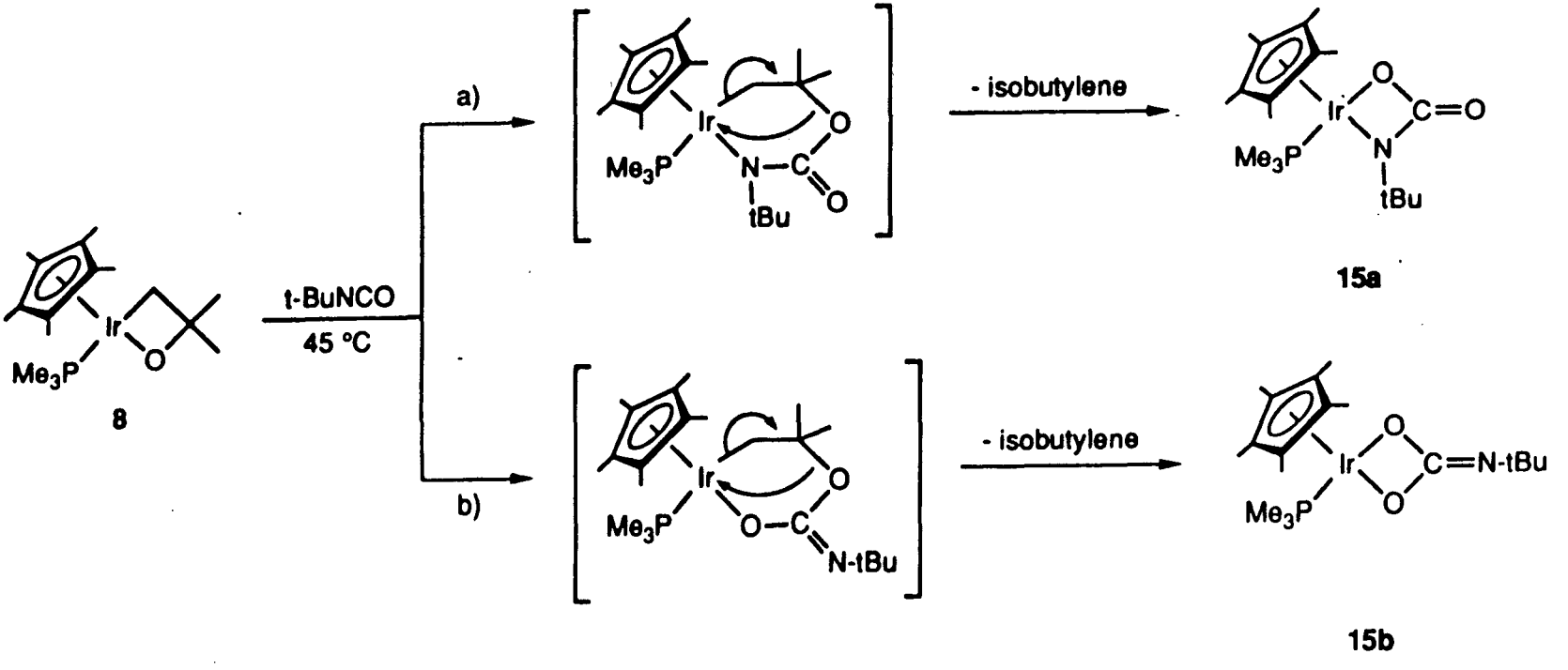

Scheme XIX

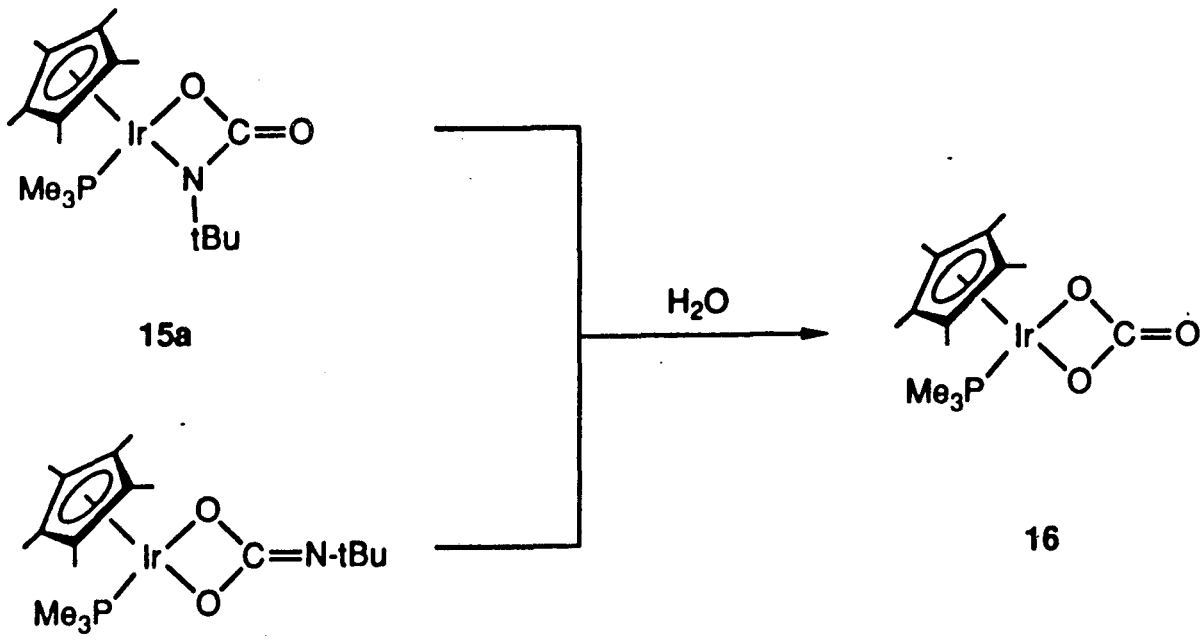

Scheme XX

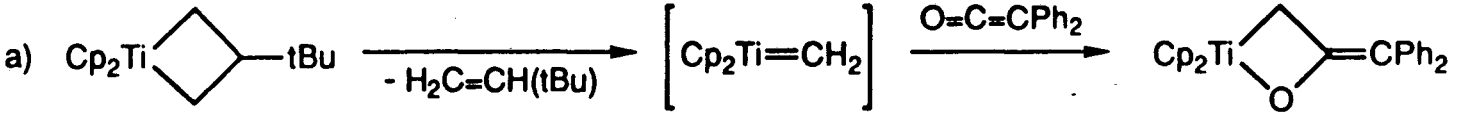
a)
Cp2Ti
tBu
- H2C=CH(tBu)
[Cp2Ti=CH2]
O=C=CPh2
Cp2Ti
O
=CPh2

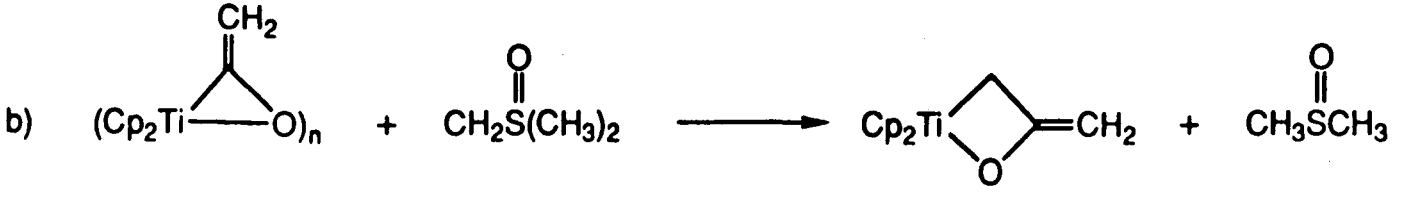
b)
CH2
(Cp2Ti
O)n
+
O
CH2S(CH3)2
Cp2Ti
O
=CH2
+
O
CH3SCH3

methylene fragment to a titanium ketene complex (Scheme XX, Path b). More recently, it has been discovered that reaction of $Cp^*_2Ta(CH_3)(=CH_2)$ with aldehydes also gives stable 2-oxametallacyclobutane complexes.[9b]

To the best of our knowledge, no other stable 2-azametallacyclobutane complexes exist. However, it has been found that a number of metal dichloride complexes react with two equivalents of lithium hexamethyldisilazide to give related silyl-substituted 2-azametallacyclobutanes (Scheme XXI).[17]

All attempts to reductively eliminate aziridine or epoxide from complexes **7** and **8** have been unsuccessful. Thermolysis of these materials in d^6-benzene (80 - 100 °C) led to the complete disappearance of observable organometallic species in the ^1H NMR spectrum and small amounts of t-$BuNH_2$ or t-BuOH. Chemical oxidation with $Cp_2Fe^+BF_4^-$ gave intractable materials. Photolysis of **7** led to many organometallic products, but no 2,2-dimethylaziridine. The photolysis of **8** was remarkably clean, giving the monomeric methylene complex $Cp^*(PMe_3)Ir{=}CH_2$ and acetone as the only products. Details of this reaction are presented in chapter 2.

As was mentioned in the results section, the chemical shift of the methylene carbon was found to be indicative of the structure of the complex in question. The heteroatom-substituted metallacyclobutane complexes described here, as well as the analogous unsubstituted metallacyclobutanes previously synthesized in these laboratories,[18] all exhibit characteristically high-field resonances in the $^{13}C\{^1H\}$ NMR spectrum for the ring carbon(s) attached to iridium (Table II). This observation allows us to assign the structure of complex **14** as the N-substituted metallacyclobutane complex rather than the six-membered metallacycle that would be formed by insertion of isocyanate into the iridium-nitrogen bond.

The insertion processes presented in this chapter are relevant to the mechanism of several reactions described in the literature. As mentioned in the introduction, Alper's work on the catalytic conversion of aziridines to β-lactams[7] is thought to proceed by initial formation of a 2-azametallacyclobutane complex. The next step in this transformation is the formal insertion of carbon monoxide (CO) into either the metal-carbon or metal-nitrogen bond, to give a new

Scheme XXI

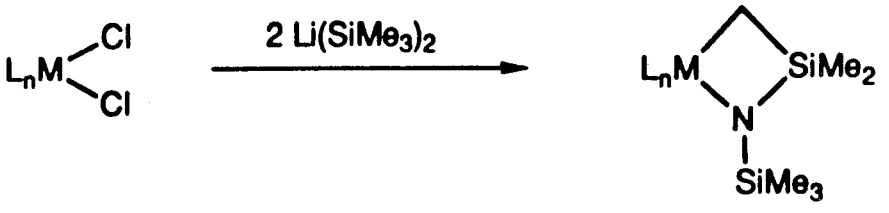

L_nM = Cp_2Ti
Cp_2Zr
$(TMS)_2Zr$
$(TMS)_2Hf$
$(TMS)_2Th$
$(TMS)_2U$

Table II. Characteristic resonances in the $^{13}C\{^1H\}$ NMR spectrum for the carbon attached to iridium in metallacyclobutane complexes.

Complex	$\delta_{(Ir\text{-}\underline{C}H_2)}$ (ppm)	Ref.
$[Cp^*(PMe_3)Ir(CH_2CMe_2NH_2)]^+(Cl^-)$ (**4**)	-10.3	a
$[Cp^*(PMe_3)Ir(CH_2CMe_2NH_2)]^+(PF_6^-)$ (**5**)	-10.8	a
$Cp^*(PMe_3)Ir(CH_2CMe_2NH)$ (**7**)	-21.7	a
$Cp^*(PMe_3)Ir(CH_2CMe_2O)$ (**8**)	-16.8	a
$Cp^*(PMe_3)Ir[CH_2CMe_2NC(O)NH(tBu)]$ (**14**)	-10.3	a
$Cp^*(PMe_3)Ir(CH_2CH_2CH_2)$	-43.9	b
$Cp^*(PMe_3)Ir(CH_2CH(Me)CH_2)$	-26.6	b

[a] This work. [b] Ref. 19.

metallacycle (Scheme IV). We have shown that 2-azametallacyclobutane **7** reacts with t-BuNC (isoelectronic with CO) to give exclusively the product of insertion into the metal-nitrogen bond. More recently, Puddephatt and coworkers have described the coupling of epoxides and CO_2 with platinum complexes to give cyclic metallacarbonates.[19] The mechanism of this reaction is thought to involve oxidative addition of the epoxide to give a 2-oxametallacyclobutane complex, followed by insertion of CO_2 into the metal-oxygen bond. This is consistent with our results on the reaction of CO_2 with the 2-oxametallacyclobutane complex **8**, in which a similar cyclic metallacarbonate is formed.

Experimental

General. Unless otherwise noted, all manipulations were performed under nitrogen using standard drybox, Schlenk, or vacuum line techniques. Drybox experiments were conducted in a Vacuum Atmospheres HE-533 Dri-Lab with attached MO-40-1 or MO-40-2 Dri-Train, equipped with a -40 °C freezer. Oxygen levels were maintained below one part per million and were monitored with a Teledyne Model 316 trace oxygen analyzer.

Nuclear magnetic resonance (NMR) spectra were obtained at ambient temperature unless otherwise noted. ^1H NMR spectra were recorded at 200, 250, or 300 MHz using Fourier transform NMR spectrometers consisting of Cryomagnetics Inc. magnets, Nicolet Model 1180 or 1280 data collection systems, and electronics assembled by Mr. Rudi Nunlist of the University of California, Berkeley (UCB). ^{13}C and $^{31}P\{^1H\}$ spectra were recorded at 75.5 and 121.5 MHz respectively. ^1H and ^{13}C chemical shifts are reported in parts per million (ppm) (δ) downfield from tetramethylsilane (TMS) using residual ^1H and ^{13}C resonances of the deuterated solvent as reference. ^{31}P resonances are reported in ppm downfield from external 85% H_3PO_4 as reference. Splitting patterns are designated as s, singlet; d, doublet; t, triplet; q, quartet; m, multiplet. Coupling constants are reported in hertz.

Infrared (IR) spectra were recorded on either a Perkin-Elmer Model 1550 Fourier transform spectrometer equipped with a Model 7500 professional computer or a Nicolet Model 510 Fourier transform spectrometer equipped with a Model 620 computer.

Mass spectra were obtained at the UCB mass spectrometry facility on AEI MS-12 and Finnegan 4000 mass spectrometers. Elemental analyses were performed by the UCB microanalytical laboratory. Melting points were recorded in sealed capillary tubes under nitrogen on a Thomas-Hoover melting point apparatus and are uncorrected.

Sealed NMR tubes were prepared by inserting a Wilmad 505-PS NMR tube into a Cajon Model SS-6-UT-6-4 3/8"-1/4" reducing union which was attached to a Kontes Model K-826500 high vacuum stopcock. Glass bombs refer to cylindrical, medium-walled Pyrex vessels joined to either a Kontes Model K-826500 or K-826510 high vacuum stopcock. Gas phase mass measurements were performed by measuring the pressure of the reagent in calibrated known-volume bulbs with a MKS Baratron pressure gauge connected to a high vacuum line.

Photochemical experiments were performed using a 450-watt Conrad-Hanovia Model PC451.050 medium-pressure mercury vapor lamp. The lamp was placed in an Ace Glass Model 7875-30 or 7857-05 water-cooled borosilicate glass immersion well. For exploratory reactions, samples were contained in sealed NMR tubes. Small scale (0.1 - 0.5 mmol) preparatory reactions were run in a pyrex vessel assembled by the UCB glass shop. The vessel is a glass "donut" 5 cm tall with an inner diameter of 5.5 cm and an outer diameter of 7.5 cm. On opposite sides of the "donut" are side arms with 14/20 female ground glass joints. Attachment of an Ace Glass Model 9080-02 adapter with stopcock allowed the use of standard Schlenk techniques for sample manipulation. Large scale (2.0 - 5.0 mmol) preparatory reactions were performed in a modified Ace Glass Model 7841-03 photochemical reaction vessel. The UCB glass shop removed the threaded side arm and sealed the vessel at this point. Attachment of an Ace Glass Model 5200-10 adapter with stopcock allowed the use of standard Schlenk techniques for sample manipulation. Constant temperature was maintained using a Forma Scientific Model 2095 refrigerated bath circulator, a Neslab Model ULT-80DD refrigerated bath circulator, a Neslab Model LT-50DD refrigerated bath circulator, or a Neslab Model CC-100 immersion cooler.

Unless otherwise stated, all solvents and reagents were purchased from commercial suppliers and used without further purification. Benzene, tetrahydrofuran (THF), and toluene were distilled

from sodium benzophenone ketyl under nitrogen. Pentane was distilled from $LiAlH_4$ under nitrogen. Hexamethyldisiloxane, *tert*-butylamine (t-$BuNH_2$), and isopropanol were refluxed over CaH_2 under nitrogen and vacuum transfered prior to use. d^6-benzene was dried over sodium benzophenone ketyl and vacuum transfered prior to use. Trimethylphosphine (PMe_3) was purchased from Strem and dried over 1:5 Na:K alloy. Chloroform ($CHCl_3$), *tert*-butylisocyanide (t-BuNC), and *tert*-butylisocyanate (t-BuNCO) were dried over P_2O_5 and distilled prior to use. *tert*-butanol was dried over sodium *tert*-butoxide and distilled prior to use. Carbon dioxide was purchased from Matheson Gas Products and used as received. Potassium hexamethyldisilazide [$KN(TMS)_2$] was prepared by the reaction of hexamethyldisilizane [$HN(TMS)_2$] and potassium hydride (KH) in THF under nitrogen. $Cp^*(PMe_3)IrH_2$[10,20] was prepared by literature procedures.

$Cp^*(PMe_3)Ir(CH_2CMe_2NH_2)H$ (2). In the drybox, 143.0 mg (0.35 mmol) of $Cp^*(PMe_3)IrH_2$ (**1**) was placed in the glass "donut" reactor described above. An adapter with stopcock was attached to one side arm and a rubber septum was placed on the other. The photoreactor was removed from the drybox and approximately 30 ml of dry t-$BuNH_2$ was cannulated onto the dihydride. The resulting pale yellow solution was irradiated for 12.5 h at 5 °C. After irradiation, the brown solution was cannulated into a 100 ml Schlenk flask and the t-$BuNH_2$ removed under vacuum. Analysis of the tan solid isolated in this manner showed approximately 90% conversion of **1** to the alkyl hydride $Cp^*(PMe_3)Ir(CH_2CMe_2NH_2)H$ (**2**). ^1H NMR (d^6-benzene) δ 1.83 (d, J = 1.6 Hz, 15H), 1.48 (s, 3H), 1.46 (s, 3H), 1.24 (d, J = 9.7 Hz, 9H), -17.81 (d, J = 35.4 Hz, 1H). Because of similar solubility properties, we were unable to separate **2** from residual dihydride remaining in the reaction mixture.

$Cp^*(PMe_3)Ir(CH_2CMe_2OH)H$ (3). In the drybox, 1.21 g (2.99 mmol) of $Cp^*(PMe_3)IrH_2$ (**1**) was placed in the modified Ace Glass Model 7841-03 photochemical reaction vessel described above. An adapter with stopcock was attached to one side arm and a rubber septum was placed on the other. The photoreactor was removed from the drybox and approximately 350 ml of dry t-BuOH was cannulated onto the dihydride. The resulting pale yellow solution was irradiated for 4 h at 30 °C. After irradiation, the brown solution was cannulated into a 500 ml

Schlenk flask and the t-BuOH removed under vacuum. Analysis of the tan solid isolated in this manner showed approximately 95% conversion of **1** to the alkyl hydride $Cp^*(PMe_3)Ir(CH_2CMe_2OH)H$ (**3**). Pure **3** can be isolated in poor yield by crystallization from diethyl ether at -40 °C in the drybox.[11] ^1H NMR (d^6-benzene) δ 2.79 (s, 1H), 2.05 (d, J = 11.8 Hz, 1H), 1.82 (d, J = 2.0 Hz, 15H), 1.70 (s, 3H), 1.63 (dd, J = 13.5, 11.8 Hz, 1H), 1.56 (s, 3H), 1.16 (d, J = 9.8 Hz, 9H), -17.76 (d, J = 34.8 Hz, 1H); $^{13}C\{^1H\}$ NMR (d^6-benzene) δ 92.1 (d, J = 2.4 Hz), 71.6 (s), 32.7 (s), 32.3 (s), 19.2 (d, J = 37.4 Hz), 10.3 (s), 9.7 (d, J = 7.0 Hz); IR (KBr pellet) : 3385, 2975, 2959, 2075, 1381, 1350, 959 cm^{-1}; MS (EI) : m/e 478/476 (M^+, $^{193}Ir/^{191}Ir$); Anal. Calcd. for $C_{17}H_{34}OPIr$: C, 42.75%; H, 7.17%. Found: C, 42.52%; H, 7.08%.

$[Cp^*(PMe_3)Ir(CH_2CMe_2NH_2)]^+(Cl^-)$ (4). In the drybox, a 0.78 g of a crude photolysis mixture consisting of 91% (0.72 g, 1.50 mmol) $Cp^*(PMe_3)Ir(CH_2CMe_2NH_2)H$ (**2**) and 9% (0.06 g, 0.15 mmol) $Cp^*(PMe_3)IrH_2$ (**1**) was placed in a 100 ml round bottom flask equipped with a magnetic stirbar. The material was dissolved in 50 ml of benzene and 150 µl (1.85 mmol) of $CHCl_3$ was added. The volatile materials were removed under vacuum. The residue was returned to the drybox, extracted with toluene, and filtered through celite. Crystallization at -40 °C from toluene layered with pentane gave 0.49 g (0.96 mmol, 64.3%) of **4** as yellow crystals. ^1H NMR (d^6-benzene) δ 6.04 (m, 2H), 1.70 (d, J = 10.3 Hz, 9H), 1.64 (d, J = 1.8 Hz, 15H), 1.57 (s, 3H), 1.51 (s, 3H), 1.30 (dd, J = 14.1, 8.5 Hz, 1H), 0.98 (d, J = 8.5 Hz, 1H); $^{13}C\{^1H\}$ NMR (d^6-benzene) δ 92.4 (s), 73.0 (d, J = 11.8 Hz), 35.8 (s), 30.5 (s), 17.4 (d, J = 36.1 Hz), 10.1 (s), -10.3 (d, J = 6.4 Hz); $^{31}P\{^1H\}$ NMR (d^6-benzene) δ -37.1 (s); IR (KBr pellet) : 3205, 3110, 2919, 955 cm^{-1}; MS (EI) : m/e 511/509 (M^+, $^{193}Ir/^{191}Ir$); MS (FAB) : m/e 476/474 (cation, $^{193}Ir/^{191}Ir$)). mp, 170°C (dec). Repeated attempts to obtain satisfactory elemental analysis for **4** failed, presumably due to its hygroscopic nature.

X-ray Crystal Structure Determination of Complex 4. Clear yellow crystals of compound **4** were obtained by slow crystallization from toluene/ hexamethyldisiloxane at -40 °C. Fragments cleaved from some of these crystals were mounted on glass fibers using

polycyanoacrylate cement. Preliminary precession photographs indicated triclinic Laue symmetry and yielded approximate cell dimensions.

The crystal used for data collection was then transferred to our Enraf-Nonius CAD-4 diffractometer and centered in the beam. Automatic peak search and indexing procedures yielded a triclinic reduced primitive cell. Inspection of the Niggli values revealed no conventional cell of higher symmetry. The final cell parameters and specific data collection parameters for this data set are given in Table III.

The 2893 unique raw intensity data were converted to structure factor amplitudes and their esd's by correction for scan speed, background, and Lorentz and polarization effects. No correction for crystal decomposition was necessary. Inspection of the azimuthal scan data showed a variation $I_{min}/I_{max} = 0.86$ for the average curve. An empirical correction based on the observed variation was applied to the data prior to solving the structure. After determination of the true contents of the asymmetric unit, an absorption correction based on the measured shape and size of the crystal and a 20x8x6 Gaussian grid of internal points was applied to the data ($T_{max} = 0.393$, $T_{min} = 0.331$). The choice of the centric triclinic space group was confirmed by the successful solution and refinement of the structure.

The structure was solved by Patterson methods and refined via standard least-squares and Fourier techniques. In a difference Fourier map calculated following the refinement of all non-hydrogen atoms with anisotropic thermal parameters, peaks were found corresponding to the positions of most of the hydrogen atoms. The hydrogen atoms on the water molecules were included in their discovered locations. All other hydrogen atoms were assigned idealized locations. All H atoms were assigned values of B_{iso} approximately 1.2 times the B_{eqv} of the atoms to which they were attached. They were included in structure factor calculations, but not refined. One reflection which suffered badly from extinction and eight reflections which were affected by multiple reflection were removed from the data set before the final refinement.

Table III. Crystal and data collection parameters for complex 4.

A)Crystal Parameters at T = 25 C

a = 8.7124(10) A	Space Group: $P\bar{1}$ (No. 2)
b = 9.8169(10) A	Formula weight = 547.13 amu
c = 14.3097(12) A	Z = 2
alpha = 91.824(8) deg	d(calc) = 1.64 g cm-3
beta = 95.831(8) deg	
gamma = 114.275(9) deg	μ(calc) = 62.13 cm-1
V = 1186.2(4) A**3	
Size: 0.19x0.22x0.29 mm	

B) Data Measurement Parameters

Radiation : Mo Kalpha (lambda= 0.71073 A)

Monochromator : Highly-oriented graphite (2theta = 12.2)

Detector : Crystal scintillation counter, with PHA.

Reflections measured : +H, +/-K, +/-L

2theta range: 3 -> 45 deg Scan Type: theta-2theta

Scan width: delta theta = 0.55 + 0.35 tan(theta)

Scan speed: 0.67 -> 6.7 (theta, deg/min)

Background: Measured over 0.25*(scan width) added to each end of the scan.

Vert. aperture = 3.0 mm Horiz. aperture = 2.0 + 1.0 tan(theta) mm

No. of unique reflections collected: 2893

The final residuals for 209 variables refined against the 2792 "accepted" data for which $F^2 > 3\sigma(F^2)$ were R = 1.63 %, wR = 2.42 % and GOF = 1.45. The R value for all 2884 accepted data was 1.78 %. In the final cycles of refinement a secondary extinction parameter was included.

The quantity minimized by the least squares program was $\Sigma\, w(|F_o|-|F_c|)^2$, where w is the weight of a given observation. The p-factor, used to reduce the weight of intense reflections, was set to 0.03 throughout the refinement. The analytical forms of the scattering factor tables for the neutral atoms were used and all scattering factors were corrected for both the real and imaginary components of anomalous dispersion.

Inspection of the residuals ordered in ranges of $\sin(\theta/\lambda)$, $|F_o|$, and parity and value of the individual indexes showed no unusual features or trends. The largest peak in the final difference Fourier map had an electron density of 0.80 e^-/A^3, and the lowest excursion -0.40 e^-/A^3. Both were located near the iridium atom.

The positional and thermal parameters of all the atoms and anisotropic thermal parameters (B's) are given in Table IV.

$[Cp^*(PMe_3)Ir(CH_2CMe_2NH_2)]^+(PF_6^-)$ (5). In the drybox, 51.0 mg (0.10 mmol) of the chloride salt **4** and 36.7 mg (0.20 mmol) of KPF_6 were weighed into a 50 ml round bottom flask equipped with a vacuum stopcock and magnetic stirbar. The reaction flask was evacuated on a vacuum line, and approximately 20 ml of i-PrOH was transferred onto the solids under vacuum. The volatile materials were then removed under vacuum and the residue was returned to the drybox and extracted with toluene. Crystallization by vapor diffusion of pentane into the toluene solution at -40 °C in the drybox gave 47.2 mg (0.08 mmol, 76.2%) of **5** as yellow needles. ^1H NMR (d^6-benzene) δ 3.44 (d, J = 8.2 Hz, 1H), 2.37 (d, J = 8.2 Hz, 1H), 1.37 (d, J = 10.4 Hz, 9H), 1.35 (d, J = 1.8 Hz, 15H), 0.89 (s, 3H), 0.81 (s, 3H); $^{13}C\{^1H\}$ NMR (d^6-benzene) δ 92.0 (s), 73.5 (s), 35.0 (s), 29.7 (s), 15.3 (d, J = 37.6 Hz), 9.2 (s), -10.8 (d, J = 7.4 Hz); $^{31}P\{^1H\}$ NMR (d^6-benzene) δ -34.5 (s), -142.5 (septet, J = 711.5 Hz); Anal. Calcd. for $C_{17}H_{34}F_6IrNP_2$: C, 32.90%; H, 5.52%; N, 2.26. Found: C, 33.05%; H, 5.51%; N, 2.23%.

Table IV. Positional parameters and their estimated standard deviations for complex **4**.

Atom	x	y	z	B(A2)
IR	0.00422(1)	0.41660(1)	0.22042(1)	2.147(3)
CL	0.6233(1)	0.2012(1)	0.40017(7)	5.16(2)
P	-0.0350(1)	0.56942(8)	0.26768(6)	2.89(2)
N1	-0.1302(3)	0.2194(3)	0.2405(2)	3.33(6)
O1	0.2555(3)	-0.0030(3)	0.4699(2)	5.63(7)
O2	0.0831(4)	0.0366(3)	0.6202(2)	6.49(8)
C1	-0.2040(4)	0.1869(4)	0.1381(3)	3.98(8)
C2	-0.0987(4)	0.3356(4)	0.0998(2)	3.54(8)
C3	-0.1676(5)	0.0580(4)	0.0966(4)	6.2(1)
C4	-0.3959(5)	0.1414(4)	0.1274(3)	5.3(1)
C5	-0.0126(4)	0.6000(4)	0.3934(3)	4.29(9)
C6	-0.2629(4)	0.5145(4)	0.2391(3)	4.61(9)
C7	0.0488(5)	0.7521(4)	0.2211(3)	4.82(9)
C11	0.3378(4)	0.5544(3)	0.1870(2)	2.90(7)
C12	0.2988(3)	0.4023(3)	0.1547(2)	2.85(7)
C13	0.2749(3)	0.3160(3)	0.2349(2)	2.76(7)
C14	0.3024(3)	0.4147(3)	0.3167(2)	2.86(7)
C15	0.3493(4)	0.5615(3)	0.2879(2)	3.03(7)
C16	0.3980(5)	0.6867(4)	0.1284(3)	4.63(9)
C17	0.2945(4)	0.3494(4)	0.0558(2)	4.24(9)
C18	0.2413(4)	0.1555(3)	0.2359(3)	3.80(8)
C19	0.3022(4)	0.3711(4)	0.4171(2)	4.18(9)
C20	0.4214(4)	0.7059(4)	0.3511(3)	4.56(9)

Table IV. Positional parameters and their estimated standard deviations for complex **4** (cont.).

Atom	x	y	z	B(A2)
H1A	-0.2025	0.2377	0.2797	4.0*
H1B	-0.1009	0.1428	0.2640	4.0*
H2A	-0.0518	0.3232	0.0446	4.3*
H2B	-0.1594	0.3955	0.0881	4.3*
H3A	-0.0488	0.0865	0.1032	7.3*
H3B	-0.2208	-0.0287	0.1289	7.3*
H3C	-0.2116	0.0371	0.0315	7.3*
H4A	-0.4176	0.2211	0.1530	6.4*
H4B	-0.4396	0.1205	0.0623	6.4*
H4C	-0.4488	0.0545	0.1598	6.4*
H5A	-0.0545	0.5161	0.4225	5.2*
H5B	0.1036	0.6643	0.4165	5.2*
H5C	-0.0756	0.6636	0.4076	5.2*
H6A	-0.2937	0.4904	0.1731	5.6*
H6B	-0.3232	0.4297	0.2716	5.6*
H6C	-0.2891	0.5954	0.2577	5.6*
H7A	0.1691	0.7945	0.2324	5.8*
H7B	0.0122	0.7422	0.1562	5.8*
H7C	0.0086	0.8156	0.2531	5.8*

Table IV. Positional parameters and their estimated standard deviations for complex **4** (cont.).

Atom	x	y	z	B(A2)
H16A	0.5173	0.7220	0.1276	5.5*
H16B	0.3421	0.6573	0.0658	5.5*
H16C	0.3736	0.7643	0.1548	5.5*
H17A	0.4031	0.3548	0.0460	5.1*
H17B	0.2126	0.2485	0.0435	5.1*
H17C	0.2649	0.4107	0.0141	5.1*
H18A	0.3381	0.1464	0.2665	4.6*
H18B	0.1465	0.1052	0.2685	4.6*
H18C	0.2174	0.1116	0.1728	4.6*
H19A	0.4119	0.3806	0.4408	6.0*
H19B	0.2711	0.4349	0.4545	6.0*
H19C	0.2223	0.2700	0.4182	6.0*
H20A	0.5400	0.7370	0.3669	5.5*
H20B	0.4010	0.7811	0.3190	5.5*
H20C	0.3681	0.6896	0.4070	5.5*
H(O1)A	0.3046	-0.0566	0.5000	7.5*
H(O1)B	0.3593	0.0546	0.4375	7.5*
H(O2)A	0.1660	0.0273	0.5820	8.5*
H(O2)B	0.0000	0.0546	0.6035	8.5*

Starred atoms were included with isotropic thermal parameters.

$Cp^*(PMe_3)Ir(CH_2CMe_2OH)Cl$ (6). In the drybox, 269 mg of a crude photolysis mixture consisting of 96% (260 mg, 0.54 mmol) $Cp^*(PMe_3)Ir(CH_2CMe_2OH)H$ (**3**) and 4% (9.3 mg, 0.02 mmol) $Cp^*(PMe_3)IrH_2$ (**1**) was placed in a 50 ml round bottom flask equipped with a magnetic stirbar. The material was dissolved in 25 ml of benzene and 50 µl (0.60 mmol) of $CHCl_3$ was added. The volatile materials were removed under vacuum. The residue was returned to the drybox and extracted with pentane. Crystallization at -40 °C from pentane gave 237 mg (0.46 mmol, 84.8%) of **6** as orange crystals. ^1H NMR (d^6-benzene) δ 4.12 (s, 1H), 2.36 (d, J = 12.0 Hz, 1H), 1.80 (s, 3H), 1.75 (dd, J = 15.6, 12.0 Hz, 1H), 1.59 (s, 3H), 1.36 (d, J = 2.0 Hz, 15H), 1.21 (d, J = 10.3 Hz, 9H); $^{13}C\{^1H\}$ NMR (d^6-benzene) δ 92.0 (d, J = 2.9 Hz), 75.4 (s), 35.9 (s), 32.6 (s), 14.0 (d, J = 38.2 Hz), 12.8 (d, J = 10.0 Hz), 8.7 (s); $^{31}P\{^1H\}$ NMR (d^6-benzene) δ -32.2 (s); IR (KBr pellet) : 3421, 2967, 2912, 1378, 1354, 957 cm^{-1}; MS (EI) : m/e 512/510 (M^+, $^{193}Ir/^{191}Ir$); mp, 128-129°C; Anal. Calcd. for $C_{17}H_{33}ClOPIr$: C, 39.87%; H, 6.50%. Found: C, 39.75%; H, 6.64%.

$Cp^*(PMe_3)Ir(CH_2CMe_2NH)$ (7). In the drybox, 108 mg (0.21 mmol) of the chloride salt **4** was weighed into a vial equipped with a magnetic stirbar and dissolved in 5 ml of toluene. In a separate vial, 42.2 mg (0.21 mmol) of $KN(SiMe_3)_2$ was also dissolved in 5 ml of toluene. Both vials were cooled to -40 °C in the drybox freezer. After removal from the freezer, the toluene solution of $KN(SiMe_3)_2$ was immediately added dropwise to the toluene solution of **4** with rapid stirring. The mixture was allowed to warm to box temperature and, after stirring an additional 10 min at box temperature, the contents was placed into a 50 ml round bottom flask equipped with a magnetic stirbar and vacuum stopcock and brought to the vacuum line. The volatile materials were removed under vacuum and the residue was returned to the drybox. The product was extracted into pentane, filtered through celite, and dried under vacuum. Lyophilization from benzene gave 91.1 mg (0.19 mmol, 90.9%) of **7** as a white powder, pure by ^1H NMR spectroscopy. ^1H NMR (d^6-benzene) δ 1.70 (d, J = 1.6 Hz, 15H), 1.30 (d, J = 9.5 Hz, 9H), 1.25 (s, 3H), 1.24 (s, 3H), 1.05 (m, 2H), -0.35 (br s, 1H); $^{13}C\{^1H\}$ NMR (d^6-benzene) δ 91.9 (d, J = 3.9 Hz), 71.1 (d, J = 1.3 Hz), 38.9 (s), 34.7 (s), 16.8 (d, J = 36.3 Hz), 10.0 (s), -21.7 (d, J = 6.6); $^{31}P\{^1H\}$ NMR (d^6-benzene) δ - 41.6

(s); IR (d^6-benzene) : 3415, 2957, 2926, 971 cm^{-1}; High resolution mass spectrum (EI), m/e calcd for $C_{17}H_{33}NPIr$: 475.1984/473.1960 (M^+, $^{193}Ir/^{191}Ir$); m/e found 475.1987/473.1950 (M^+, $^{193}Ir/^{191}Ir$, deviation = 0.6/-2.1 ppm).

$Cp^*(PMe_3)Ir(CH_2CMe_2O)$ (8). In the drybox, 31.0 mg (0.06 mmol) of the alkyl chloride **6** was weighed into a vial equipped with a magnetic stirbar and dissolved in 5 ml of benzene. In a separate vial, 13.3 mg (0.06 mmol) of $KN(SiMe_3)_2$ was also dissolved in 5 ml of benzene. The benzene solution of $KN(SiMe_3)_2$ was added dropwise to the rapidly stirring benzene solution of **6**. After stirring for 10 min, the contents were placed into a 50 ml round bottom flask equipped with a magnetic stirbar and vacuum stopcock and brought to the vacuum line. The volatile materials were removed under vacuum and the residue returned to the drybox. The product was extracted into pentane, filtered through celite, and dried under vacuum. Lyophilization from benzene gave 23.4 mg (0.05 mmol, 81.3%) of **8** as a white powder. ^1H NMR (d^6-benzene) δ 1.63 (d, J = 1.9 Hz, 15H), 1.49 (dd, J = 7.3, 2.7 Hz, 1H), 1.42 (dd, J = 11.6, 7.3 Hz, 1H), 1.36 (s, 3H), 1.34 (d, J = 9.9 Hz, 9H), 1.30 (s, 3H); $^{13}C\{^1H\}$ NMR (d^6-benzene) δ 91.2 (s), 90.6 (d, J = 3.9 Hz), 38.5 (s), 34.4 (s), 16.0 (d, J = 36.2 Hz), 10.0 (s), -16.8(d, J = 6.1 Hz); $^{31}P\{^1H\}$ NMR (d^6-benzene) δ -33.0 (s); IR (KBr pellet) : 2976, 2911, 954 cm^{-1}; High resolution mass spectrum (EI), m/e calcd for $C_{17}H_{32}OPIr$: 476.1824/474.1800 (M^+, $^{193}Ir/^{191}Ir$); m/e found 476.1827/474.1796 (M^+, $^{193}Ir/^{191}Ir$, deviation = 0.6/-0.8 ppm); mp, 90-93°C (dec).

$Cp^*(PMe_3)Ir[CH_2CMe_2N(H)C(N\text{-}tBu)]$ (9). In the drybox, 32.5 mg (0.07 mmol) of the metallacycle **7** was loaded into a bomb and dissolved in 5 ml of benzene. The bomb was removed to a vacuum line and the solution was degassed with a freeze-pump-thaw cycle. From a known-volume bulb, 1.25 equiv t-BuNC (56.1 torr, 28.36 ml at 298K, 0.09 mmol) was condensed into the solution at -196 °C. The solution was thawed and left at room temperature for 8 h. The volatile materials were removed under vacuum and the residue returned to the drybox. The product was extracted into pentane, filtered through celite, and dried under vacuum. Lyophilization from benzene gave 34.6 mg (0.06 mmol, 90.6%) of **9** as a white powder. ^1H NMR (d^6-benzene) δ 3.12 (br s, 1H), 2.35 (dd, J = 16.2, 10.8 Hz, 1H), 2.05 (d, J = 10.8, 1H), 1.83 (s, 3H), 1.68 (d, J = 1.7 Hz,

15H), 1.57 (s, 9H), 1.32 (s, 3H), 1.21 (d, J = 9.8 Hz, 9H); ^{13}C {^{1}H} NMR (d^6-benzene) δ 155.6 (d, J = 14.4 Hz), 92.4 (d, J = 2.9 Hz), 73.3 (s), 51.8 (s), 34.4 (s), 32.3 (s), 30.1 (s), 25.2 (d, J = 7.3 Hz), 15.6 (d, J = 38.2 Hz), 9.8 (s); ^{31}P {^{1}H} NMR (d^6-benzene) δ -33.6 (s); IR (KBr pellet) : 2953, 2905, 1558, 953 cm^{-1}; High resolution mass spectrum (EI), m/e calcd for $C_{22}H_{42}N_2PIr$: 558.2718/556.2694 (M^+, $^{193}Ir/^{191}Ir$); m/e found 558.2718/556.2686 (M^+, $^{193}Ir/^{191}Ir$, deviation = 0.0/-1.4 ppm).

$Cp^*(PMe_3)Ir[CH_2CMe_2OC(N\text{-}tBu)]$ (10). In the drybox, 24.3 mg (0.05 mmol) of the metallacycle **8** was loaded into a Wilmad 505-PS 8" NMR tube fitted with a Cajon adaptor and dissolved in 0.5 ml d^6-benzene. The tube was removed to a vacuum line and the solution was degassed with a freeze-pump-thaw cycle. From a known-volume bulb, 1.25 equiv t-BuNC (42.4 torr, 28.36 ml at 298K, 0.09 mmol) was condensed into the solution at -196 °C. The tube was sealed and placed in a 45 °C constant temperature bath for 2 d. The tube was returned to the drybox where the volatile materials were removed under vacuum. The product was extracted into pentane, filtered through celite, and dried under vacuum. Lyophilization from benzene gave 17.9 mg (0.03 mmol, 62.7%) of **10** as a yellow powder, judged to be greater than 90% pure by ^{1}H NMR spectroscopy. ^{1}H NMR (d^6-benzene) δ 2.05 (dd, J = 15.0, 10.9 Hz, 1H), 1.80 (s, 3H), 1.73 (d, J = 10.9 Hz, 1H), 1.70 (d, J = 1.8 Hz, 15H), 1.64 (s, 3H), 1.60 (s, 9H), 1.18 (d, J = 10.1 Hz, 9H); ^{13}C {^{1}H} NMR (d^6-benzene) δ 160.5 (d, J = 20.0 Hz), 93.1 (d, J = 2.8 Hz), 83.9 (s), 54.4 (s), 31.8 (s), 30.5 (s), 29.1 (s), 15.9 (d, J = 7.1 Hz), 14.5 (d, J = 38.1 Hz), 9.2 (s); ^{31}P {^{1}H} NMR (d^6-benzene) δ -32.8 (s); IR (neat oil) : 2960, 2906, 1586, 952 cm^{-1}.

$[Cp^*(PMe_3)Ir[CH_2CMe_2N(H)C(O)O]$ (11). In the drybox, 24.5 mg (0.05 mmol) of the metallacycle **7** was loaded into a Wilmad 505-PS 8" NMR tube fitted with a Cajon adaptor and dissolved in 0.5 ml d^6-benzene. The tube was removed to a vacuum line and the solution was degassed with a freeze-pump-thaw cycle. 605 torr of CO_2 was placed above the solution and the NMR tube was sealed. Analysis of the reaction by ^{1}H NMR spectroscopy showed the immediate formation of complex **12**. Spectroscopic data for **12**: ^{1}H NMR (d^6-benzene) δ 12.71 (br s, 1H), 1.67 (s, 3H), 1.55 (d, J = 1.9 Hz, 15H), 1.50 (s, 3H), 1.27 (dd, J = 13.5, 9.4 Hz, 1H), 1.18 (d, J =

10.1 Hz, 9H), 1.07 (d, J = 9.4 Hz, 1H). IR (d^6-benzene) : 2975, 2909, 1605, 953 cm^{-1}. After standing for 3 d at room temperature, conversion of **12** to complex **11** was complete. The tube was returned to the drybox where the volatile materials were removed under vacuum. The product was extracted into pentane, filtered through celite, and dried under vacuum. Lyophilization from benzene gave 21.4 mg (0.04 mmol, 80.0%) of **11** as a white powder, judged to be greater than 90% pure by ^1H NMR spectroscopy. ^1H NMR (d^6-benzene) δ 4.26 (br s, 1H), 2.11 (dd, J = 11.2, 1.4 Hz, 1H), 1.97 (dd, J = 15.9, 11.2 Hz, 1H), 1.31 (d, J = 2.0 Hz, 15H), 1.19 (s, 3H), 1.18 (s, 3H), 1.15 (d, J = 10.2 Hz, 9H); ^{13}C {^1H} NMR (d^6-benzene) δ 162.6 (s), 90.8 (d, J = 3.2 Hz), 53.6 (s), 35.4 (s), 31.2 (s), 16.0 (d, J = 8.5 Hz), 14.4 (d, J = 35.2 Hz), 9.1 (s); IR (d^6-benzene) : 2956, 2912, 1626, 956 cm^{-1}.

[Cp*(PMe$_3$)Ir[CH$_2$CMe$_2$OC(O)O] (13). In the drybox, 23.4 mg (0.05 mmol) of the metallacycle **8** was loaded into a Wilmad 505-PS 8" NMR tube fitted with a Cajon adaptor and dissolved in 0.5 ml d^6-benzene. The tube was removed to a vacuum line and the solution was degassed with a freeze-pump-thaw cycle. 580 torr of CO_2 was placed above the solution and the NMR tube was sealed. After standing for 1 d at room temperature, the reaction was complete. The tube was returned to the drybox where the volatile materials were removed under vacuum. The product was extracted into pentane, filtered through celite, and dried under vacuum. Lyophilization from benzene gave 20.5 mg (0.04 mmol, 80.2%) of **13** as a yellow powder. ^1H NMR (d^6-benzene) δ 2.24 (d, J = 11.8 Hz, 1H), 2.05 (dd, J = 15.8, 11.8 Hz, 1H), 1.63 (s, 3H), 1.33 (s, 3H), 1.26 (d, J = 2.0 Hz, 15H), 1.15 (d, J = 10.2 Hz, 9H); ^{13}C {^1H} NMR (d^6-benzene) δ 157.0 (s), 90.8 (d, J = 1.7 Hz), 79.1 (s), 34.9 (s), 28.6 (s), 14.8 (d, J = 8.5 Hz), 14.3 (d, J = 35.5 Hz), 9.0 (s); ^{31}P {^1H} NMR (d^6-benzene) δ -29.2 (s); IR (KBr pellet) : 2968, 2916, 1644, 960 cm^{-1}; Anal. Calcd. for $C_{18}H_{32}O_3PIr$: C, 41.61%; H, 6.21%. Found: C, 41.81%; H, 6.28%.

Cp*(PMe$_3$)Ir[CH$_2$CMe$_2$NC(O)NH(tBu)] (14). In the drybox, 24.3 mg (0.05 mmol) of the metallacycle **7** was loaded into a Wilmad 505-PS 8" NMR tube fitted with a Cajon adaptor and dissolved in 0.5 ml d^6-benzene. The tube was removed to a vacuum line and the solution was degassed with a freeze-pump-thaw cycle. From a known-volume bulb, 1.25 equiv t-BuNCO (45.2

torr, 28.36 ml at 298K, 0.07 mmol) was condensed into the solution at -196 °C. The tube was sealed; upon thawing the product immediately precipitated from solution. After returning the tube to the drybox, the product was collected on a filter funnel with a fine porosity fritted disc and washed with pentane to give 31.2 mg (0.05 mmol, 98.9%) of **14** as a white powder. ^{1}H NMR (d^{6}-benzene) δ 3.59 (br s, 1H), 1.84 (s, 3H), 1.54 (s, 3H), 1.53 (d, J = 1.9 Hz, 15H), 1.52 (s, 9H), 1.22 (d, J = 9.8 Hz, 9H), 1.15 (dd, J = 12.1, 7.7 Hz, 1H), 1.03 (dd, J = 7.7, 1.1 Hz, 1H); $^{13}C\{^{1}H\}$ NMR (d^{6}-benzene) δ 159.5 (s), 91.6 (d, J = 3.4 Hz), 74.8 (s), 49.4 (s), 33.6 (s), 30.9 (s), 29.2 (s), 16.9 (d, J = 37.3 Hz), 9.8 (s), -10.3 (d, J = 6.5 Hz); $^{31}P\{^{1}H\}$ NMR (d^{6}-benzene) δ -30.9 (s); IR (KBr pellet) : 2955, 2915, 1601, 957 cm^{-1}; MS (EI) : m/e 574/572 (M^{+}, $^{193}Ir/^{191}Ir$); Anal. Calcd. for $C_{22}H_{42}N_{2}OPIr$: C, 46.05%; H, 7.38%; N, 4.88 Found: C, 46.14%; H, 7.36%; N, 4.85%.

Cp*(PMe3)Ir(OC(O)N-tBu) (15). In the drybox, 11.2 mg (0.02 mmol) of the metallacycle **8** was loaded into a Wilmad 505-PS 8" NMR tube fitted with a Cajon adaptor and dissolved in 0.5 ml d^{6}-benzene. The tube was removed to a vacuum line and the solution was degassed with a freeze-pump-thaw cycle. From a known-volume bulb, 1.45 equiv t-BuNCO (22.0 torr, 28.36 ml at 298K, 0.03 mmol) was condensed into the solution at -196 °C. The tube was sealed, thawed, and placed in a 45 °C constant temperature bath. After 2 d, the solution was bright green and analysis by ^{1}H NMR spectroscopy showed complete disappearance of **8**. The tube was returned to the drybox where the volatile materials were removed under vacuum. The product was extracted into pentane, filtered through celite and crystallized at -40 °C to give 9.7 mg (0.02 mmol, 71.8%) of **15** (contaminated with ca. 2% of the metallacarbonate **16**) as yellow crystals. All attempts to isolate pure **15** failed due to its reactivity with trace amounts of water. ^{1}H NMR (d^{6}-benzene) δ 1.60 (s, 9H), 1.35 (d, J = 2.0 Hz, 15H), 1.06 (d, J = 10.4 Hz, 9H).

References

1. For some specific examples and leading references, see: (a) Chong, A. O.; Sharpless, K. B. *J. Org. Chem.* **1977**, *42*, 1587. (b) Sheldon, R. A.; Van Doorn, J. A. *J. Catal.*, **1973**, *31*, 427. (c) Mimoun, H.; Mignard, M.; Brechot, P.; Saussine, L. *J. Am. Chem. Soc.* **1986**, *108*, 3711. (d) Chaumette, P.; Mimoun, H.; Saussine, L.; Fischer, J.; Mitschler, A. *J. Organomet. Chem.* **1983**, *250*, 291. (e) Sheldon, R. A.; Kochi, J. K. *Metal Oxidations of Organic Compounds*, Academic Press: New York, 1981.
2. See, *Cytochrome P-450*, Ortiz de Montellano, P. R., Ed., Plenum Press: New York, 1986, and references therein.
3. (a) Groves, J. T.; Subramanian, D. V. *J. Am. Chem. Soc.* **1984**, *106*, 2177. (b) Groves, J. T., in *Advances in Inorganic Biochemistry*, Eichorn, G. L., Marzilli, L. G., Eds., Elsevier, New York, 1979: pp. 119-145. (c) Renaud, J. -P.; Battioni, P.; Bartoli, J. F.; Mansuy, D. *J. C. S. Chem. Comm.* **1985**, 888, and references therein.
4. See, for example: (a) Gould, E. S.; Hiatt, R. R.; Irwin, K. C. *J. Am. Chem. Soc.* **1968**, *90*, 4573. (b) Sheng, M. N.; Zajacek, J. G. *J. Org. Chem.* **1970**, *35*, 1839. (c) Strukul, G.; Michelin, R. A. *J. Am. Chem. Soc.* **1985**, *107*, 7563. (d) Srinivasan, K.; Perrier, S.; Kochi, J. K. *J. Mol. Catal.* **1986**, *36*, 297. (e) Jorgenson, K. A.; Hoffmann, R. *Acta. Chem. Scand.* **1986**, *B40*, 411.
5. See, for example: (a) Sharpless, K. B.; Teranishi, A. Y.; Bacvkvall, J.-E. *J. Am. Chem. Soc.* **1977**, *99*, 3120. (b) Rappe, A. K.; Goddard, W. A. *J. Am. Chem. Soc.* **1982**, *104*, 3287. (c) Collman, J. P.; Brauman, J. I.; Meunier, B.; Raybuck, S. A.; Kodadek, T. *Proc. Natl. Acad. Sci. USA* **1984**, *81*, 3245. (d) Walba, D. M.; DePuy, C. H.; Grabowski, J. J.; Bierbaum, V. M. *Organometallics* **1984**, *3*, 498. (e) Collman, J. P.; Kodadek, T.; Raybuck, S. A.; Brauman, J. I.; Papazian, L. M. *J. Am. Chem. Soc.* **1985**, *107*, 4343. (f) Collman, J. P.; Brauman, J. I.; Meunier, B.; Hayashi, T.; Kodadek, T.; Raybuck, S. A. *J. Am. Chem. Soc.* **1985**, *107*, 2000. (g) Mock, W. L.; Bieniarz, C. *Organometallics* **1985**, *4*, 1917. (h) Groves, J. T.; Avaria-Neisser,

G. E.; Fish, K. M.; Imachi, M.; Kuczkowski, R. L. *J. Am. Chem. Soc.* **1986**, *108*, 3837. (i) Girardet, M.; Meunier, B. *Tetrahedron Lett.*.**1987**, 2955.

6. Schrock, R. R. *J. Am. Chem. Soc.* **1976**, *98*, 5399.
7. Miyashita, A; Ishida, J; Nohira, H. *Tetrahedron Lett.* **1986**, *27*, 2127.
8. Alper, H.; Urso, F, Smith, D. J. H. *J. Am. Chem. Soc.* **1983**, *105*, 6737.
9. (a) Ho, S. C.; Hentges, S.; Grubbs, R. H. *Organometallics* **1988**, *7*, 780. (b) L. Whinnery and J. Bercaw, personal communication.
10. Janowicz, A. H.; Bergman, R. G. *J. Am. Chem. Soc.* **1983**, *105*, 3929.
11. Work on the photolysis of **1** in t-BuOH was begun by Dr. J. C. Hayes of these laboratories.
12. Dr. J. C. Hayes, unpublished results.
13. Dr. M. B. Sponsler, unpublished results.
14. Newman, L. J.; Bergman, R. G. *J. Am. Chem. Soc.* **1985**, *107*, 5314.
15. (a) Schlodder, R.; Ibers, J. A.; Lenarda, M.; Graziani, M. *J. Am. Chem. Soc.* **1974**, *96*, 6893. (b) Lenarda, M.; Ros, R.; Traverso, O.; Pitts, W. D.; Bradley, W. H., Graziani, M. *Inorg. Chem.* **1977**, *16*, 3178.
16. Klein, D. P.; Hayes, J. C.; Bergman, R. G. *J. Am. Chem. Soc.* **1988**, *110*, 3704.
17. (a) Bennett, C. R.; Bradley, D. C. *J. C. S. Chem. Commun.* **1974**, 29. (b) Simpson, S. J.; Turner, H. W.; Andersen, R. A. *J. Am. Chem. Soc.* **1979**, *101*, 7728. (c) Simpson, S. J.; Turner, H. W.; Andersen, R. A. *Inorg. Chem.* **1981**, *20*, 2921. (d) Simpson, S. J.; Andersen, R. A. *Inorg. Chem.* **1981**, *20*, 3627.
18. McGhee, W. D.; Bergman, R. G. *J. Am. Chem. Soc.* **1985**, *107*, 3388.
19. Aye, K.; Ferguson, G.; Lough, A. J.; Puddephatt, R. J. *Angew. Chem. Int. Ed. Engl.* **1989**, *28*, 767.
20. Isobe, K.; Bailey, P. M.; Maitlis, P. M. *J. Chem. Soc., Dalton Trans.*, **1981**, 2003.

Chapter 2

Synthesis and Reactivity of $Cp^*(PMe_3)Ir{=}CH_2$: A Monomeric (Pentamethylcyclopentadienyl)iridium Methylene Complex

Introduction

Complexes with metal-carbon double bonds are the key reactive species in olefin metathesis[1] and are potentially relevant to the mechanism of the Fischer-Tropsch process.[2] The first stable molecules of this type were reported by Fischer in 1964.[3] These complexes, commonly referred to as Fischer carbenes, contain heteroatom substituents on the α-carbon. Nearly ten years passed before stable nonheteroatom-substituted carbene (alkylidene) complexes were discovered.[4] Soon after, Schrock reported the first stable alkylidene complex with a hydrogen on the α-carbon[5] and, one year later, the first stable methylene ($L_nM{=}CH_2$) complex.[6] Since these initial discoveries, transition-metal carbene and alkylidene complexes have been extensively studied.[7]

Monomeric iridium alkylidene complexes, however, are still quite rare,[8] and although a large number of dinuclear cyclopentadienyl and pentamethylcyclopentadienyl cobalt, rhodium, and iridium alkylidene complexes are known,[9] no monomeric alkylidene complex in this well studied series has ever been made. In this chapter, we report the generation of a monomeric pentamethylcyclopentadienyl iridium methylene complex, as well as a study on the reactivity of this molecule.

Results

Irradiation of a toluene solution of the 2-oxametallacyclobutane complex $Cp^*(PMe_3)Ir(CH_2CMe_2O)$ (**1**)[10] at -70 °C for 8 h led to the disappearance of starting material and the generation of one equivalent of acetone (δ 1.54 ppm) and a single new organometallic species as determined by NMR spectroscopy. This new species exhibits typical absorptions in both the ^1H and ^{13}C NMR spectra due to simple PMe_3 and η^5-coordinated pentamethylcyclopentadienyl ligands. The only other resonances observable confirm the identity of this species as the methylene complex $Cp^*(PMe_3)Ir{=}CH_2$ (**2**) (Scheme I). As shown in Figure I, signals for two protons are evident in the ^1H NMR spectrum at very low field (δ 14.08 and 13.08 ppm). These hydrogens are coupled weakly to one another ($J_{H\text{-}H}$ = 3.3 Hz). One exhibits a large trans coupling to phosphorus ($J(H_T\text{-}P)$ = 23.8 Hz) and the other a smaller cis coupling ($J(H_C\text{-}P)$ =

Scheme I

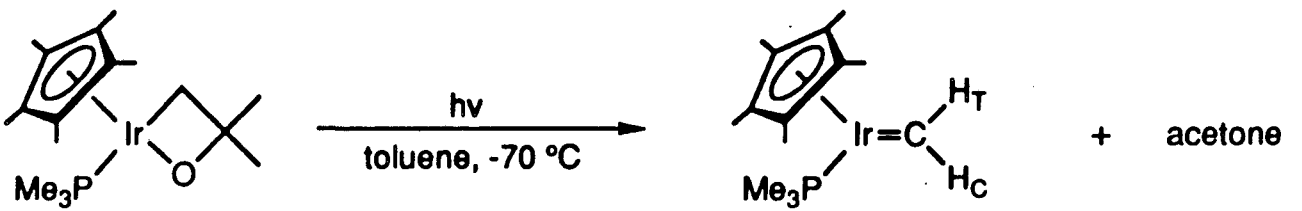

1 2

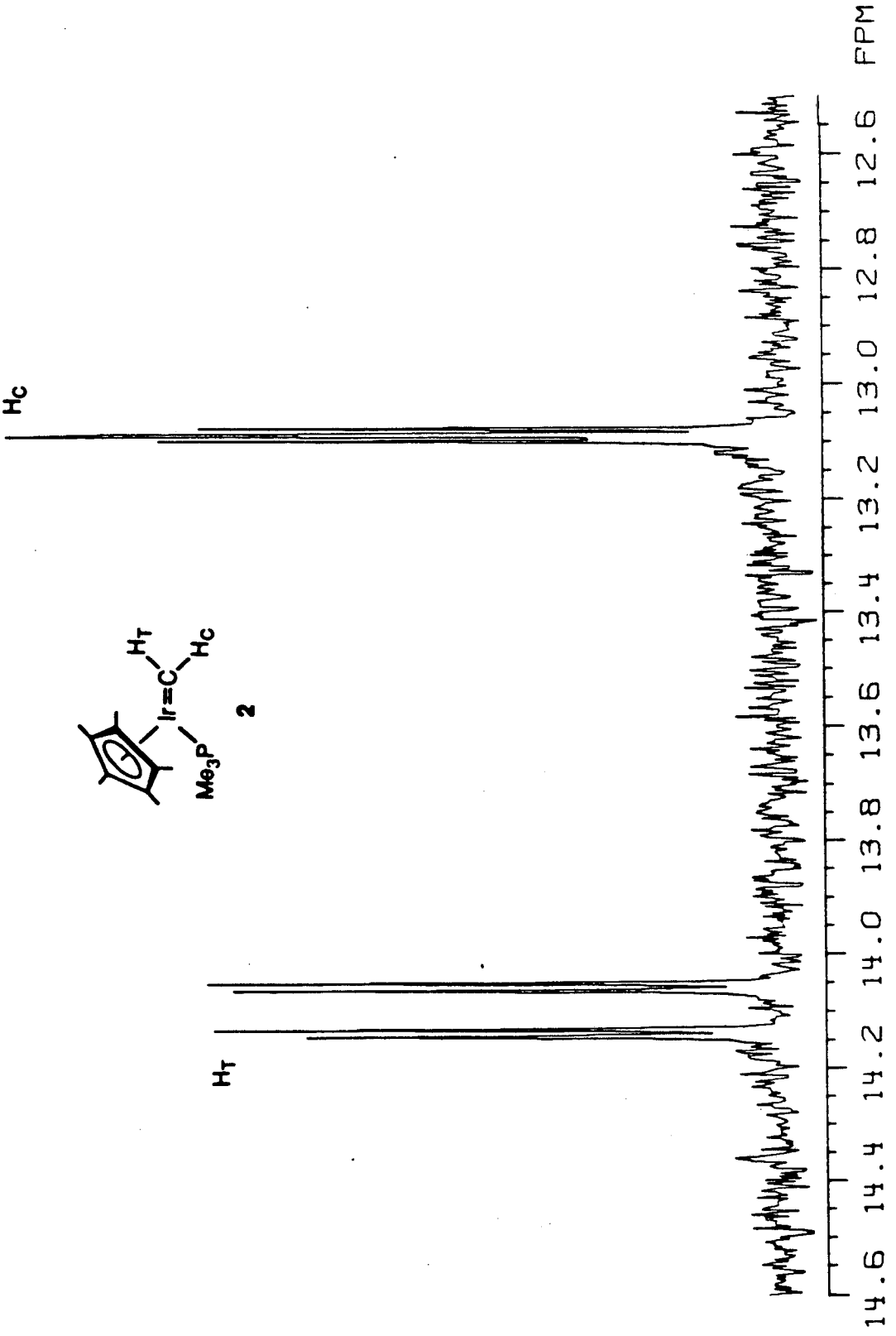

Figure I. Low field region of the ^1H NMR spectrum of **2** at -45 °C in d^8-toluene.

2.8 Hz). The $^{13}C\{^1H\}$ NMR spectrum shows a low field resonance at δ 189.9 ppm; a proton-coupled spectrum establishes this as a carbon to which two hydrogens are attached (J_{C-H} = 146.4, 133.8 Hz). The chemical shifts of these hydrogen and carbon resonances (as well as its reactivity; see below) confirm the existence of **2** as a monomer; bridging CH_2, CHR and CR_2 groups in dinuclear transition metal complexes uniformly resonate at substantially higher field.[11] Analysis of the volatile materials by GC confirmed the production of one equivalent of acetone in this reaction.

Methylene complex **2** is air-sensitive and indefinitely stable only below -40 °C. Toluene solutions of **2** contained in sealed tubes decomposed over 48 h at room temperature, but showed no decomposition after one month at -60 °C. Attempts to isolate **2** have proven unsuccessful; removal of solvent, even at low temperature, resulted in decomposition to an uncharacterized brown oil.

Reaction of $Cp^*(PMe_3)Ir{=}CH_2$ (2) With Organic Acids. Although we have been unable to isolate methylene complex **2**, its stability in solution has allowed us to explore its chemistry. Complex **2** shows ubiquitous reactivity toward a variety of organic acids. Treatment of a toluene solution of **2** with one equivalent of aniline hydrochloride resulted in the instantaneous formation of the known[12] (methyl)chloride complex $Cp^*(PMe_3)Ir(Me)Cl$ (**3**) in 71% isolated yield (Scheme II). Compound **2** was also found to react with phenols. Addition of an excess of α,α,α-trifluoro-p-cresol gave the methyl phenoxide complex $Cp^*(PMe_3)Ir(Me)(O\text{-}C_6H_4\text{-}p\text{-}CF_3)$ (**4**) in 85% isolated yield (Scheme III). Likewise, complex **2** reacted with succinimide to give the (methyl)succinimate $Cp^*(PMe_3)Ir(Me)[NC(O)CH_2CH_2C(O)]$ (**5**) as a yellow powder in 77% isolated yield (Scheme IV). Finally, complex **2** reacted with hydrogen sulfide (H_2S) to give the (thiol)methyl complex $Cp^*(PMe_3)Ir(SH)Me$ (**6**) in 76% isolated yield (Scheme V).

Acids of much higher pK_a also react readily with complex **2**. Treatment of **2** with *tert*-butanethiol (t-BuSH) proceeded slowly at -40 °C, giving the (methyl)*tert*-butylthiolate complex $Cp^*(PMe_3)Ir(Me)(S\text{-}tBu)$ (**7**) in 85% yield (Scheme VI). This material shows a characteristic iridium-methyl resonance at δ 0.84 ppm (doublet, J_{P-H} = 6.7 Hz) in the ^1H NMR spectrum. Primary

Scheme II

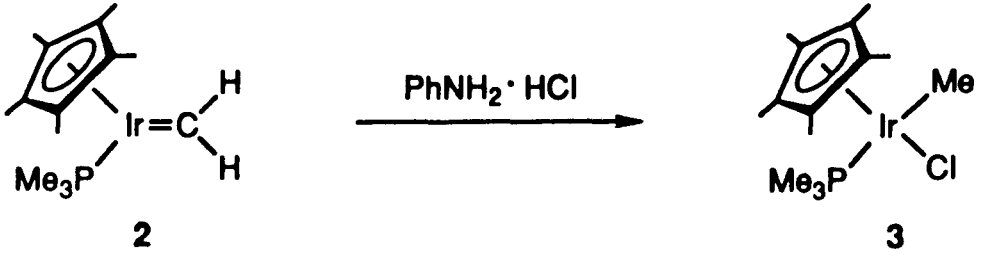

2 3

Scheme III

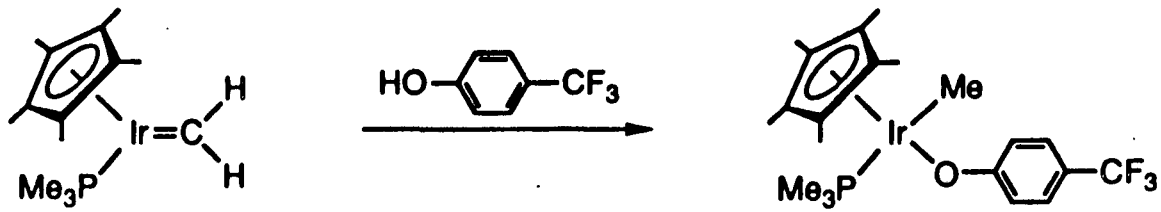

2 4

Scheme IV

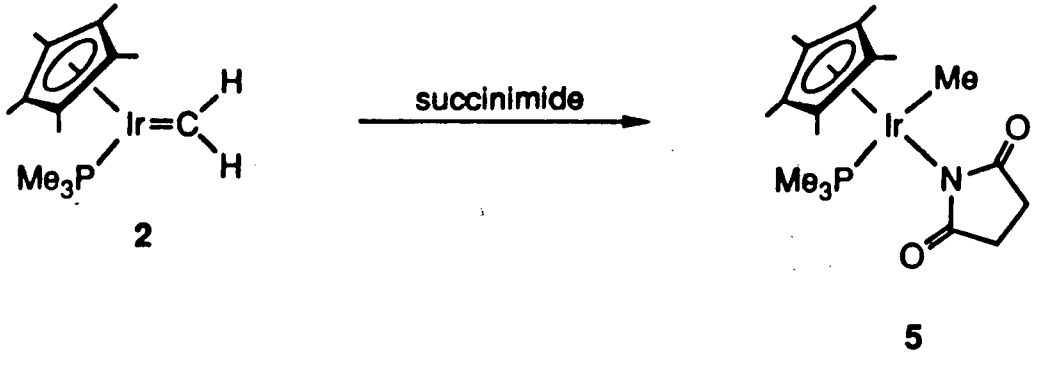

2 **5**

Scheme V

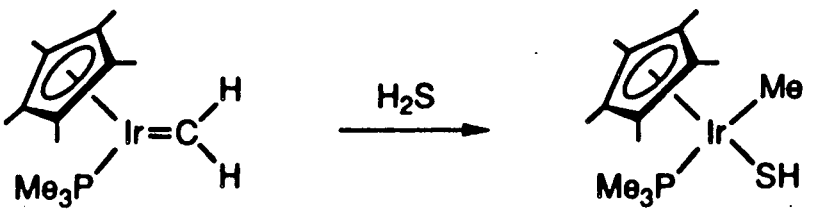

2 **6**

Scheme VI

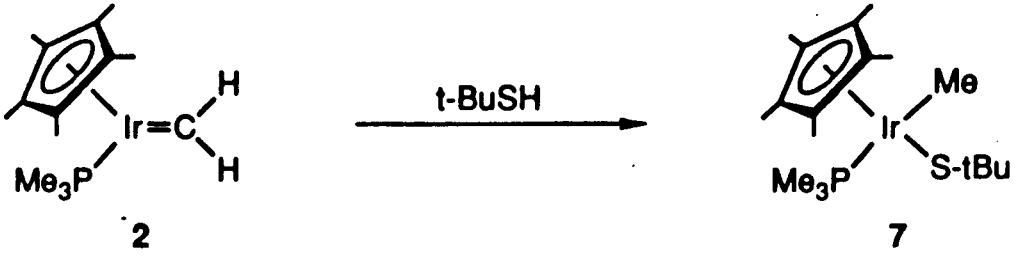

2 7

alcohols also reacted with the methylene complex. These reactions invariably led to the formation of the known[13] (methyl)hydride complex $Cp^*(PMe_3)Ir(Me)H$ (**8**) rather than to methyl alkoxide complexes, even at low temperature. Methanol induced this reaction immediately at -60 °C, presumably giving formaldehyde polymer (not detected) as coproduct (Scheme VII). Benzyl alcohol reacted with **2** over 10 h at -40 °C , leading to the (methyl)hydride **8** and benzaldehyde (95% yield by NMR) (Scheme VIII). A possible mechanism for this transformation is given in Scheme IX. Analogous to the reaction of **2** with other acids, treatment of **2** with the primary alcohol should give either the methyl alkoxide **9a** and/or ion pair **9b**, which could then undergo hydride transfer to give the observed products. No trace of **9**, however, was observed when the reaction was monitored by ^1H NMR spectroscopy.

Reaction of $Cp^*(PMe_3)IrMe_2$ (10) With Organic Acids: Independent Synthesis of Complexes 4 and 5. Reaction of the dimethyl compound $Cp^*(PMe_3)IrMe_2$ (**10**) with relatively strong acids results in the replacement of one of the methyl groups by the conjugate base of the acid used.[14] Thus, treatment of a toluene solution of **8** with α,α,α-trifluoro-p-cresol at -40 °C gave the methyl phenoxide complex $Cp^*(PMe_3)Ir(Me)(O\text{-}C_6H_4\text{-}p\text{-}CF_3)\cdot(HO\text{-}C_6H_4\text{-}p\text{-}CF_3)$ (**4**) (Scheme X), isolated in 44% yield. Reaction of dimethyl complex **10** with succinimide was more sluggish. Heating a solution of **8** in acetone at 130 °C for two days led to the (methyl)succinimate $Cp^*(PMe_3)Ir(Me)[NC(O)CH_2CH_2C(O)]$ (**5**) in 74% isolated yield (Scheme XI).[14]

Reaction of $Cp^*(PMe_3)Ir{=}CH_2$ (2) With Non-protic Reagents. Addition of dihydrogen to a toluene solution of **2** at -40 °C led to a slow reaction (Scheme XII). After two weeks the reaction was complete and the (methyl)hydride **8** was formed in 74% yield (NMR). More interestingly, carbon dioxide reacted slowly with **2** to give the addition product $Cp^*(PMe_3)Ir(CH_2C(O)O)$ (**11**) as yellow crystals in 45% isolated yield (Scheme XIII). The methylene protons shift dramatically upfield in the ^1H NMR spectrum (δ 1.96 and 1.56 ppm), and a C-O stretching band is observed at 1662 cm^{-1} in the IR spectrum. Degradation of **11** with an

Scheme VII

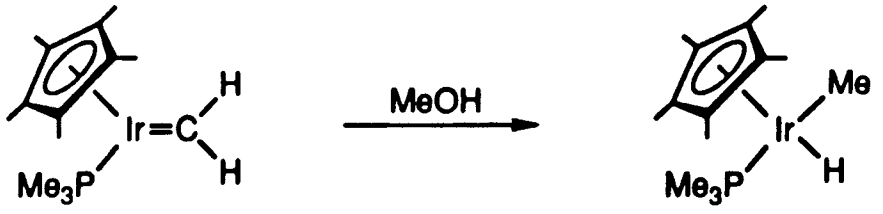

2 **8**

Scheme VIII

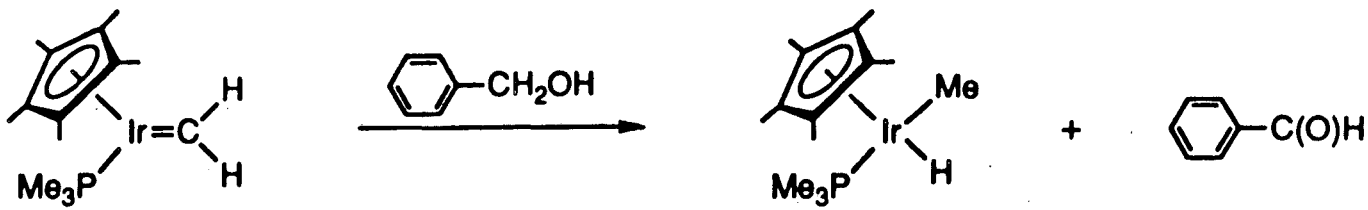

2 **8**

Scheme IX

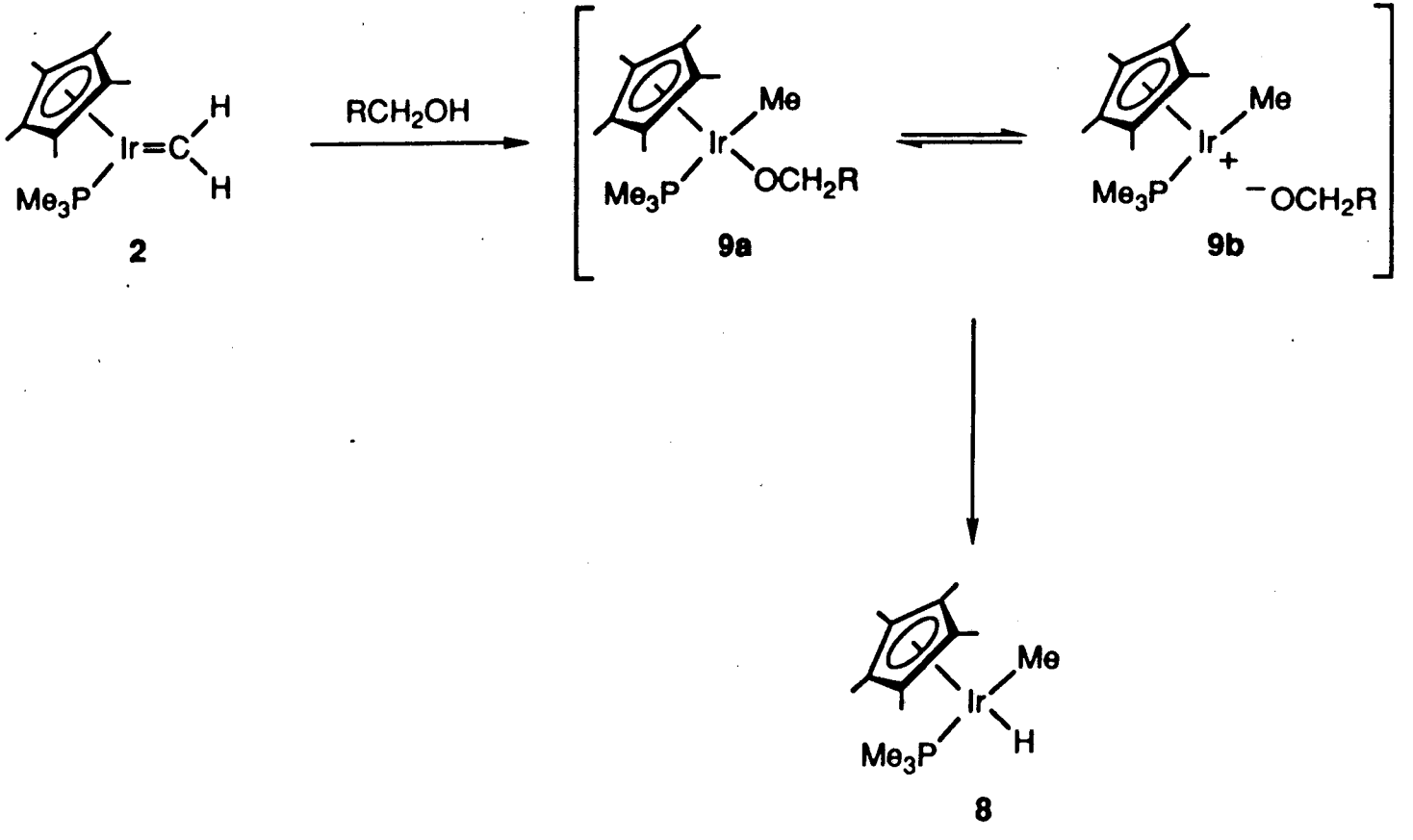
Ir=C
H
H
Me3P
2
RCH2OH
Me
Ir
Me3P
OCH2R
9a
Me
Ir+
Me3P
−OCH2R
9b
Me
Ir
H
Me3P
8

Scheme X

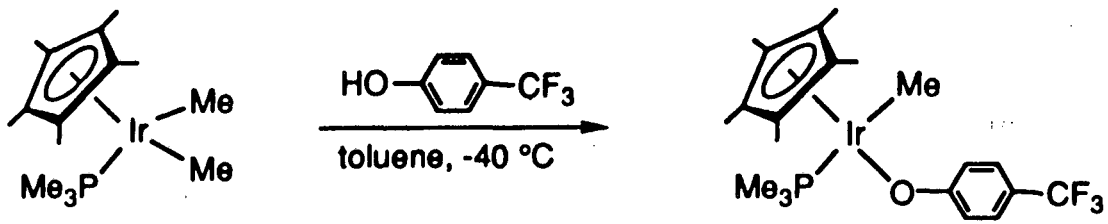

10 **5**

Scheme XI

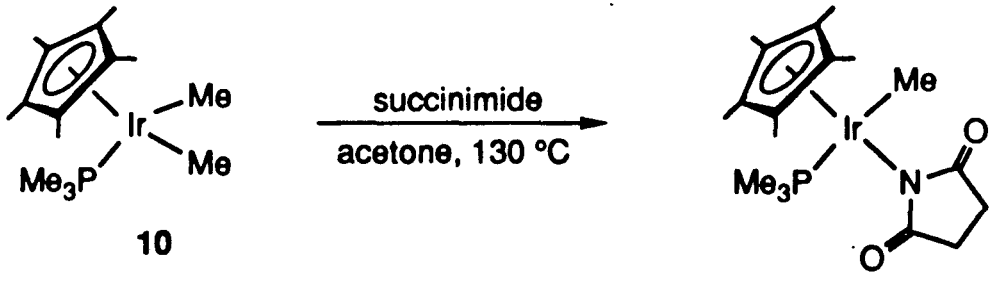

10 **4**

Scheme XII

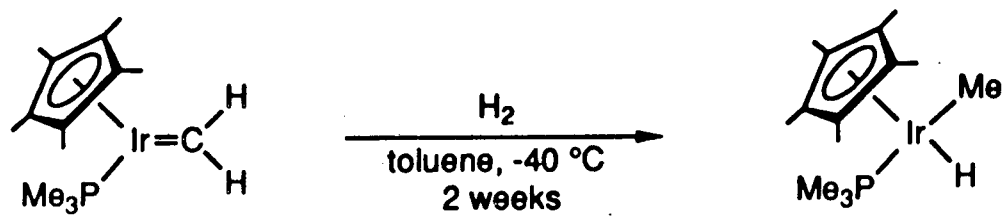

2 **8**

Scheme XIII

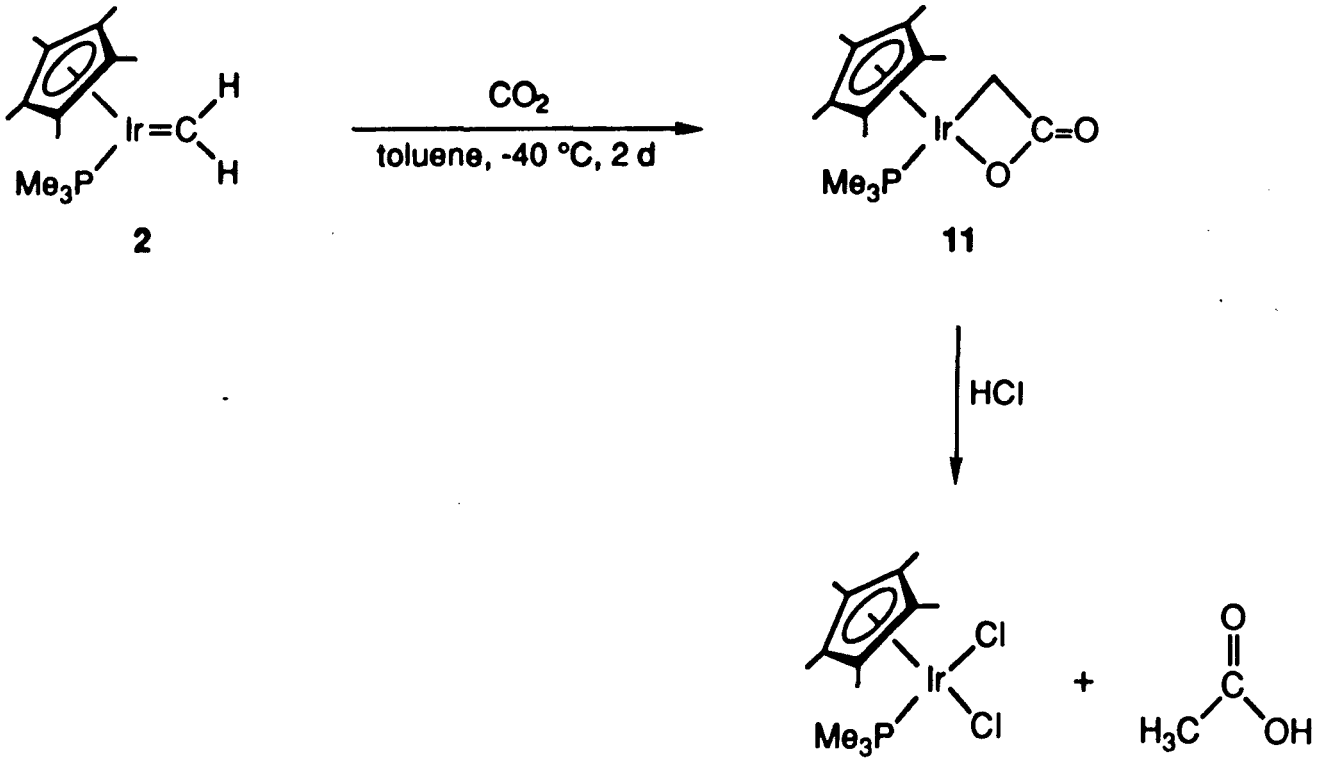
Ir=C
H
H
Me3P
2
CO2
toluene, -40 °C, 2 d
Ir
C=O
O
Me3P
11
HCl
Ir
Cl
Cl
Me3P
+
O
C
H3C
OH

excess of dry HCl in toluene gives the known[15] $Cp^*(PMe_3)IrCl_2$ and one equivalent of acetic acid (as determined by ^1H NMR and GC analysis of the volatile materials).

Discussion

The photoextrusion reaction reported here represents a novel route to late transition-metal alkylidene complexes. It is essentially the reverse of the organic Paterno-Büchi reaction, wherein a photochemical addition of a carbonyl compound and an alkene takes place to form an oxetane.[16] Unfortunately, compound **1** is the only example of a stable late transition-metal 2-oxametallacyclobutane complex yet known and the methodology used to synthesize it (see Chapter 1) does not easily allow analogues of **1** to be made. Until new methodology is developed in this regard, complex **2** will remain the only alkylidene compound in this series we can generate. The related 2-azametallacyclobutane complex $Cp^*(PMe_3)Ir(CH_2CMe_2NH)$[17] and the unsubstituted metallacyclobutane complex $Cp^*(PMe_3)Ir(CH_2CH_2CH_2)$ react photochemically to give only small amounts (<10% yield by NMR) of the methylene complex **2** and large amounts of the dihydride $Cp^*(PMe_3)IrH_2$.[18]

The wide reactivity of the methylene complex $Cp^*(PMe_3)Ir{=}CH_2$ (**2**) toward organic acids shows that the alkylidene carbon is exceptionally basic. Traditionally nucleophilic reactivity at the carbene carbon has been attributed to early transition-metal carbene complexes and electrophilic reactivity to their late transition-metal analogues. However, the complexes on which these comparisons have been based often differ greatly in either molecular charge or the substituents on the carbene carbon. The results reported here affirm that the nucleo- or electrophilicity of a carbene ligand is more dependent upon the substituents on the carbene and the ligands on the metal center than upon the position of the metal in the periodic table.[19]

Experimental

General. For a description of general experimental procedures, see Chapter 1. d^8-toluene was dried over sodium benzophenone ketyl and vacuum transferred prior to use. Aniline hydrochloride ($PhNH_2{\cdot}HCl$) was purchased from Aldrich and recrystallized from ethanol/diethyl ether prior to use. α,α,α-trifluoro-p-cresol was purchased from Aldrich and used as received.

Succinimide was crystallized from ethanol prior to use. *tert*-butanethiol (t-BuSH) was purchased from Aldrich, dried over calcium oxide, and distilled prior to use. Hydrogen sulfide (H_2S) was purchased from Matheson Gas Products and used as received. Methanol was dried over magnesium methoxide and vacuum transferred prior to use. Benzyl alcohol was purified by literature methods.[20] The 2-oxametallcyclobutane complex $Cp^*(PMe_3)Ir(CH_2CMe_2O)$ (**1**) was prepared as described in Chapter 1. The dimethyl complex $Cp^*(PMe_3)IrMe_2$ (**10**) was prepared as described in the literature.[12]

$Cp^*(PMe_3)Ir{=}CH_2$ (2). In the drybox, 7.8 mg (0.016mmol) of $Cp^*(PMe_3)Ir(CH_2CMe_2O)$ and 1 μl of hexamethyldisiloxane were placed in a Wilmad 505-PS 8" NMR tube fitted with a Cajon adaptor. The tube was evacuated on a vacuum line and sealed. Irradiation for 6 h at -68 °C gave a 95% yield of the methylene complex $Cp^*(PMe_3)Ir{=}CH_2$ (**2**) as determined by integration of the Cp^* resonance of **2** in the ^1H NMR spectrum versus the internal standard hexamethyldisiloxane. ^1H NMR (d^8-toluene, -45 °C) δ 14.08 (dd, J = 23.8, 3.3, 1H), 13.08 (dd, J = 3.3, 2.8, 1H), 2.03 (d, J = 1.3 Hz, 15H), 1.34 (d, J = 9.5 Hz, 9H); ^{13}C NMR (d^8-toluene, -45 °C) δ 189.9 (ddd, J = 146.4, 133.8, 15.6 Hz), 92.1(d, J = 1.4 Hz), 20.1 (dq, J = 127.2, 35.8), 11.0 (q, J = 126.3); $^{31}P\{^1H\}$ NMR (d^8-toluene, -40 °C) δ -32.8 (s); IR (d^8-toluene, 25 °C) : 2971, 2955, 2905, 2858, 949 cm^{-1}.

Reaction of $Cp^*(PMe_3)Ir{=}CH_2$ (2) with Aniline Hydrochloride. The methylene complex $Cp^*(PMe_3)Ir{=}CH_2$ (**2**) was generated in 95% yield as described above starting with 6.8 mg (0.014 mmol) of metallacycle **1**. An acetone solution of 1.85 mg (0.014 mmol) of aniline hydrochloride was added to the toluene solution of **2** at -40 °C with rapid stirring. After 5 min, the volatile materials were removed under vacuum. Chromatography on silica gel gave 5.2 mg (0.010 mmol, 71%) of the (methyl)chloride $Cp^*(PMe_3)Ir(CH_3)Cl$ (**3**) as a yellow powder. ^1H NMR (d^6-benzene) δ 1.48 (d, J = 1.8 Hz, 15 H), 1.17 (d, J = 10.3 Hz, 9H), 1.09 (d, J = 6.9 Hz). [Lit.[13] ^1H NMR (C_6D_6) δ 1.47 (d, J = 1.9 Hz, 15 H), 1.17 (d, J = 10.3 Hz, 9H), 1.08 (d, J = 7.0 Hz, 3H)].

$Cp^*(PMe_3)Ir(Me)(O\text{-}C_6H_4\text{-}p\text{-}CF_3)$ (4). In the drybox, 53.0 mg (0.12 mmol) of $Cp^*(PMe_3)IrMe_2$ (**10**) was placed in a vial equipped with a magnetic stirbar and cooled to -40 °C. In a separate vial, 19.8 mg (0.12 mmol) of α,α,α-trifluoro-p-cresol was dissolved in 1 ml of toluene

and cooled to -40 °C. After removal from the freezer, the toluene solution of α,α,α-trifluoro-p-cresol was immediately added dropwise to the toluene solution of **10** with rapid stirring. The mixture was allowed to warm to box temperature and, after stirring an additional 10 min at box temperature, the volatile materials were removed under vacuum to afford a green oil. The crude product was dissolved in pentane, filtered through celite, and crystallized at -40 °C to give 40.0 mg (0.05 mmol, 44%) of **4**. ^{1}H NMR (d^6-benzene) δ 7.46 (d, J = 8.8 Hz, 2H), 6.71 (d, J = 8.8 Hz, 2H),1.33 (d, J = 2.0 Hz, 15H), 0.96 (d, J = 6.8 Hz, 3H), 0.94 (d, J = 10.0 Hz, 9H); ^{13}C {^{1}H} NMR (d^6-benzene) δ 173.1 (s), 126.4 (s), 120.4 (s), 118.6 (q, J = 293.6), 115.0 (q, J = 31.6), 89.8 (d, J = 3.3 Hz), 13.6 (d, J = 36.3 Hz), 9.0 (s), -10.7 (d, J = 10.5 Hz); ^{31}P {^{1}H} NMR (d^6-benzene) δ -29.5 (s); Ir(KBr pellet): 2915, 2891, 1604, 1322, 1291, 1277, 1157, 1113, 1098, 1063, 952 cm^{-1}; MS(EI): m/e 580/578 (M^+, ^{193}Ir/^{191}Ir); Anal. Calcd. for $C_{28}H_{36}F_6IrO_2P$ (compound **4** crystallizes with one equiv. of α,α,α-trifluoro-p-cresol, confirmed by ^{1}H NMR): C, 45.34%; H, 4.89%. Found C, 45.66%; H, 4.93%; mp, 110-113 °C (dec).

Reaction of $Cp^*(PMe_3)Ir{=}CH_2$ (2) with α,α,α-trifluoro-p-cresol. The methylene complex $Cp^*(PMe_3)Ir{=}CH_2$ (**2**) was generated in 80% yield as described above starting with 9.0 mg (0.019 mmol) of metallacycle **1**. A toluene solution of 2.4 mg (0.015 mmol) of α,α,α-trifluoro-p-cresol was added to the d^8-toluene solution of **2** at -40 °C with rapid stirring. After 5 min, the volatile materials were removed under vacuum to give 7.4 mg (0.013 mmol, 85%) of **4** as a yellow oil. The residue was extracted into d^6-benzene and filtered to afford an NMR sample. The material produced in this reaction was identical to **4** described above and found to be at least 95% pure by ^{1}H NMR spectroscopy.

$Cp^*(PMe_3)Ir(Me)[NC(O)CH_2CH_2C(O)]$ (5). In the drybox, 48.2 mg (0.11 mmol) of $Cp^*(PMe_3)IrMe_2$ (**10**) and 11.0 mg (0.11 mmol) of succinimide were dissolved in 1 ml d^6-acetone and placed in a Wilmad 505-PS 8" NMR tube fitted with a Cajon adaptor. After freezing the solution, the tube was evacuated on a vacuum line and sealed. The NMR tube was then placed in a stainless steel tube with approximately 1 ml of acetone and sealed with a threaded plug equipped with a pressure relief valve. The stainless steel tube was then placed in a 130 °C

constant temperature bath for 2 d. The NMR tube was returned to the drybox and the volatile materials were removed under vacuum to afford a yellow powder. The crude product was dissolved in pentane, filtered through celite, and crystallized at -40 °C to give 42.7 mg (0.08 mmol, 74%) of **5**. ^{1}H NMR (d^8-toluene, -40 °C) δ 2.21(m, 4H), 1.48 (d, J = 1.9 Hz, 15H), 1.17 (d, J = 10.2 Hz, 9H), 0.94 (d, J = 7.4 Hz, 3H); ^{13}C {^{1}H} NMR (d^8-toluene, -40 °C) δ 189.2 (s), 187.2 (s), 90.4 (d, J = 3.0 Hz), 32.4 (s), 30.6 (s), 14.4 (d, J = 37.0 Hz), 9.1 (s), -20.6 (d, J = 10.4); ^{31}P {^{1}H} NMR (d^8-toluene) δ -36.2 (s); IR (KBr pellet) : 2918, 1650, 967 cm^{-1}; High resolution mass spectrum (EI), m/e calcd for $C_{18}H_{31}NO_2PIr$: 517.1723/515.1699 (M^+, ^{193}Ir/^{191}Ir); m/e found 517.1718/515.1697 (M^+, ^{193}Ir/^{191}Ir, deviation = -0.8/-0.3 ppm); mp, 168-170 °C.

Reaction of Cp*(PMe$_3$)Ir=CH$_2$ (2) with Succinimide. The methylene complex Cp*(PMe$_3$)Ir=CH$_2$ (**2**) was generated as described above starting with 17.1 mg (0.036 mmol) of metallacycle **1**. An acetone solution of 3.6 mg (0.036 mmol) of succinimide was added to the d^8-toluene solution of **2** at -40 °C with rapid stirring. After 30 min, the volatile materials were removed under vacuum. The crude product was extracted into pentane, filtered through celite, and dried under vacuum to give 14.3 mg (0.028 mmol, 77%) of **5** as a yellow powder. The material produced in this reaction was identical to **5** described above and found to be at least 95% pure by ^{1}H NMR spectroscopy.

Reaction of Cp*(PMe$_3$)Ir=CH$_2$ (2) with Hydrogen Sulfide. The methylene complex Cp*(PMe$_3$)Ir=CH$_2$ (**2**) was generated using a modification of the procedure described above, starting with 8.0 mg (0.017 mmol) of metallacycle **1**. The NMR tube was left on the Cajon adapter during photolysis and after irradiation for 6 h, the tube was transferred to a high vacuum line. From a known-volume bulb, 2 equiv H_2S (110 torr, 5.72 ml at 298K, 0.034 mmol) was condensed into the solution at -196 °C. The solution was thawed and placed in a constant temperature bath held at -45 °C for 2 h. The NMR tube was returned to the drybox and the volatile materials were removed under vacuum to give 5.8 mg (0.013 mmol, 76 %) of the (thiol)methyl complex Cp*(PMe$_3$)Ir(SH)Me (**6**) as a yellow powder. This material was identical to that described in Chapter 3 and was found to be at least 95% pure by ^{1}H NMR spectroscopy. ^{1}H NMR (d^6-

benzene) δ 1.55 (d, J = 1.9 Hz, 15H), 1.17 (d, J = 10.0 Hz, 9H), 0.66 (d, J = 6.3 Hz, 3H), -2.57 (d, J = 4.4 Hz, 1H).

Reaction of $Cp^*(PMe_3)Ir=CH_2$ (2) with *tert*-butanethiol. The methylene complex $Cp^*(PMe_3)Ir=CH_2$ (2) was generated using a modification of the procedure described above, starting with 22.1 mg (0.047 mmol) of metallacycle **1**. The NMR tube was left on the Cajon adapter during photolysis. After irradiation for 6 h, the NMR tube was transferred to a high vacuum line. From a known-volume bulb, 1.25 equiv t-BuSH (40 torr, 28.36 ml at 298K, 0.060 mmol) was condensed into the solution at -196 °C. The solution was thawed and placed in a constant temperature bath held at -45 °C for 4 h. The NMR tube was returned to the drybox and the volatile materials were removed under vacuum to give 20.2 mg (0.039 mmol, 85%) of the (*tert*-butylthiolate)methyl complex $Cp^*(PMe_3)Ir(S\text{-}tBu)Me$ (**7**) as a yellow oil. We have been unable to isolate pure **7**, but the material produced in this reaction was found to be approximately 90% pure by ^1H NMR spectroscopy. Spectroscopic data for **7**: ^1H NMR (d^6-benzene) δ 1.61 (s, 9H), 1.54 (d, J = 2.0 Hz, 15H), 1.26 (d, J = 10.1 Hz, 9H), 0.84 (d, J = 6.7, 3H); $^{13}C\{^1H\}$ NMR (d^6-benzene) δ 92.6 (d, J = 3.8 Hz), 37.4(s), 37.1 (s), 13.7 (d, J = 40.0 Hz), 8.8 (s), -30.0 (d, J = 10.3); $^{31}P\{^1H\}$ NMR (d^6-benzene) δ -34.6 (s); IR (d^6-benzene) : 2960, 2910, 2856, 952 cm^{-1}.

Reaction of $Cp^*(PMe_3)Ir=CH_2$ (2) with Methanol. The methylene complex $Cp^*(PMe_3)Ir=CH_2$ (2) was generated using a modification of the procedure described above, starting with 5.0 mg (0.010 mmol) of metallacycle **1**. The NMR tube was left on the Cajon adapter during photolysis. After irradiation for 8 h, the NMR tube was transferred to a high vacuum line. From a known-volume bulb, 2 equiv MeOH (68 torr, 5.72 ml at 298K, 0.020 mmol) was condensed into the solution at -196 °C. The solution was thawed and placed in a constant temperature bath held at -40 °C for 1 h. The NMR tube was returned to the drybox and the volatile materials were removed under vacuum to give 3.9 mg (0.009 mmol, 88 %) of the (methyl)hydride complex $Cp^*(PMe_3)Ir(Me)H$ (**8**) as a pale yellow oil, judged to be greater than 95% pure by ^1H NMR spectroscopy. ^1H NMR (d^6-benzene) δ 1.86 (d, J = 2.2 Hz, 15H), 1.22 (d, J = 10.0 Hz, 9H), 0.70

(d, J = 7.0 Hz, 3H), -17.22 (d, J = 35.9 Hz, 1H). [Lit.[13] ^{1}H NMR (d^6-benzene) δ 1.87 (d, J = 2.0 Hz, 15H), 1.22 (d, J = 9.8 Hz, 9H), 0.71 (d, J = 7.0 Hz, 3H), -17.22 (d, J = 35.9 Hz, 1H)].

Reaction of $Cp^*(PMe_3)Ir{=}CH_2$ (2) with Benzyl Alcohol. The methylene complex $Cp^*(PMe_3)Ir{=}CH_2$ (2) was generated as described above starting with 7.4 mg (0.016 mmol) of metallacycle **1** and 3 μl of hexamethyldisiloxane as internal standard. After irradiation, the NMR tube was warmed to room temperature, returned to the drybox, opened, and 1.7 μl of benzyl alcohol was added. The tube was quickly refitted with a Cajon adapter, removed from the drybox, and sealed under vacuum. The sealed tube was placed in a constant temperature bath held at -40 °C for 10 h. Analysis of the reaction mixture by ^{1}H NMR spectroscopy showed that $Cp^*(PMe_3)Ir(Me)H$ (**8**) was produced in quantitative yield while benzaldehyde was produced in 95% yield.

Reaction of $Cp^*(PMe_3)Ir{=}CH_2$ (2) with Dihydrogen. The methylene complex $Cp^*(PMe_3)Ir{=}CH_2$ (2) was generated using a modification of the procedure described above, starting with 24.0 mg (0.051 mmol) of metallacycle **1** and 3 μl of hexamethyldisiloxane as internal standard. The NMR tube was left on the Cajon adapter during photolysis. After irradiation for 8 h, the NMR tube was transferred to a high vacuum line. Approximately 600 torr of H_2 was placed above the solution and the NMR tube was sealed. The NMR tube was placed in a constant temperature bath held at -40 °C for 2 wk. Analysis of the reaction mixture by ^{1}H NMR spectroscopy showed that $Cp^*(PMe_3)Ir(Me)H$ (**8**) was produced in 70% yield.

$Cp^*(PMe_3)Ir(CH_2C(O)O)$ (11). The methylene complex $Cp^*(PMe_3)Ir{=}CH_2$ (2) was generated using a modification of the procedure described above, starting with 30.0 mg (0.063 mmol) of metallacycle **1**. After irradiation for 8 h, the NMR tube was transferred to a high vacuum line. Approximately 600 torr of CO_2 was placed above the solution and the NMR tube was sealed. The NMR tube was placed in a constant temperature bath held at -45 °C for 3 d and then returned to the drybox where the volatile materials were removed under vacuum. The product was extracted into toluene, filtered through celite, and crystallized at -40 °C by slow diffusion of hexamethyldisiloxane into the toluene solution, giving 13.0 mg (0.028 mmol, 45%) of **11** as

yellow crystals. ^{1}H NMR (d^{8}-toluene) δ 1.96 (dd, J = 13.2, 3.0, 1H), 1.56 (dd, J = 13.2, 9.7, 1H), 1.46 (d, J = 1.7 Hz, 15H), 1.05 (d, J = 10.0 Hz, 9H); ^{13}C {^{1}H} NMR (d^{8}-toluene) δ 185.0 (s), 90.3 (d, J = 3.6 Hz), 14.1(d, J = 35.7 Hz), 9.2 (s), -0.6 (d, J = 6.0 Hz); ^{31}P {^{1}H} NMR (d^{8}-toluene) δ -30.5 (s); IR (KBr pellet) : 2975, 2956, 2907, 1662, 946 cm^{-1}; High resolution mass spectrum (FAB), m/e calcd. for $C_{15}H_{27}O_{2}PIr$: 463.1378/461.1355 (MH^{+}, $^{193}Ir/^{191}Ir$); m/e found 463.1387/461.1367 (MH^{+}, $^{193}Ir/^{191}Ir$, deviation = -0.9/-1.2 ppm).

Reaction of Complex 11 with HCl. In the drybox, 0.9 mg (0.002 mmol) of **11** was dissolved in 0.5 ml d^{8}-toluene and loaded into an NMR tube. The tube was sealed with a rubber septum and removed from the drybox. After cooling to -77 °C, 120 μl (0.005 mmol) of dry HCl was added *via* gas tight syringe. Analysis by ^{1}H NMR spectroscopy showed the formation of $Cp^{*}(PMe_{3})IrCl_{2}$ (quantitative) and acetic acid (96%). The volatile materials were removed under vacuum and analysis by GC confirmed the formation of 1 equiv of acetic acid in this reaction.

References

1. (a) Dragutan, V.; Balaban, A. T.; Dimonie, M. *Olefin Metathesis and Ring-Opening Polymerization of Cyclo-Olefins*, 2nd edition; Wiley-Interscience, New York, 1985. (b) Ivin, K. J. *Olefin Metathesis*; Academic Press: New York, 1983.
2. See Herrmann, W. A. *Angew. Chem. Int. Ed. Engl.* **1982**, *21*, 117, and references therein.
3. Fischer, E. O.; Maasböl, A. *Angew. Chem. Int. Ed. Engl.* **1964**, *3*, 580.
4. (a) Casey, C. P.; Burkhardt, T. J. *J. Am. Chem. Soc.* **1973**, *95*, 5833. (b) Sanders, A.; Cohen, L.; Giering, W. P.; Kenedy, D.; Magatti, C. V. *J. Am. Chem. Soc.* **1973**, *95*, 5431.
5. Schrock, R. R. *J. Am. Chem. Soc.* **1974**, *96*, 6796.
6. Schrock, R. R. *J. Am. Chem. Soc.* **1975**, *97*, 6577.
7. For reviews see: (a) Fischer, E. O. *Adv. Organometal. Chem.*, **1976**, *14*, 1. (b) Schrock, R. R. *Acc. Chem. Rev.*, **1979**, *12*, 98. (c) Schrock, R. R. *Science*, **1983**, *219*, 13. (d) Gallop, M. A.; Roper, W. R. *Adv. Organometal. Chem.*, **1986**, *25*, 121.
8. (a) Fryzuk, M. D.; MacNeil, P. A.; Rettig, S. J. *J. Am. Chem. Soc.* **1985**, *107*, 6708. (b) Clark, G. R.; Roper, W. R.; Wright, A. H. *J. Organomet. Chem.* **1984**, *273*, C17. (c) Empsall, H. D.; Hyde, E. M.; Markham, R.; McDonald, W. S.; Norton, M. C.; Shaw, B. L.; Weeks, B. *J. Chem. Soc., Chem. Commun.*, **1977**, 589. (d) Mango, F. D.; Dvoretzky, I. *J. Am. Chem. Soc.* **1965**, *88*, 1654.
9. For some specific examples, see: (a) Herrmann, W. A.; Kruger, C.; Goddard, R.; Bernal, I. *Angew. Chem. Int. Ed. Engl.*, **1977**, *16*, 334. (b) Herrmann, W. A.; Kruger, C.; Goddard, R.; Bernal, I. *J. Organomet. Chem.*, **1977**, *140*, 73. (c) Herrmann, W. A. *Chem. Ber.*, **1978**, *111*, 1077. (d) Theopold, K. H.; Bergman, R. G. *J. Am. Chem. Soc.*, **1981**, *103*, 2489. (e) Vasquez de Miguel, A.; Isobe, K.; Taylor, B. F.; Nutton, A.; Maitlis, P. M. *J. Chem. Soc., Chem. Commun.*, **1982**, 758.
10. The synthesis and other reactions of this complex are reported in Chapter 1.

11. Herrmann, W. A. *Adv. Organometal. Chem.*, **1982**, *20*, 159 and references cited therein.

12. Buchanan, J. M.; Stryker, J. M.; Bergman, R. G. *J. Am. Chem. Soc.* **1986**, *108*, 1537.

13. Wax, M. J.; Stryker, J. M.; Buchanan, J. M.; Kovac, C. A.; Bergman, R. G. *J. Am. Chem. Soc.*, **1984**, *106*, 1121.

14. Dr. Jeffrey C. Hayes, unpublished results.

15. Isobe, K.; Bailey, P. M.; Maitlis, P. M. *J. Chem. Soc., Dalton Trans.*, **1981**, 2003.

16. (a) Paterno, E.; Chieffi, G. *Gazz. Chim. Ital.* **1909**, *39*, 341. (b) Büchi, G.; Inman, C. G.; Lipinsky, E. S. *J. Am. Chem. Soc.*, **1954**, *76*, 4327. For reviews, see (c) Coyle, J. D. *Chem. Soc. Rev.* **1974**, *3*, 329. (d) Coyle, J. D.; Carless, H. A. J. *Chem. Soc. Rev.* **1972**, *1*, 465. (e) Arnold, D. R. *Adv. Photochem.* **1968**, *6*, 301.

17. The synthesis and reactivity of this molecule are discussed in Chapter 1.

18. William D. McGhee, unpublished results.

19. For an excellent discussion on the reactivity patterns of transition metal carbene complexes, see ref. 7d.

20. Perrin, D. D.; Armarego, W. L. F.; Perrin, D. R. *Purification of Laboratory Chemicals*; Pergamon Press, New York, 1966.

Chapter 3

Synthesis and Reactivity of (Pentamethylcyclopentadienyl)Iridium and Rhodium Thiolate Complexes

Introduction

The behavior of transition metal complexes with metal-sulfur bonds is potentially relevant to the mechanism of hydrodesulfurization (HDS),[1] one of the most important modern industrial heterogeneous catalytic processes.[1g] Binary sulfides of most of the transition metals show at least some activity in this regard. The degree of activity shows periodic trends, with the highest activity observed for osmium, ruthenium, iridium, and rhodium.[1c]

Thiophene, benzothiophene, and dibenzothiophene have been used as standards for measuring HDS catalyst activity, as these types of compounds are the main sulfur-containing contaminants in most hydrocarbon feedstocks that are processed. Much of the debate on the mechanism of HDS is focused on the initial mode of binding of these substrates to the catalyst surface, which could initially occur through a metal-sulfur interaction or by π-complexation to the metal center. Theoretical studies and the lack of stable π-thiophene complexes of the transition metals before 1985 seemed to favor initial sulfur coordination. Recently, however, several π-thiophene complexes of highly HDS-active metals have been synthesized.[2]

In contrast to the large number of solid materials and polynuclear complexes containing metal-sulfur bonds that are known, mononuclear organometallic thiol (M-SH) and thiolate (M-SR) complexes (especially those involving late transition metals) are relatively rare.[3,4] Consequently, little is yet known about the detailed reactivity of these functionalities. The majority of the reactivity reported thus far for these species involves protonation and alkylation of the sulfur ligand[4d,5] and the formation of μ-thiolato heterobimetallic complexes.[3g,4e] Reaction with highly activated alkynes has also been reported.[4g,6]

In this chapter, the synthesis of a series of iridium and rhodium mono- and bis-thiolate complexes is discussed. The X-ray crystal structures of several of these materials are presented, including only the fourth crystallographically characterized metalladithiol, as well as a preliminary investigation of the reactivity of these species.

Results

Photolysis of $Cp^*(PMe_3)IrH_2$ (1) in *tert*-butylthiol and Di-*tert*-butyldisulfide. Photolysis of the dihydride **1** in neat t-BuSH at 5 °C leads to greater than 95% disappearance of **1** in less than six hours, as monitored by $^{31}P\{^1H\}$ NMR spectroscopy. This is in marked contrast to the photolysis of **1** in *tert*-butylamine or *tert*-butanol. Under similar conditions, these substrates require on the order of 18 hours to approach 90% conversion of the starting dihydride (see Chapter 1). Removal of t-BuSH leaves a yellow solid. Analysis of this material by ^1H NMR spectroscopy reveals four new complexes, one of which shows a characteristic iridium-hydride doublet at high field (δ -16.47, J_{P-H} = 35.1 Hz). Subsequent syntheses have established the identity of these complexes as $Cp^*(PMe_3)Ir(S\text{-}tBu)H$ (**2**), $Cp^*(PMe_3)Ir(S\text{-}tBu)_2$ (**3**), $Cp^*(PMe_3)Ir(S\text{-}tBu)(SH)$ (**4**), and $Cp^*(PMe_3)Ir(SH)_2$ (**5**) (Scheme I). At early conversion (less than two hours), approximately 40% of the dihydride remained and complexes **2** and **4** were produced in equal amounts. Only a trace of complexes **3** and **5** were observed. Further irradiation of the sample led to a decrease of both the dihydride **1** and the (*tert*-butylthiolate)hydride **2** and an increase in the amount of the bis-thiolates **4** and **5**. Again, only a trace of complex **3** was observed. To the limits of detection (<5%), none of the alkyl hydride complex $Cp^*(PMe_3)Ir(CH_2CMe_2SH)H$ was formed.

The formation of the (*tert*-butylthiolate)hydride **2** can be explained in two ways. Oxidative addition of the S-H bond of t-BuSH to the unsaturated intermediate $[Cp^*(PMe_3)Ir]$[7] would lead to complex **2**. The absence of the alkyl hydride complex $Cp^*(PMe_3)Ir(CH_2CMe_2SH)H$ could be explained by comparing the S-H bond strength of t-BuSH (88.6 kcal/mole)[8] with those of typical sp^3 C-H bonds (~100 kcal/mole).[9] Formation of **2**, however, would also be consistent with attack of **1** by *tert*-butylthiyl radical.[10]

The formation of bis-thiolate products supports the existence of a radical pathway, one possible route to these materials is shown in Scheme II. *tert*-butylthiyl radical could abstract hydride from initially formed (*tert*-butylthiolate)hydride **2**. The organometallic radical formed could then be trapped by a second *tert*-butylthiyl radical to give the bis-(*tert*-butylthiolate) $Cp^*(PMe_3)Ir(S\text{-}tBu)_2$ (**3**). Photochemical cleavage of one or both of the carbon-sulfur bonds of

Scheme I

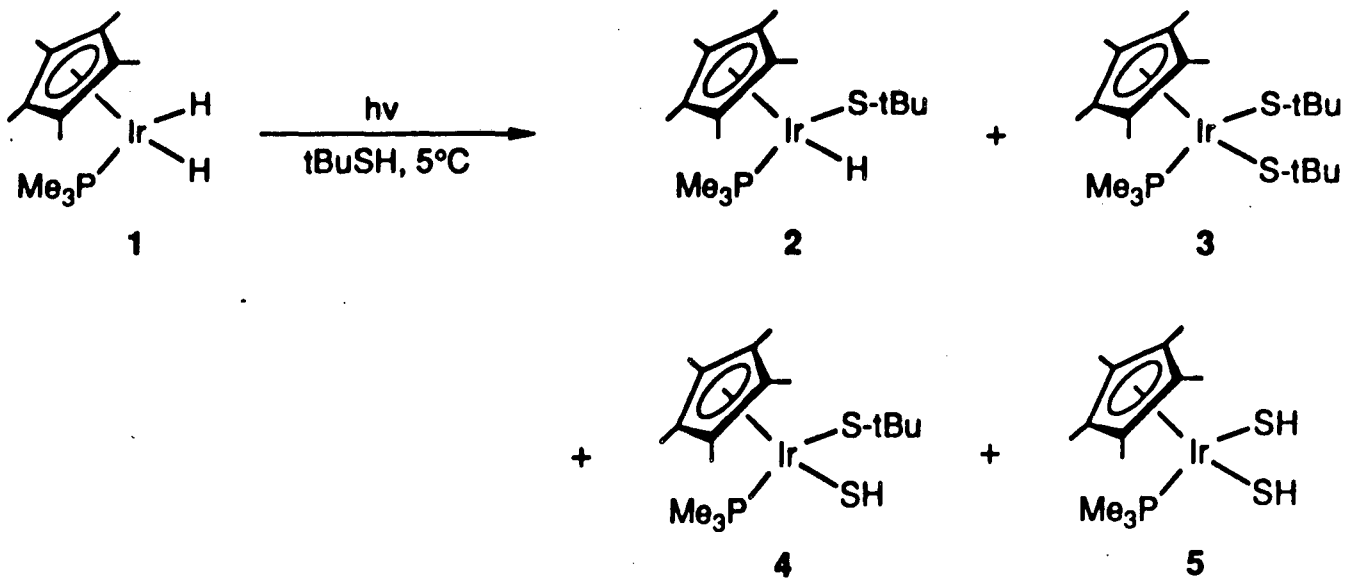

Scheme II

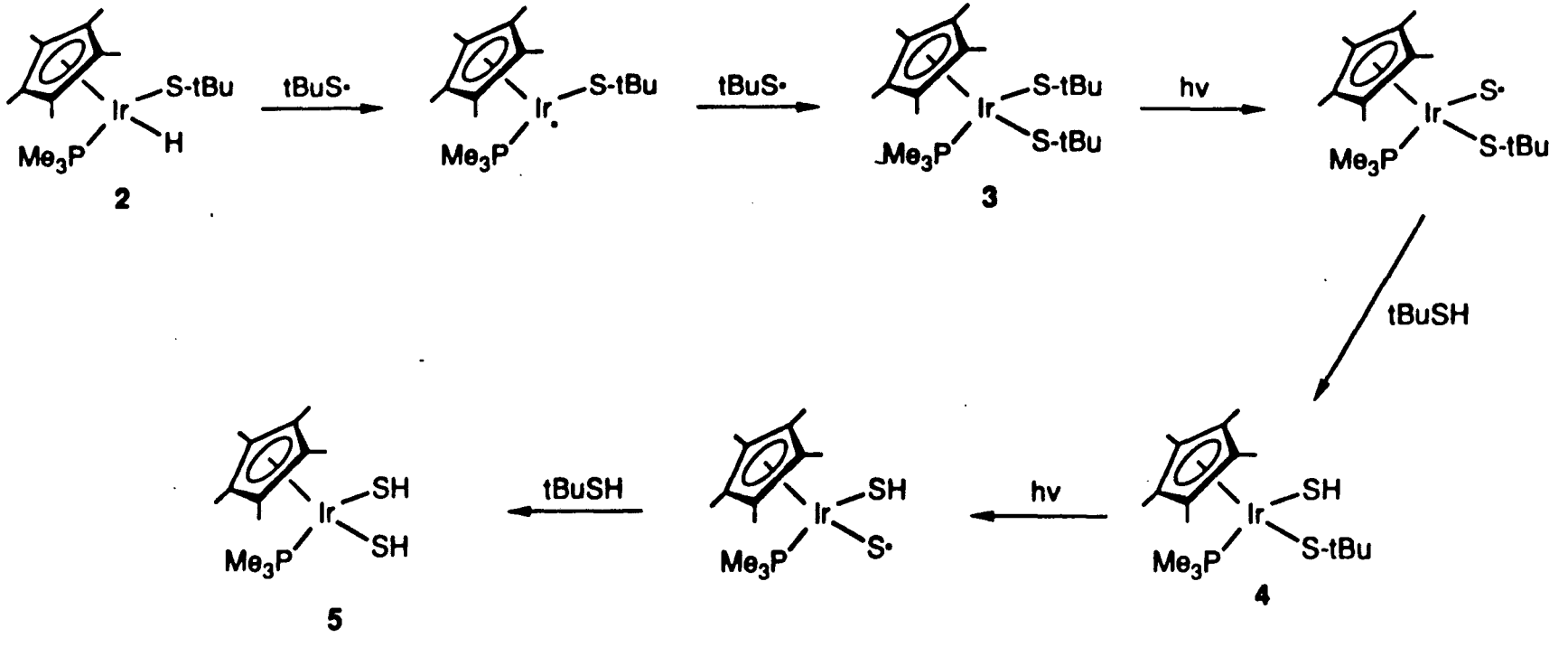
S-tBu
tBuS·
Ir
Me3P
H
2
S-tBu
tBuS·
3
hv
S·
tBuSH
4
SH
S-tBu
hv
S·
tBuSH
5
SH
SH

the bis-(*tert*-butylthiolate), followed by hydrogen abstraction from t-BuSH, would lead to the bis-thiolate products **4** and **5**. Photolysis of a sample of **3** and two equivalents of t-BuSH in d^6-benzene gave some of the (*tert*-butylthiolate)thiol complex **4** and isobutane. Recent work by Dr. Christian Schade of these laboratories has shown that photolysis of the dimethyl complex $Cp^*(PMe_3)Ir(Me)_2$ in the presence of *tert*-butylthiol leads to production of $Cp^*(PMe_3)Ir(S\text{-}tBu)Me$,[11] consistent with the operation of a radical process in this system as well.

More evidence supporting a radical pathway for this reaction is found by performing the photolysis of the dihydride **1** in di-*tert*-butyldisulfide. Irradiation of a sample of **1** in neat di-*tert*-butyldisulfide at 5 °C led to the formation of the same four products observed upon photolysis of **1** in t-BuSH (Scheme III). Disappearance of the dihydride was faster (>95% conversion in less than four hours) and more of the bis-(*tert*-butylthiolate) **3** was observed. We are uncertain which species is absorbing the light in this reaction, but di-*tert*-butyldisulfide has been shown to generate t-butylthiyl radicals upon irradiation by ultraviolet light.[12] Although formation of the bis-thiolate products could be explained by initial oxidative addition of the sulfur-sulfur bond of di-*tert*-butyldisulfide to the unsaturated intermediate $[Cp^*(PMe_3)Ir]$, the formation of the (*tert*-butylthiolate)hydride in this reaction is more consistent with the proposed radical pathway. We cannot rule out the possibility, however, that both oxidative addition and radical pathways are operating in these reactions.

Exchange Reactions of $Cp^*(PMe_3)Ir(OEt)H$ (6) with Organic Thiols: Synthesis of $Cp^*(PMe_3)Ir(SR)H$; R = H (8), R = Me (9), and R = tBu (2). Having formed a stable iridium thiolate hydride in the photochemical experiments described above, a rational route to these types of complexes was sought. It has been shown that the (ethoxy)hydride $Cp^*(PPh_3)Ir(OEt)H$ undergoes efficient exchange reactions with acids stronger than ethanol.[13] Thus, we guessed that reaction of the PMe_3-substituted (ethoxy)hydride $Cp^*(PMe_3)Ir(OEt)H$ (**6**) with organic thiols (RSH) would give the corresponding thiolate hydrides $Cp^*(PMe_3)Ir(SR)H$.

Scheme III

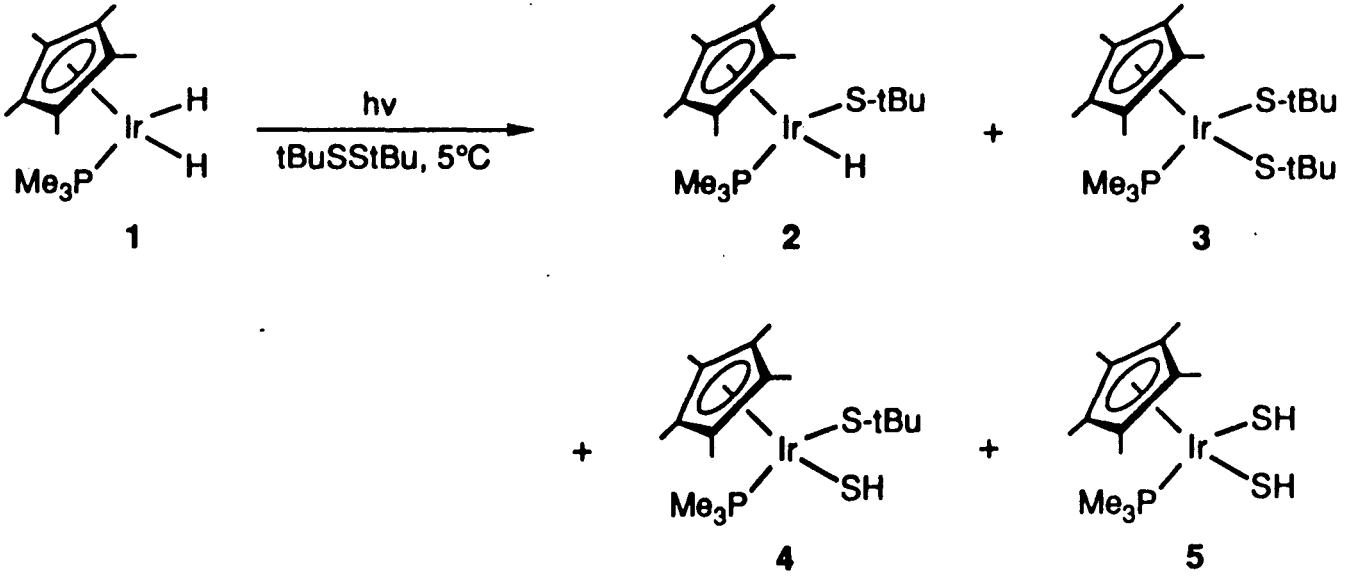
H
Ir
H
Me3P
1
hv
tBuSStBu, 5°C
S-tBu
Ir
H
Me3P
2
+
S-tBu
Ir
S-tBu
Me3P
3
+
S-tBu
Ir
SH
Me3P
4
+
SH
Ir
SH
Me3P
5

Treatment of the dichloride $Cp^*(PMe_3)IrCl_2$[14] (**7**) with two equivalents of sodium ethoxide in ethanol gave the iridium (ethoxy)hydride $Cp^*(PMe_3)Ir(OEt)H$ (**6**).[15] Unlike its PPh_3-substituted analogue, which can be purified,[13] we have been unable to separate this complex from small amounts of the (hydrido)chloride $Cp^*(PMe_3)Ir(H)(Cl)$[14] and/or dihydride $Cp^*(PMe_3)IrH_2$[7,14] that also form in the reaction. However, treatment of crude (ethoxy)hydride **6** with H_2S, methanethiol, or *tert*-butanethiol in benzene led to the rapid formation of $Cp^*(PMe_3)Ir(SH)H$ (**8**), $Cp^*(PMe_3)Ir(SMe)H$ (**9**), and $Cp^*(PMe_3)Ir(S\text{-}tBu)H$ (**2**), respectively (Scheme IV). Complex **8** is extremely air-sensitive in the solid state. Samples exposed to air darkened within minutes. Complex **9** is moderately air-stable, while **2** seems indefinitely stable in air. All three complexes can be isolated in pure form (60-80% yield) and fully characterized, and show characteristic hydride doublets at high field in the ^1H NMR spectrum and iridium-hydride stretches in the infrared spectrum (Table I). The (thiol)hydride **8** also shows a doublet of doublets at δ -2.18 ppm ($J_{P\text{-}H}$ = 4.6 Hz, $J_{H\text{-}H}$ = 1.8 Hz) for the thiol proton in the ^1H NMR spectrum (Figure I) and a weak S-H stretch at 2524 cm^{-1} in the infrared spectrum.

A single crystal X-ray diffraction study of (*tert*-butylthiolate)hydride **2** was performed by Dr. F. J. Hollander of the U.C. Berkeley College of Chemistry X-ray Diffraction Facility. Details are given in the experimental section. Suitable crystals for the determination were grown from a saturated pentane solution at -40 °C, giving large yellow/brown octahedral crystals. An ORTEP diagram of **2** is shown in Figure II and selected bond distances and angles are given in Table II. The structure shows the expected three-legged piano stool geometry at iridium. The iridium-sulfur bond length of 2.366(1) Å is quite similar to those found in the other X-ray diffraction studies reported in this chapter.

Reaction of Sodium Alkyl Thiolates with $Cp^*(PMe_3)MCl_2$; M = Ir (7) and M = Rh (12). The stability of complexes **2**, **8**, and **9** encouraged us to attempt the preparation of materials with iridium-sulfur and rhodium-sulfur bonds by more straightforward nucleophilic substitution routes. Accordingly, addition of dry ethanol to a mixture of the iridium dichloride **7** and slightly more than two equivalents of sodium methyl thiolate or sodium *tert*-butyl thiolate led to

Scheme IV

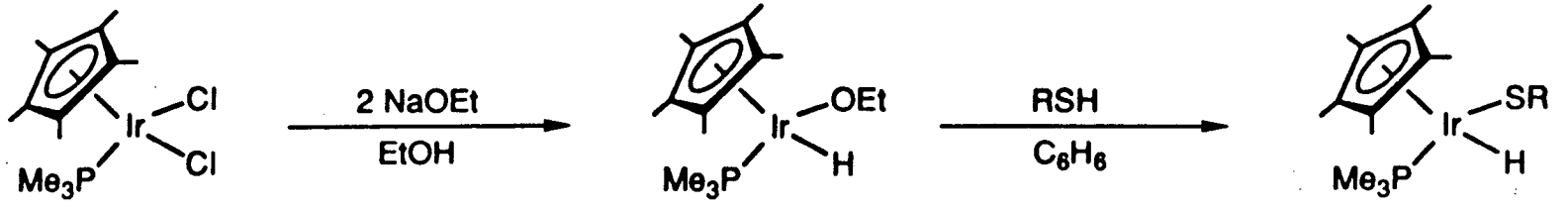

7 **6**

8, R = H
9, R = Me
2, R = tBu

Table I. Characteristic iridium hydride resonances (^{1}H NMR) and iridium hydride stretches (IR) for the (thiol)hydride complexes **8**, **9**, and **2**.

Complex	$\delta_{Ir\text{-}H}$ (d^6-benzene)	$\upsilon_{Ir\text{-}H}$ (KBr pellet)
$Cp^*(PMe_3)Ir(SH)H$ (**8**)	- 16.01 ($J_{P\text{-}H}$ = 36.7 Hz)	2093 cm^{-1}
$Cp^*(PMe_3)Ir(SMe)H$ (**9**)	- 16.58 ($J_{P\text{-}H}$ = 36.4 Hz)	2114 cm^{-1}
$Cp^*(PMe_3)Ir(S\text{-}tBu)$ (**2**)	- 16.47 ($J_{P\text{-}H}$ = 35.1 Hz)	2069 cm^{-1}

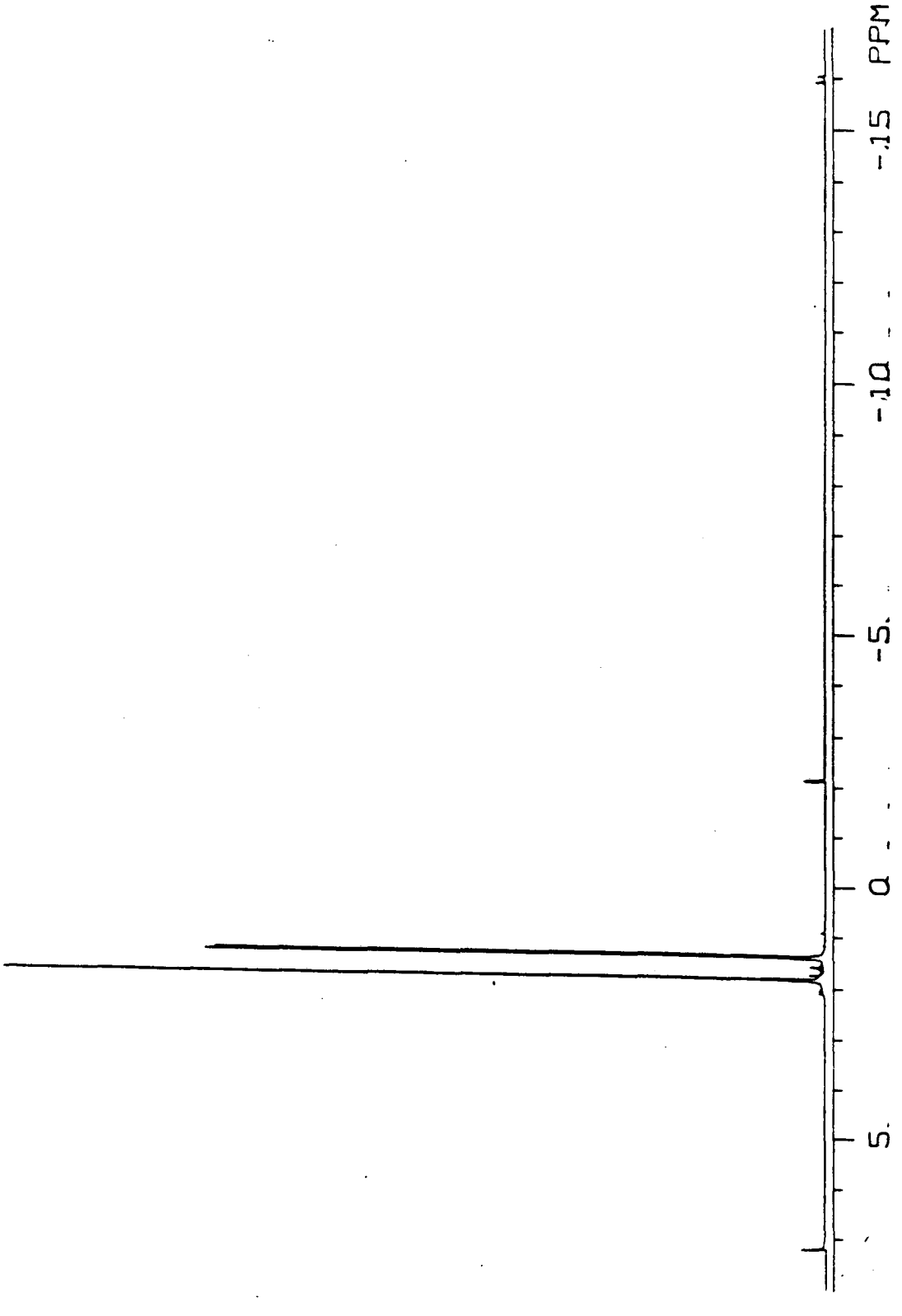

Figure I. ^{1}H NMR spectrum of $Cp^{*}(PMe_3)Ir(SH)H$ (8) in d^6-benzene.

Figure II. ORTEP diagram and labelling scheme for complex **2**.

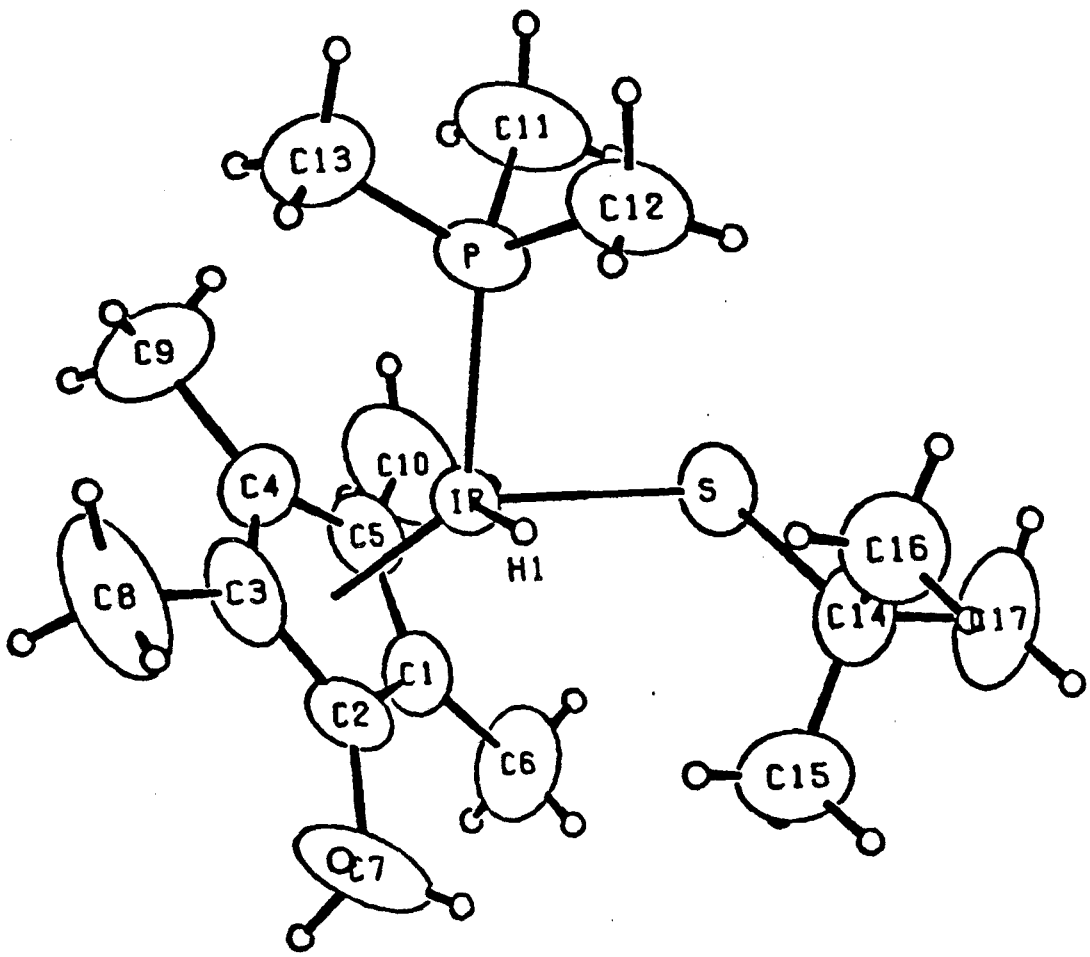

Table II. Selected bond distances and angles for complex **2**.

Intramolecular Distances

ATOM 1	ATOM 2	DISTANCE
IR	S	2.366(1)
IR	P	2.228(1)
IR	H1	1.69(4)
IR	C1	2.272(4)
IR	C2	2.246(4)
IR	C3	2.193(4)
IR	C4	2.227(4)
IR	C5	2.260(4)
IR	CP	1.893
P	C11	1.811(6)
P	C12	1.809(6)
P	C13	1.815(5)
S	C14	1.854(4)
C14	C15	1.503(7)
C14	C16	1.518(6)
C14	C17	1.529(6)
C1	C2	1.386(6)
C1	C5	1.412(6)
C2	C3	1.432(6)
C3	C4	1.404(6)
C4	C5	1.400(6)
C1	C6	1.522(6)
C2	C7	1.512(6)
C3	C8	1.520(7)
C4	C9	1.512(7)
C5	C10	1.507(7)

Intramolecular Angles

ATOM 1	ATOM 2	ATOM 3	ANGLE
CP	IR	S	124.56
CP	IR	P	132.43
CP	IR	H1	129.63
S	IR	P	87.37(5)
S	IR	H1	87.7(13)
P	IR	H1	79.5(14)
IR	P	C11	115.0(2)
IR	P	C12	117.2(2)
IR	P	C13	117.0(2)
C11	P	C12	102.4(3)
C11	P	C13	102.4(3)
C12	P	C13	100.5(3)
IR	S	C14	113.14(15)
S	C14	C15	112.0(3)
S	C14	C16	111.6(3)
S	C14	C17	104.6(3)
C15	C14	C16	109.5(4)
C15	C14	C17	109.8(5)
C16	C14	C17	109.1(4)
C2	C1	C5	109.0(4)
C1	C2	C3	107.8(4)
C2	C3	C4	106.9(4)
C3	C4	C5	109.0(4)
C1	C5	C4	107.3(4)
C2	C1	C6	127.2(5)
C5	C1	C6	123.7(5)
C1	C2	C7	126.1(5)
C3	C2	C7	125.9(5)
C2	C3	C8	124.4(5)
C4	C3	C8	127.9(5)
C3	C4	C9	125.2(5)
C5	C4	C9	125.5(5)
C1	C5	C10	126.3(5)
C4	C5	C10	126.2(5)

the corresponding iridium bis-thiolates $Cp^*(PMe_3)Ir(SMe)_2$ (**10**) and $Cp^*(PMe_3)Ir(S\text{-}tBu)_2$ (**3**) in about 50% isolated yield (Scheme V). Use of ethanol as solvent is critical in these reactions; attempts to prepare **3** using tetrahydrofuran or t-BuSH as solvent were unsuccessful. Both complexes are air-stable orange solids. Unlike the few alkoxide complexes that have been prepared in this series, they can be purified by chromatography on Alumina III. Both have been fully characterized by standard spectroscopic and analytical techniques. The ^1H and $^{13}C\{^1H\}$ NMR spectra of these materials are, for the most part, unremarkable. The ^1H NMR spectrum of **3**, however, does show considerable broadening of the resonance attributable to the PMe_3 ligand at room temperature. This is presumably due to hindered rotation of the ligand caused by the two very bulky *tert*-butylthiolate groups. Warming the sample to 60 °C results in considerable sharpening of this resonance.

Attempts to prepare the analogous rhodium complexes met with limited success. Addition of dry ethanol to a mixture of the rhodium dichloride **11**[14] and slightly more than two equivalents of sodium methyl thiolate produced only intractable materials. This is probably due to rapid β-hydrogen elimination from the coordinated methyl thiolate ligands once formed. However, reaction of **11** with sodium *tert*-butyl thiolate resulted in successful substitution of the chloride ligands to give the rhodium bis-(*tert*-butylthiolate) complex $Cp^*(PMe_3)Rh(S\text{-}tBu)_2$ (**12**) (Scheme VI) in 68.7% isolated yield. This material exhibits ^1H and $^{13}C\{^1H\}$ NMR spectra which are very similar to those of the iridium analogue **3**, including the broadening of the PMe_3 resonance in the ^1H NMR spectrum at room temperature.

Reaction of the iridium dichloride **7** with sodium hydrogen sulfide (NaSH) in ethanol also led to successful substitution chemistry (Scheme VII). Upon mixing, a dramatic color change was observed, the initially yellow solution slowly turning rust red followed by a rapid change to bright green. After removal of solvent a dark green residue remained. Chromatography in the drybox on Alumina III afforded two products, one intensely green-colored and the other bright yellow.

The bright yellow material isolated in this manner is identified as the expected metalladithiol $Cp^*(PMe_3)Ir(SH)_2$ (**5**). Besides resonances for the coordinated Cp^* and PMe_3 ligands, a doublet

Scheme V

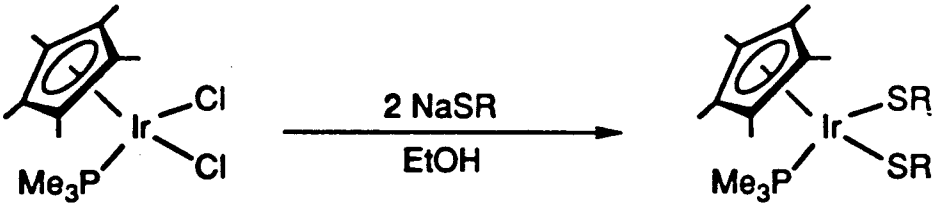

7

10, R = Me
3, R = tBu

Scheme VI

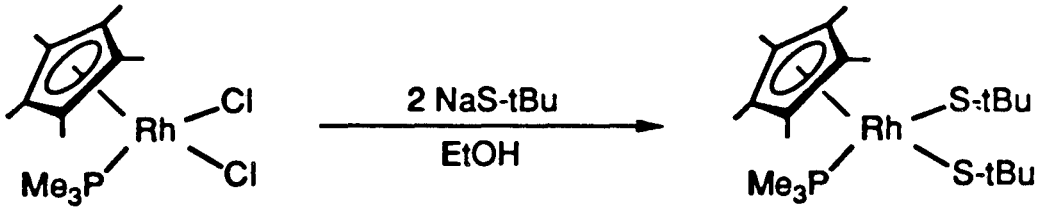

11 **12**

Scheme VII

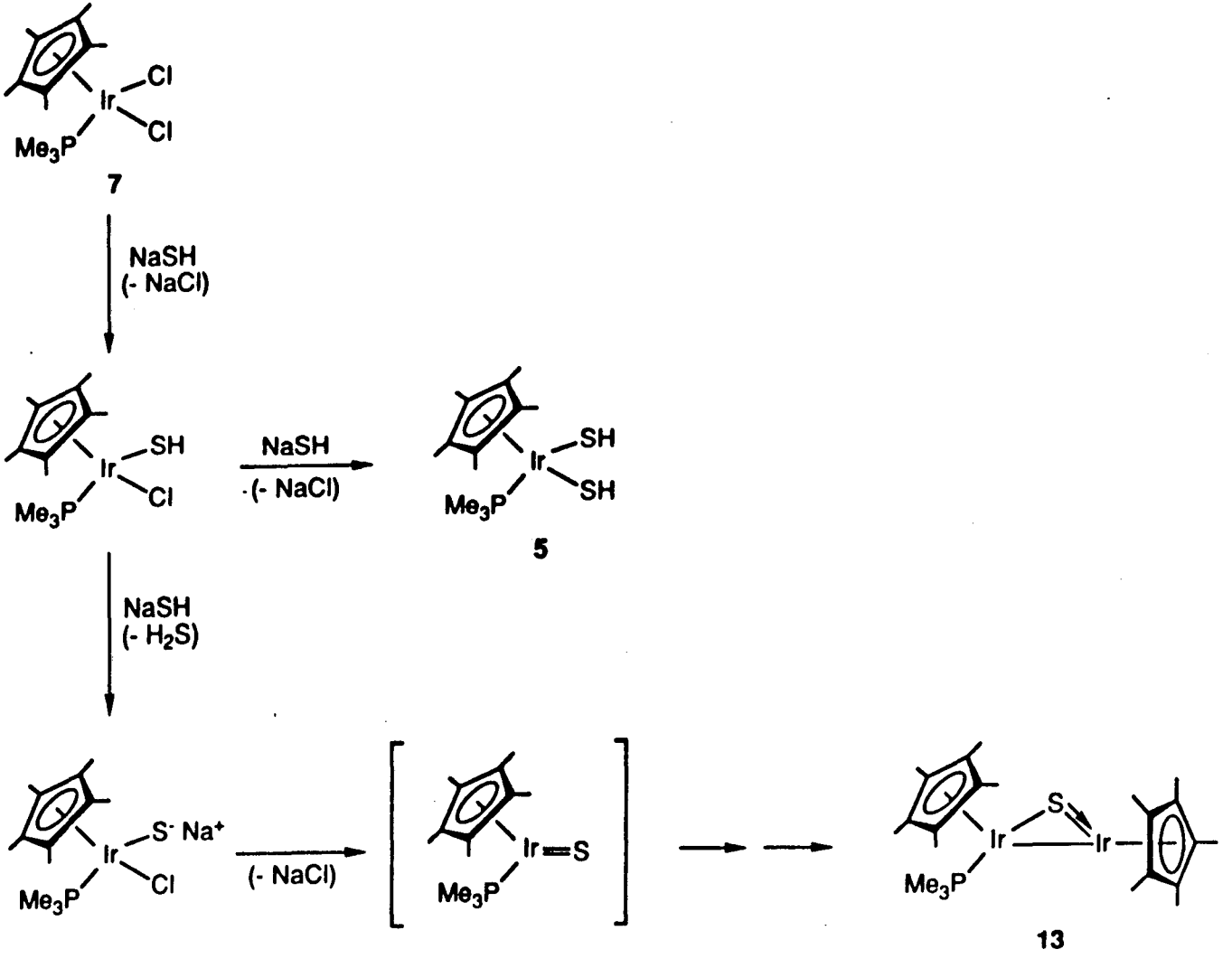
Cl
Ir
Cl
Me3P
7
NaSH
(- NaCl)
SH
Ir
Cl
Me3P
NaSH
(- NaCl)
SH
Ir
SH
Me3P
5
NaSH
(- H2S)
S- Na+
Ir
Cl
Me3P
(- NaCl)
Ir=S
Me3P
S
Ir
Ir
Me3P
13

at δ -1.93 ppm (J_{P-H} = 4.5 Hz) integrating to two protons is observed in the ^1H NMR spectrum. In addition, S-H stretching frequencies are observed at 2521 and 2496 cm^{-1} in the infrared spectrum. Addition of an excess of H_2S to the reaction mixture completely suppressed the formation of the green material, and in this manner **5** was isolated in 92% yield.

A single crystal X-ray diffraction study of the metalladithiol **5** was performed by Dr. F. J. Hollander of the U.C. Berkeley College of Chemistry X-ray Diffraction Facility. Details are given in the experimental section. Suitable crystals for the determination were grown from a toluene solution layered with heptane at -40°C, giving orange-yellow tabular crystals. An ORTEP diagram of **5** is shown in Figure III and selected bond distances and angles are given in Table III. The structure once again shows the expected three-legged piano stool geometry at iridium. The iridium-sulfur bond distances are 2.370(2) and 2.380(2) Å; very similar to those found in the other X-ray diffraction studies reported in this chapter. The thiol hydrogens were located and refined; however, motion and/or disorder gave large thermal parameters for these atoms. As can be seen in Figure III, the hydrogen attached to S2 lies between the two sulfur atoms (the S1-H2 distance is 2.68(16) Å) and the iridium atom, both sulfur atoms, and H2 all lie in approximately the same plane. This, taken with the observation of two S-H stretching frequencies in the solid-state infrared spectrum, suggest the formation of an intramolecular hydrogen bond between the two thiol ligands. Unfortunately, the error in the structural values does not allow this assertion to be made with great confidence.

The ^1H and $^{13}C\{^1H\}$ NMR spectra of the green compound exhibit resonances indicative of two types of Cp^* ligands (only one of which is coupled to phosphorus), and one PMe_3 ligand. The UV-Vis spectrum in hexanes exhibits maxima at λ 317 nm (ε = 8.8 x 10^3), 400 nm (ε = 5.4 x 10^3), and 690 nm (ε = 950). Comparison of these data with those obtained by McGhee for the dimer $Cp^*(PR_3)Ir(\mu\text{-}O)IrCp^*$ (R = Me, Ph),[16] leads us to assign the structure of this material as the analogous μ-sulfido dimer $Cp^*(PMe_3)Ir(\mu\text{-}S)IrCp^*$ (**13**).

One possible mechanism for the formation of the dimer **13** is outlined in Scheme VII. Initial attack of NaSH on the dichloride **7** should give the (thiol)chloride $Cp^*(PMe_3)Ir(SH)Cl$.

Figure III. ORTEP diagram and labelling scheme for complex **5**.

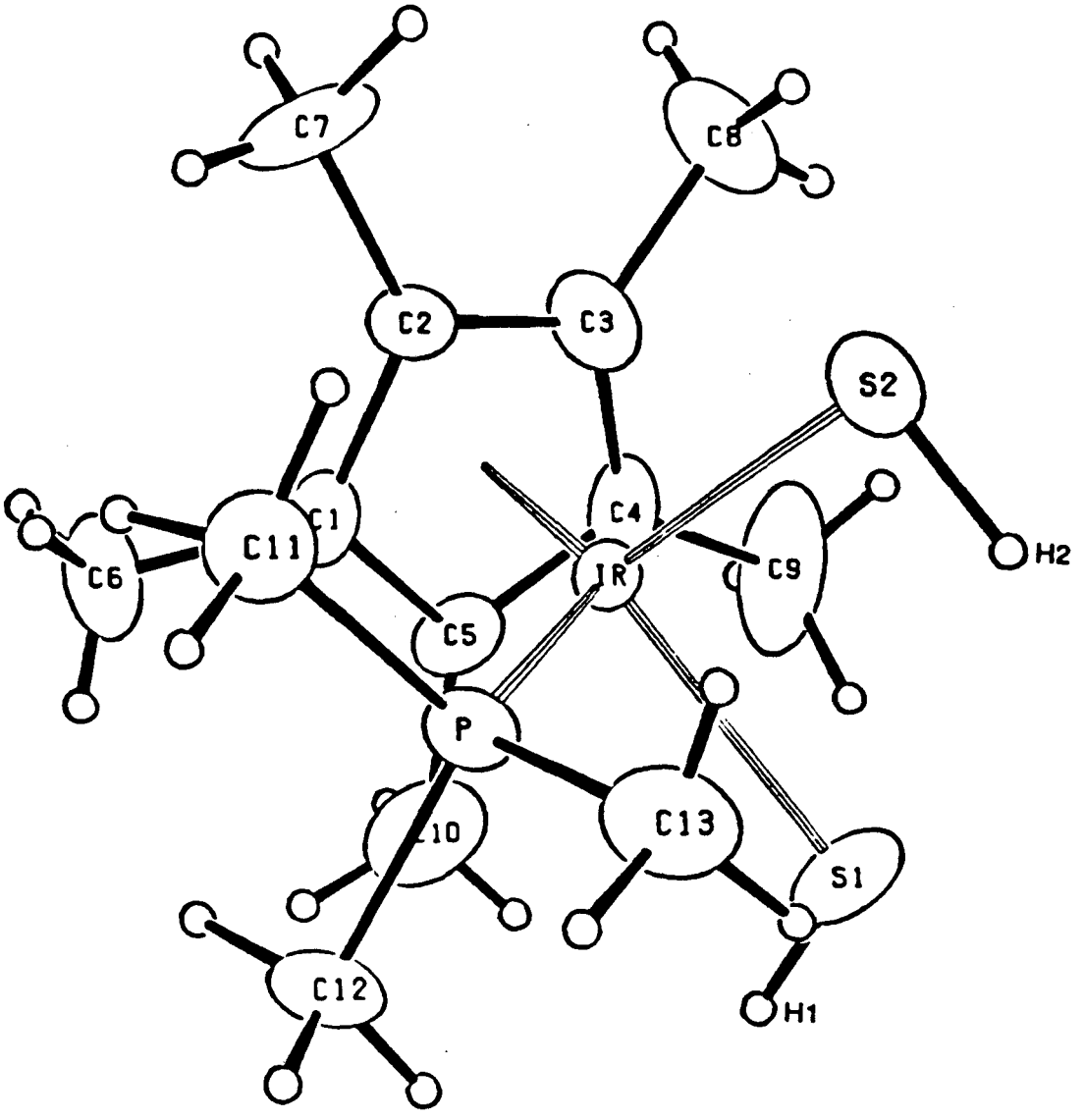

Table III. Selected bond distances and angles for complex **5**.

Intramolecular Distances

ATOM 1	ATOM 2	DISTANCE
IR	S1	2.380(2)
IR	S2	2.370(2)
IR	P	2.257(2)
IR	C1	2.205(6)
IR	C2	2.177(6)
IR	C3	2.263(6)
IR	C4	2.258(6)
IR	C5	2.195(6)
IR	CP	1.858
P	C11	1.816(7)
P	C12	1.806(7)
P	C13	1.816(8)
C1	C2	1.432(8)
C1	C5	1.428(8)
C2	C3	1.426(10)
C3	C4	1.414(10)
C4	C5	1.447(9)
C1	C6	1.485(9)
C2	C7	1.498(10)
C3	C8	1.496(11)
C4	C9	1.486(10)
C5	C10	1.493(10)
S1	H1	1.02(14)
S2	H2	1.25(18)

Intramolecular Angles

ATOM 1	ATOM 2	ATOM 3	ANGLE
CP	IR	S1	123.23
CP	IR	S2	124.03
CP.	IR	P	131.83
P	IR	S1	87.37(6)
P	IR	S2	88.86(6)
S1	IR	S2	88.74(7)
IR	S1	H1	109(7)
IR	S2	H2	95(7)
IR	P	C11	115.4(3)
IR	P	C12	113.6(2)
IR	P	C13	118.0(3)
C11	P	C12	103.3(4)
C11	P	C13	101.9(4)
C12	P	C13	102.6(4)
C2	C1	C5	107.8(5)
C1	C2	C3	107.4(5)
C2	C3	C4	109.4(6)
C3	C4	C5	106.9(6)
C1	C5	C4	108.1(5)
C2	C1	C6	126.4(7)
C5	C1	C6	125.4(7)
C1	C2	C7	126.0(7)
C3	C2	C7	125.0(7)
C2	C3	C8	122.8(9)
C4	C3	C8	127.8(9)
C3	C4	C9	127.2(8)
C5	C4	C9	125.8(8)
C1	C5	C10	126.6(7)
C4	C5	C10	124.8(7)

Deprotonation of this material followed by loss of sodium chloride (NaCl) would generate the monomeric sulfido species [$Cp^*(PMe_3)Ir(S)$]. This could then dimerize with loss of trimethylphosphine sulfide to generate **13**.

To test the hypothesis of deprotonation of $Cp^*(PMe_3)Ir(SH)Cl$, the dichloride **7** was treated with Na_2S in ethanol (Scheme VIII). This should initially generate $Cp^*(PMe_3)Ir(S^-Na^+)Cl$, which could then lose NaCl and dimerize as before. As expected, treatment of **7** with Na_2S in ethanol led to the same rapid color change described above. After workup (removal of solvent, chromatography on Alumina III) both the dimer **13** and the metalladithiol **5** were obtained. The green material can be isolated as a solid in 47% yield by lyophilization from benzene. Formation of **5** can be explained by competitive protonation of $Cp^*(PMe_3)Ir(S^-Na^+)Cl$ by ethanol to give $Cp^*(PMe_3)Ir(SH)Cl$. Subsequent reaction with Na_2S followed by protonation would generate **5**.

Reaction of the rhodium dichloride **11** with NaSH (Scheme IX) proceeded in an identical manner to the iridium chemistry described above. Addition of dry ethanol to a mixture of **11** and NaSH resulted in the formation of a red/purple solution. Chromatography in the drybox on Alumina III again afforded two products, one magenta and the other is red. The red material is the expected metalladithiol $Cp^*(PMe_3)Rh(SH)_2$ (**14**). The thiol protons are seen as a doublet of doublets at δ -2.07 ppm (J_{P-H} = 3.9 Hz, J_{Rh-H} = 0.6 Hz) in the ^1H NMR spectrum (Figure IV). As was observed in the iridium reaction, addition of H_2S suppressed the formation of the second product, and in this manner **14** was isolated in 40% yield.

As was observed for the iridium chemistry, reaction of the rhodium dichloride **11** with Na_2S in ethanol also produced the same two products as the reaction of **11** with NaSH. Chromatography in the drybox on Alumina III separated the two products. Lyophilization of the magenta product from benzene allowed its isolation in 62% yield. Its ^1H and $^{13}C\{^1H\}$ NMR spectra are very similar to that of the iridium dimer **13**. On this basis, the structure of this material is assigned as the analogous μ-sulfido dimer $Cp^*(PMe_3)Rh(\mu\text{-}S)RhCp^*$ (**15**).

Reactivity of the bis-(*tert*-butylthiolates) $Cp^*(PMe_3)M(S\text{-}tBu)_2$; M = Ir (11), M = Rh (12): an Alternate Route to (Thiolate)hydride Complexes. As was shown

Scheme VIII

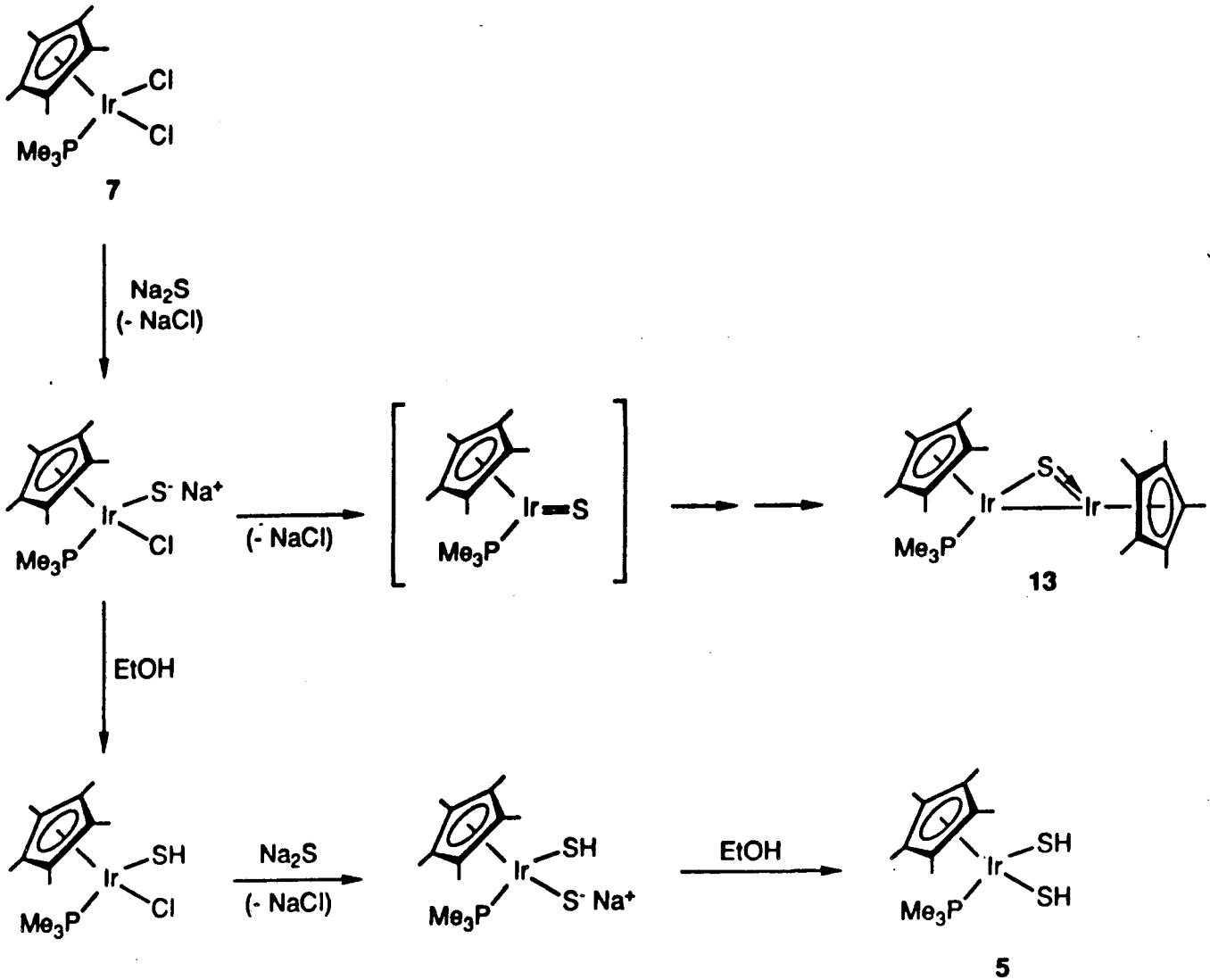
Cl
Ir
Cl
Me3P
7
Na2S
(- NaCl)
S- Na+
Ir
Cl
Me3P
(- NaCl)
Ir=S
Me3P
S
Ir
Ir
Me3P
13
EtOH
SH
Ir
Cl
Me3P
Na2S
(- NaCl)
SH
Ir
S- Na+
Me3P
EtOH
SH
Ir
SH
Me3P
5

Scheme IX

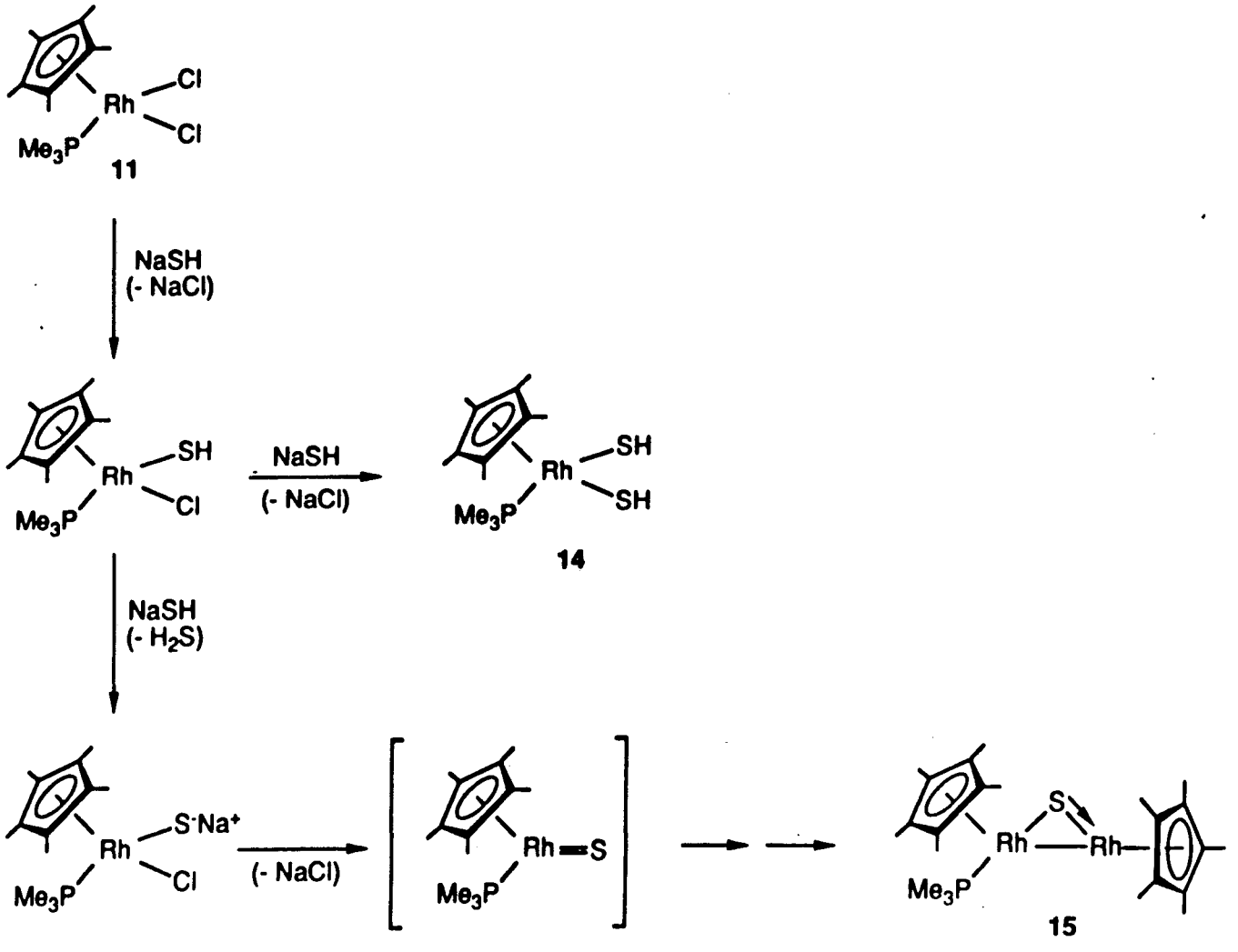
Rh
Cl
Cl
Me3P
11
NaSH
(- NaCl)
SH
Rh
Cl
Me3P
NaSH
(- NaCl)
SH
Rh
SH
Me3P
14
NaSH
(- H2S)
S-Na+
Rh
Cl
Me3P
(- NaCl)
Rh=S
Me3P
S
Rh
Rh
Me3P
15

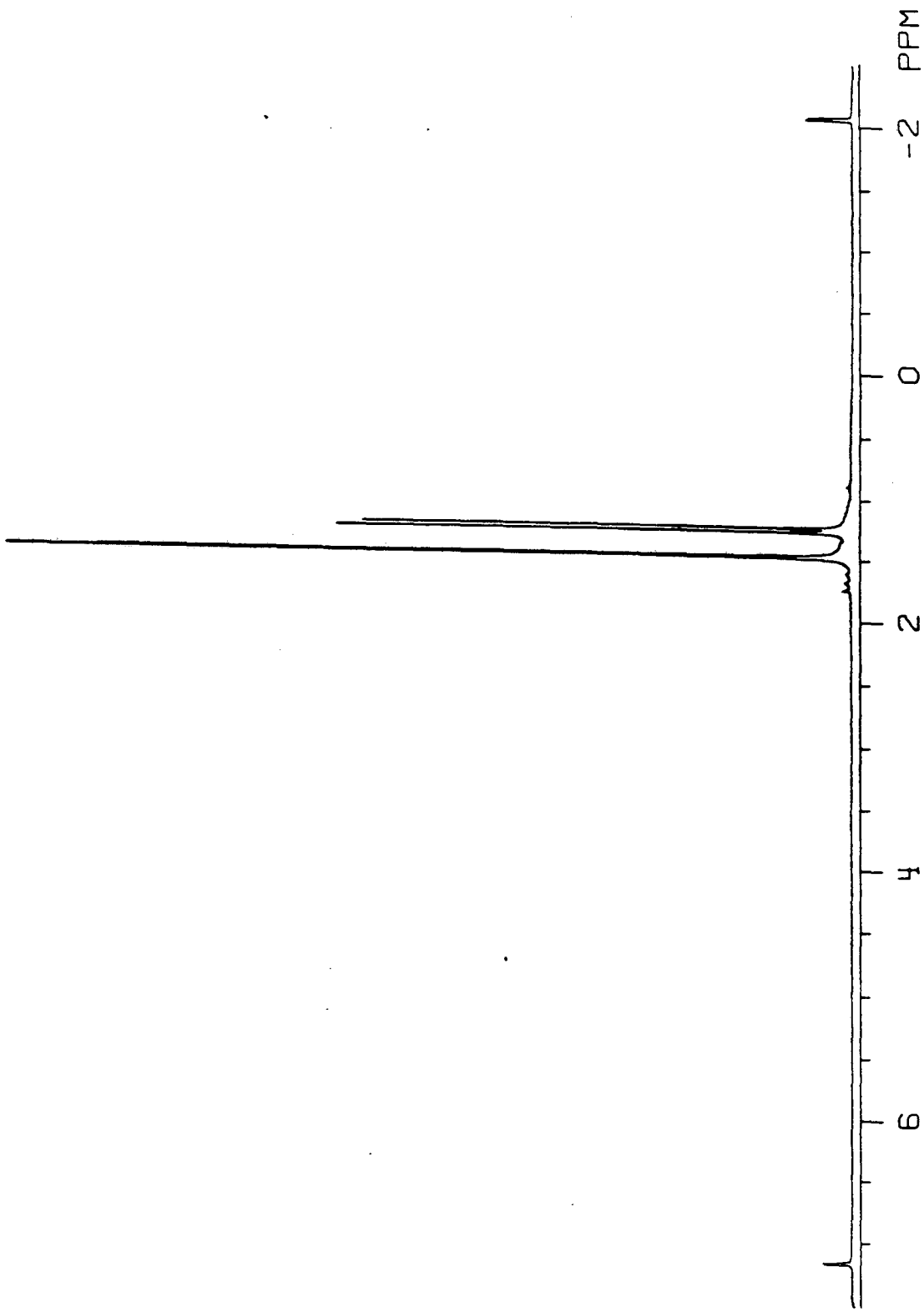

Figure IV. ^{1}H NMR spectrum of $Cp^{*}(PMe_3)Rh(SH)_2$ **(14)** in d^6-benzene.

previously, successful exchange reactions of the iridium (ethoxy)hydride **6** with organic thiols produce the corresponding thiolate hydride complexes. However, the rhodium (ethoxy)hydride $Cp^*(PMe_3)Rh(OEt)H$ has not been successfully prepared. Therefore, an alternate route to the (thiolate)hydride complexes was sought. A number of reagents are known which successfully substitute hydride ligand for halide in transition metal complexes.[5,7,17] With this in mind, a route to the thiolate chloride complexes $Cp^*(PMe_3)M(SR)Cl$ was developed.

Treatment of the iridium dimethyl complex $Cp^*(PMe_3)IrMe_2$ with aniline hydrochloride in acetone leads to the replacement of one of the methyl groups by chloride to give $Cp^*(PMe_3)Ir(Me)Cl$.[18] Similarly, reaction of the iridium bis-(*tert*-butylthiolate) **3** with slightly more than one equivalent of aniline hydrochloride in acetone also resulted in successful substitution to give the desired thiolate chloride $Cp^*(PMe_3)Ir(S\text{-}tBu)Cl$ (**16**) in 45% isolated yield. The rhodium analogue $Cp^*(PMe_3)Rh(S\text{-}tBu)Cl$ (**17**) can be prepared from **12** in the same manner (Scheme X), in 77% isolated yield.

Addition of dry ethanol to a mixture of $Cp^*(PMe_3)Ir(S\text{-}tBu)Cl$ (**16**) and sodium ethoxide resulted in a rapid reaction (Scheme XI). The initially bright yellow solution paled considerably and, after workup, $Cp^*(PMe_3)Ir(S\text{-}tBu)H$ (**2**) was recovered in 88% isolated yield. This material is identical to that formed via the exchange reaction described previously.

Synthesis of the rhodium (*tert*-butylthiolate)hydride $Cp^*(PMe_3)Rh(S\text{-}tBu)H$ (**18**) can also be accomplished by a modification of the above procedure (Scheme XII). It has been established that the rhodium (alkyl)hydride complexes $Cp^*(PMe_3)Rh(R)H$ are thermally unstable above -40 °C.[19] Therefore, the reaction of thiolate chloride **17** with sodium ethoxide was run at low temperature. Addition of a pre-cooled (-78 °C) ethanol solution of sodium ethoxide to a similarly pre-cooled ethanol solution of **17** produced no immediate color change. After stirring for two days at -40 °C, ethanol was removed under vacuum at -20 °C. The resulting solid, analyzed by ^1H NMR spectroscopy, showed approximately 50% conversion of **17** to the desired thiolate hydride complex $Cp^*(PMe_3)Rh(S\text{-}tBu)H$ (**18**). Longer reaction times are necessary to effect complete

Scheme X

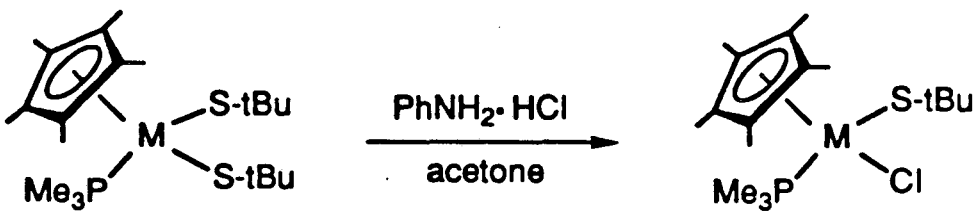

3, M = Ir
12, M = Rh

16, M = Ir
17, M = Rh

Scheme XI

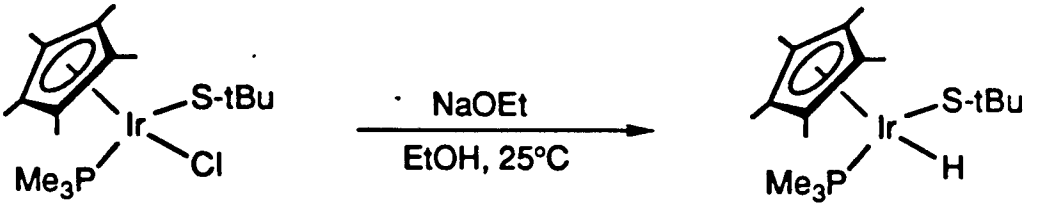

16 **2**

Scheme XII

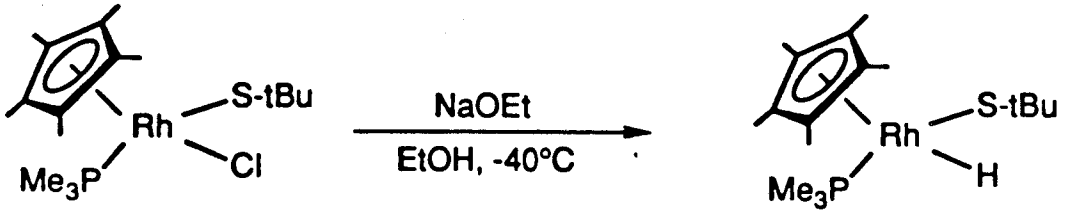

17 **18**

conversion. Warming of the sample to room temperature led to decomposition of **18** to unknown materials.

Synthesis of the (Thiol)methyl Complex $Cp^*(PMe_3)Ir(SH)Me$ (20). The (thiol)methyl complex **20** can be synthesized in two ways, both of which are shown in Scheme XIII. As was previously alluded to, reaction of the dimethyl compound $Cp^*(PMe_3)IrMe_2$ (**19**) with relatively strong acids (aniline hydrochloride, carboxylic acids, phenols, succinimide, etc.) results in the replacement of one of the methyl groups by the conjugate base of the acid used.[20] Heating a solution of **19** with excess H_2S in benzene at 65 °C led to a slow conversion to the desired (thiol)methyl complex **20** and methane. The reaction reached completion only after heating for weeks, to give **20** in 66.7% isolated yield.

A more propitious route to this molecule is the nucleophilic displacement of halide by thiol anion (see Scheme XIII). Treatment of the (chloro)methyl compound $Cp^*(PMe_3)Ir(Cl)Me$ (**21**)[18] with NaSH in ethanol at room temperature for one hour also led to the (thiol)methyl complex **20** in 96.3% isolated yield. The ^1H NMR spectrum of this material, identical to that prepared above, shows characteristic resonances for both the thiol proton (δ -2.57 ppm, J_{P-H} = 4.4 Hz) and the iridium-bound methyl group (δ 0.66 ppm, J_{P-H} = 6.3 Hz) (Figure V).

Preliminary Studies on the Reactivity of Iridium-Sulfur Complexes. The metalladithiol **5** reacted with solvent acetone in the presence of catalytic acid (either HCl or aniline hydrochloride) to give a single new complex which exhibits inequivalent methyl groups at δ 2.02 and 1.81 ppm in the ^1H NMR spectrum (Scheme XIV). This, in addition to other spectroscopic and analytical data, lead us to assign the structure of this product as the 2,4-dithiametallacyclobutane complex $Cp^*(PMe_3)Ir(SCMe_2S)$ (**22**).

An X-ray diffraction study performed by Dr. F. J. Hollander of the U.C. Berkeley College of Chemistry X-ray Diffraction Facility confirms this assignment. Details are given in the experimental section. Suitable crystals for the determination were grown from a toluene/pentane solution at -40°C, giving yellow crystals. An ORTEP diagram of **22** is shown in Figure VI and selected bond distances and angles are given in Table IV. The geometry of the molecule at iridium is the

Scheme XIII

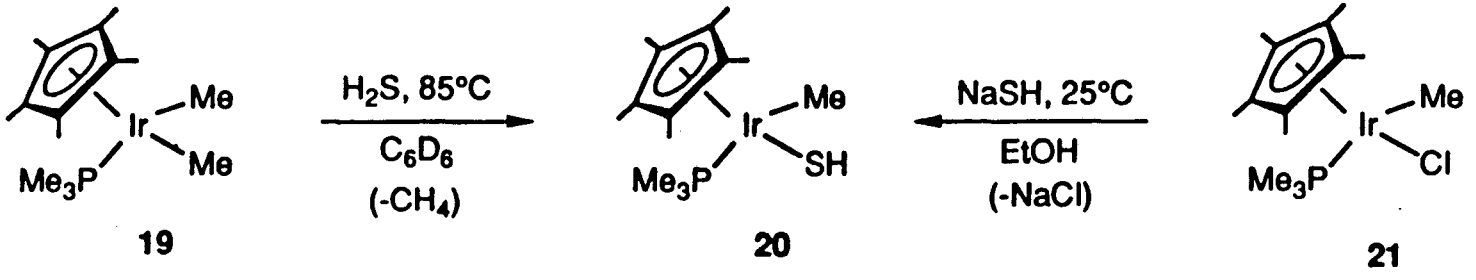
Me
Ir
Me
Me3P
19
H2S, 85°C
C6D6
(-CH4)
Me
Ir
SH
Me3P
20
NaSH, 25°C
EtOH
(-NaCl)
Me
Ir
Cl
Me3P
21

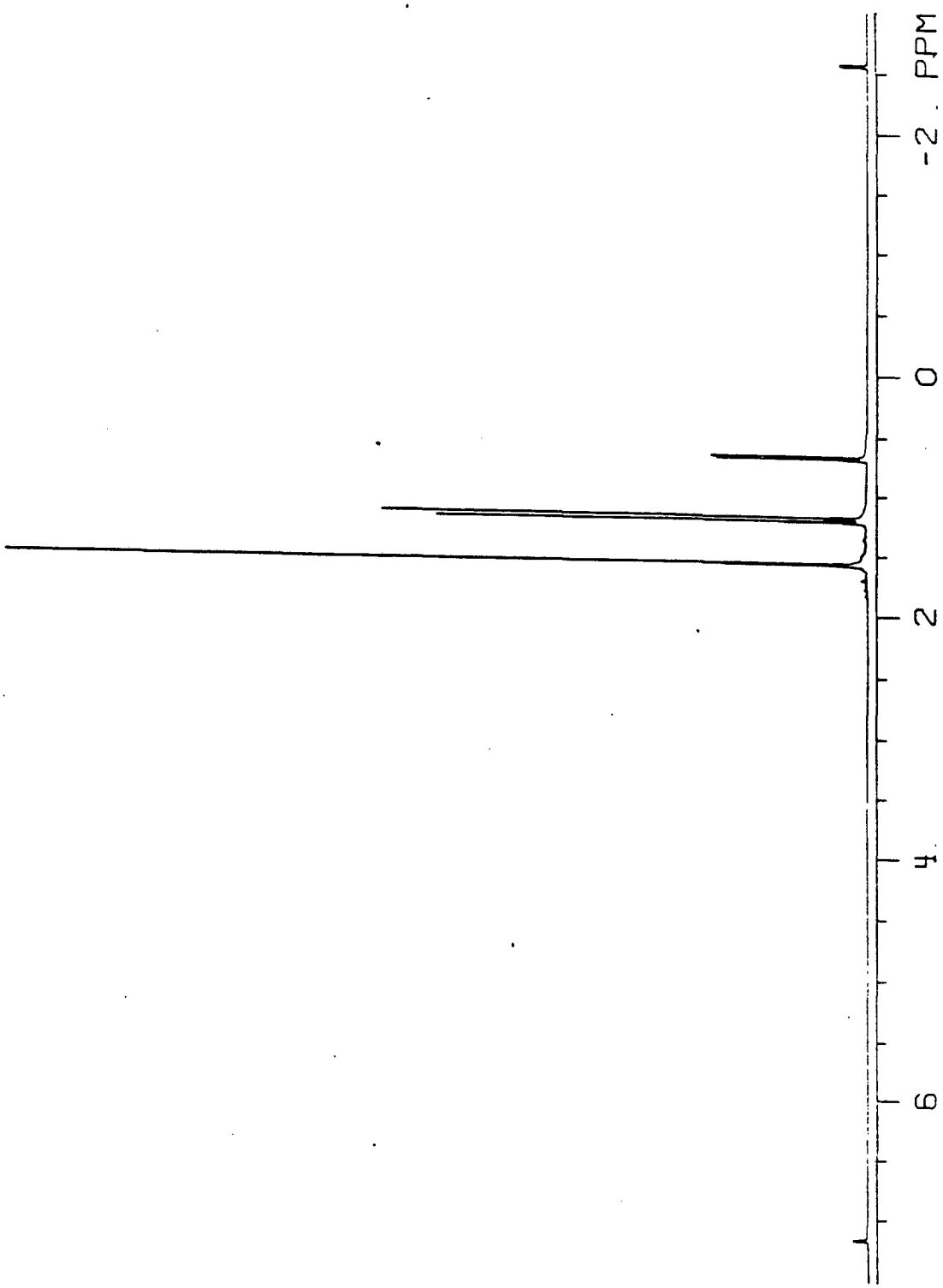

Figure V. ^{1}H NMR spectrum of $Cp^{*}(PMe_3)Ir(SH)Me$ (20) in d^6-benzene.

Scheme XIV

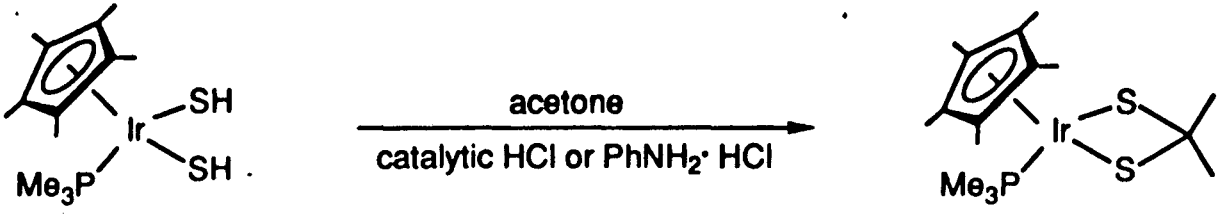

5 **22**

Figure VI. ORTEP diagram and labelling scheme for complex **22**.

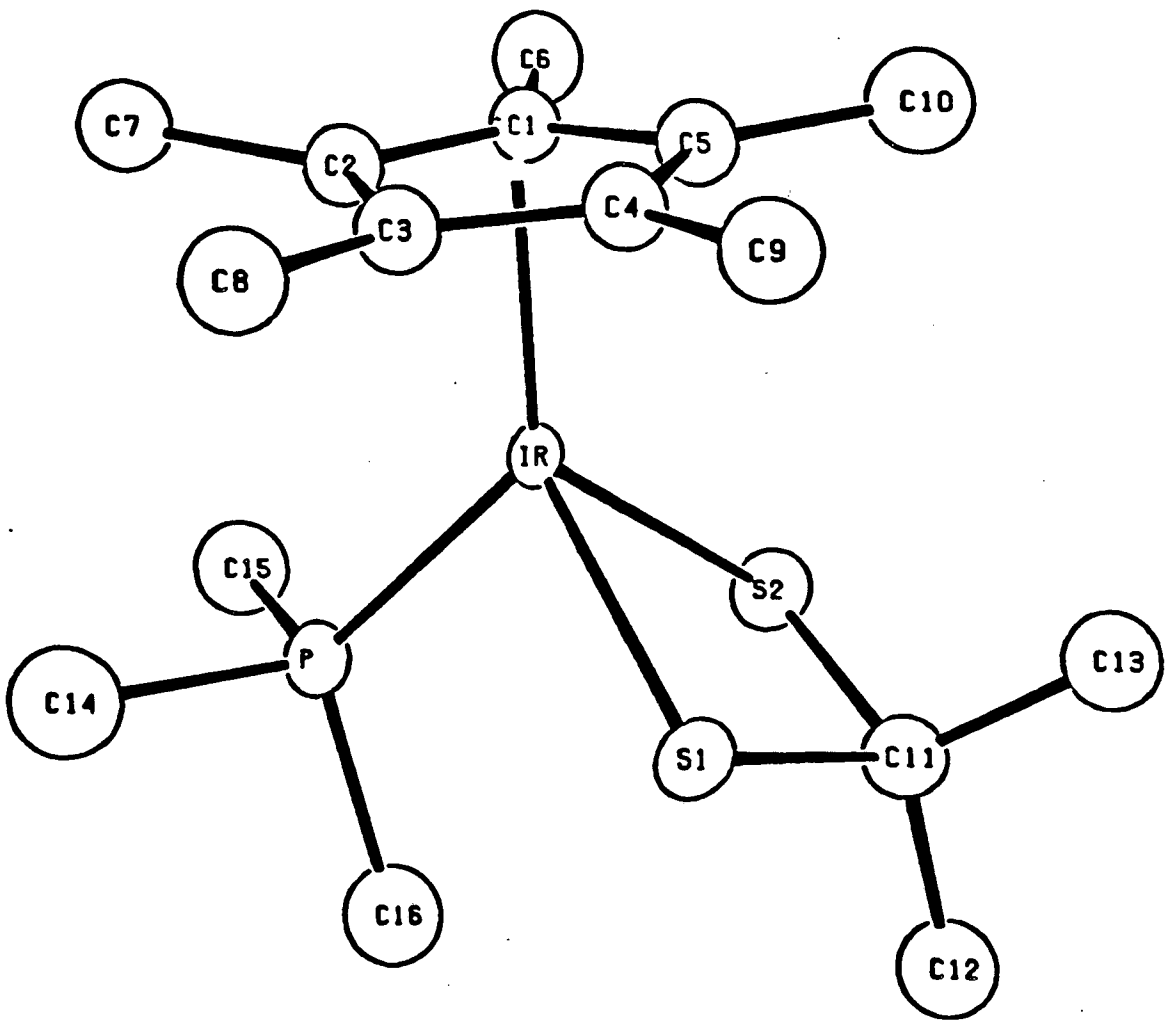

Table IV. Selected bond distances and angles for complex 22.

ATOM 1	ATOM 2	DISTANCE
IR	S1	2.358(2)
IR	S2	2.356(2)
IR	P	2.243(1)
IR	C1	2.211(6)
IR	C2	2.217(6)
IR	C3	2.210(6)
IR	C4	2.275(6)
IR	C5	2.273(6)
IR	CP1	1.868
C11	S1	1.859(6)
C11	S2	1.847(6)
C11	C12	1.508(9)
C11	C13	1.532(8)
P	C14	1.835(8)
P	C15	1.815(7)
P	C16	1.820(7)
C1	C2	1.433(8)
C1	C6	1.469(8)
C2	C3	1.480(7)
C3	C4	1.438(8)
C4	C5	1.446(9)
C1	C5	1.443(8)
C2	C7	1.507(9)
C3	C8	1.494(9)
C4	C9	1.490(9)
C5	C10	1.509(9)

ATOM 1	ATOM 2	ATOM 3	ANGLE
CP1	IR	P	131.92
CP1	IR	S1	126.96
CP1	IR	S2	126.88
P	IR	S1	90.39(6)
P	IR	S2	88.74(6)
S1	IR	S2	73.58(5)
IR	S1	C11	91.4(2)
IR	S2	C11	91.7(2)
S1	C11	S2	99.3(3)
S1	C11	C12	111.9(4)
S1	C11	C13	110.6(4)
S2	C11	C12	112.5(4)
S2	C11	C13	111.3(4)
C12	C11	C13	110.8(5)
IR	P	C14	115.2(2)
IR	P	C15	114.8(2)
IR	P	C16	118.0(2)
C14	P	C15	103.9(3)
C14	P	C16	100.7(3)
C15	P	C16	102.1(3)
C2	C1	C5	108.1(5)
C2	C1	C6	127.2(5)
C5	C1	C6	124.3(5)
C1	C2	C3	108.0(5)
C1	C2	C7	126.8(5)
C3	C2	C7	124.7(5)
C2	C3	C4	106.8(5)
C2	C3	C8	126.4(6)
C4	C3	C8	126.2(5)
C3	C4	C5	108.5(5)
C3	C4	C9	125.2(5)
C5	C4	C9	126.2(6)
C1	C5	C4	108.3(5)
C1	C5	C10	124.3(6)
C4	C5	C10	127.4(6)
C12	C11	C13	110.8(5)

expected three-legged piano stool. The metallacycle ring is flat, with inequivalent methyl groups pointing toward and away from the Cp* ring. The iridium-sulfur bond lengths of 2.358(2) and 2.356(2) Å are quite similar to those found in the other X-ray diffraction studies reported in this chapter.

Addition of H_2S to a d^6-benzene solution of the 2,4-dithiametallacyclobutane complex $Cp^*(PMe_3)Ir(SCMe_2S)$ (**22**) at room temperature gave no reaction. Upon heating to 80 °C, a slow reaction took place (Scheme XV). After 24 hours, the metallacycle **22** was quantitatively transformed into the metalladithiol **5** (as determined by integration of the ^1H NMR spectra versus an internal standard), and 2,2-propanedithiol[21] was produced in 25% yield (also determined versus the internal standard).

Treatment of the (thiol)hydride complex $Cp^*(PMe_3)Ir(SH)H$ (**8**) with CS_2 in benzene for 12 hours resulted in insertion of CS_2 into the metal-hydrogen bond of **8** to give the (dithioformate)thiol compound $Cp^*(PMe_3)Ir(SC(S)H)(SH)$ (**23**) (Scheme XVI) as the only product (^1H NMR). In addition to resonances attributable to the Cp* and PMe_3 ligands, a new thiol doublet (δ -2.01 ppm, J_{P-H} = 4.8 Hz) and a singlet integrating to one proton (δ 11.97 ppm) are seen in the ^1H NMR spectrum. Attempts to isolate pure **23** were unsuccessful due to slow decomposition of the compound in solution.

Discussion

The results presented in this chapter show that a wide variety of iridium and rhodium mono- and bis-thiolate complexes can be synthesized in a straightforward manner, isolated, and characterized. The mono-thiolate species can contain a variety of other potentially reactive ligands including hydride, halide, and alkyl groups. For the most part, these molecules are quite stable and many can be purified by chromatography. This is in sharp contrast to the alkoxide complexes thus far prepared in this series, which are unstable to chromatography supports.

The (thiolate)hydride complexes $Cp^*(PMe_3)M(SR)H$ [M = Ir, R = H (**8**), R = Me (**9**), R = tBu (**2**); M = Rh, R = tBu (**18**)] represent rare examples of monomeric, organometallic (thiolate)hydrides. Other examples are listed in Table V. As can be seen, only two types of (thiolate)hydrides are

Scheme XV

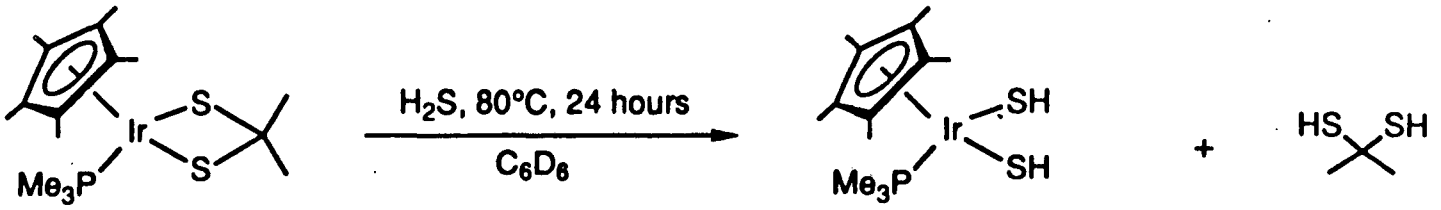

22 **5**

Scheme XVI

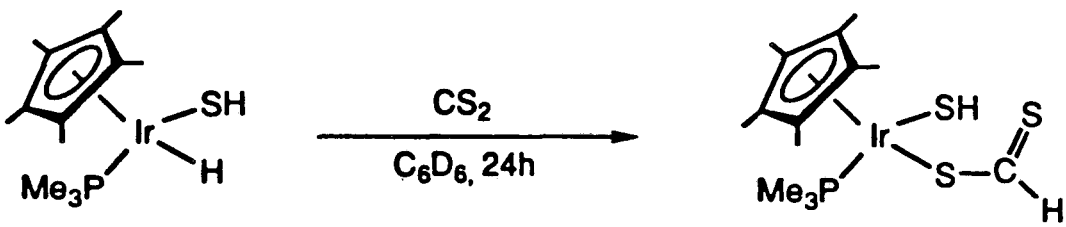

8 **23**

Table V. Examples of monomeric (thiolate)hydride complexes.

Complex		Reference
$[M(H)(SR)(X)(CO)(PPh_3)_2]$	M = Rh or Ir; R = H, alkyl or aryl	22
$[Ir(H)(SR)(PMe_3)_4]^+$	R = H only	23
$[Ru(H)(SR)(PPh_3)_3]$	R = alkyl or aryl	24
$[Mo(H)(SR)(dppe)_2]$	R = alkyl or aryl	25

known for iridium. Both of these are formed by oxidative addition of RSH to a square planar iridium(I) center. Treatment of trans-[Ir(Cl)(CO)(PPh_3)$_2$] with t-BuSH, however, does not lead to successful oxidative addition. Hence, complex **2** is the first (*tert*-butylthiolate)hydride complex of iridium. The only other crystal structure of a neutral, iridium(III) (thiolate)hydride is for [Ir(H)(SH)(Cl)(CO)(PPh_3)$_2$].[21e] The Ir-S bond length for this molecule is 2.336(4) Å, which compares favorably to that found in **2** at 2.366(1) Å. Studies on the desulfurization of cyclic sulfides and alkyl thiols on molybdenum surfaces has established that surface-bound (thiolate)hydrides may be the key intermediates in this reaction.[26] The proposed reaction sequence is given in Scheme XVII.

To date, no bis-alkoxide complexes have been prepared in this series. Reaction of Cp*(PMe_3)$IrCl_2$ with sodium methoxide gives four organometallic products, none of which contain methoxide ligand,[15] and, as was previously stated, reaction of Cp*(PR_3)$IrCl_2$ with sodium ethoxide gives the (ethoxy)hydride Cp*(PR_3)Ir(OEt)H as the sole organometallic product. The related bis-(*tert*-butoxide) complex Cp*Ir(O-tBu)$_2$ can be synthesized,[27] but reaction of this compound with phosphine gives only intractable materials.

Neutral, monomeric metalladithiol complexes are also quite rare.[3b,c,e,h,k] Structural information is scarce for these molecules,[3e,h,k] and the thiol hydrogens have only been located in one other structure, that of Cp*$_2$Ti(SH)$_2$.[3k] In contrast to the results reported here, the thiol hydrogens point away from each other, ruling out the possibility of an intramolecular hydrogen bond in the solid state.

Thus far, only a modest amount of reactivity has been discovered for the compounds presented in this chapter. As was stated in the introduction, most of the reactivity of previously described bis-thiolate complexes involves protonation and alkylation of the sulfur-containing ligands. The most interesting reaction of these molecules is the formation of the 2,4-dithiametallacyclobutane complex Cp*(PMe_3)Ir($SCMe_2S$) (**22**) by the acid-catalyzed reaction of acetone with the metalladithiol **5**. To the best of our knowledge, this is the first example of the formation of this type of metallacycle ring. Two other examples of the reaction of acetone with

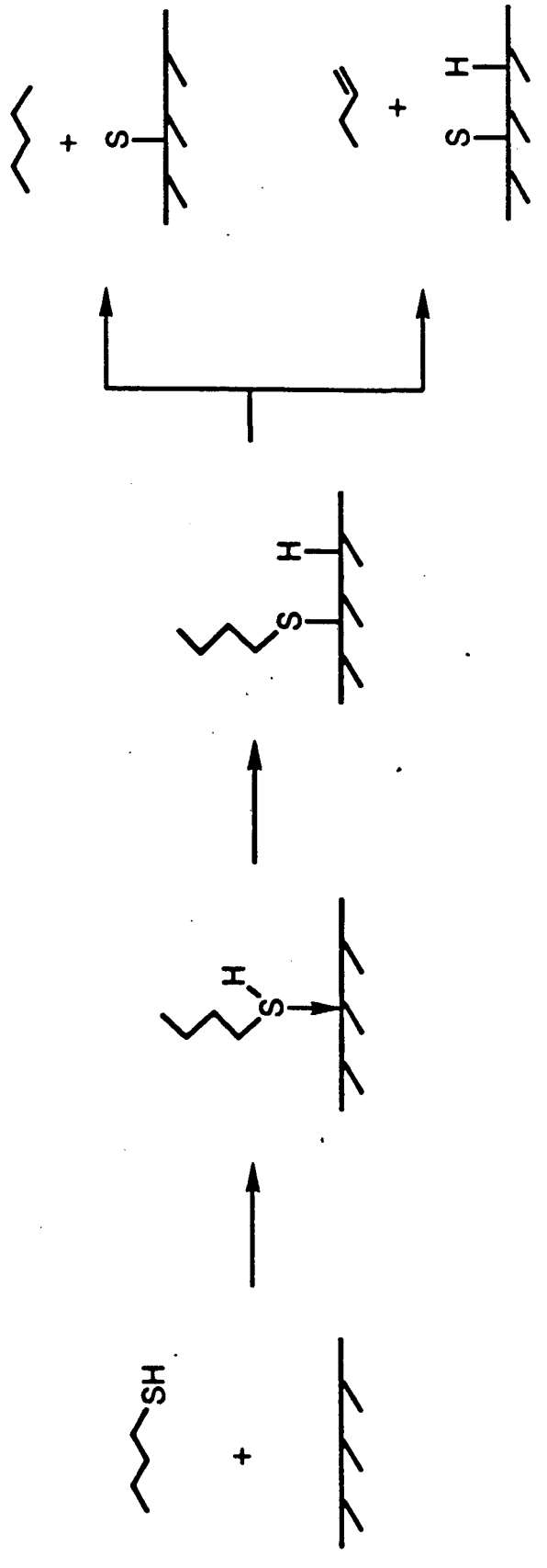

Scheme XVII

transition metal thiol groups have been reported. The first, also acid catalyzed, results in the formation of a metal-bound thioacetone ligand,[28] while the second converts a bridging thiol into a bridging isopropyl thiolate ligand.[29]

Insertion of CS_2 into a metal-hydrogen bond to give a metalladithioformate complex, as is seen in the reaction of $Cp^*(PMe_3)Ir(SH)H$ (7) with CS_2, is well precedented.[30] There has been no evidence for insertion of small molecules into the metal-sulfur bond of any of these molecules. It is possible that reactions of this type might be discovered by studying the reactivity of the rhodium or cobalt analogues.

Experimental

General. For a description of general experimental procedures, see Chapter 1. *tert*-butanethiol (t-BuSH) was purchased from Aldrich, dried over calcium oxide, and distilled prior to use. Di-*tert*-butyldisulfide was purchased from Aldrich and distilled prior to use. Hydrogen sulfide (H_2S) and methanethiol (MeSH) were purchased from Matheson Gas Products and used as received. Sodium hydrogen sulfide (NaSH) and sodium sulfide (Na_2S) were purchased from Alfa Products and used as received. Aniline hydrochloride from Aldrich was crystallized from ethanol/diethylether prior to use. Acetone was pre-dried with magnesium sulfate, dried for one week over activated 4Å molecular sieves, then distilled. Ethanol was dried over either magnesium ethoxide or sodium ethoxide, stored over activated 4Å molecular sieves, and distilled prior to use. Sodium ethoxide was prepared by reacting sodium metal with one equivalent of dry ethanol in tetrahydrofuran. Sodium methyl thiolate (NaSMe) and sodium *tert*-butyl thiolate (NaS-tBu) were prepared by reacting a slight excess of the appropriate thiol with sodium ethoxide in ethanol. The (methyl)chloride $Cp^*(PMe_3)Ir(Me)Cl$ and dimethyl $Cp^*(PMe_3)IrMe_2$ complexes were prepared according to published procedures,[18] as were the dichloride complexes $Cp^*(PMe_3)IrCl_2$ and $Cp^*(PMe_3)RhCl_2$.[14] The iridium dihydride $Cp^*(PMe_3)IrH_2$ was prepared as described in Chapter 1.

Photolysis of the Dihydride 1 in *tert*-butylthiol. In the drybox, 19.3 mg (0.05 mmol) $Cp^*(PMe_3)IrH_2$ (1) was placed in a Wilmad 505-PS 8" NMR tube fitted with a Cajon adaptor. The

tube was evacuated on a vacuum line and approximately 1 ml t-BuSH was condensed into the tube at -196 °C. The tube was sealed, thawed, and placed in a photolysis set-up (described in Chapter 1) held at 5 °C. The solution was irradiated for 4 h. The $^{31}P\{^{1}H\}$ NMR spectrum shows five singlets at δ -30.7, -32.0, -34.2, -37.0, and -45.7 ppm corresponding to $Cp^*(PMe_3)Ir(S\text{-}tBu)(SH)$ (**4**) (~35%), $Cp^*(PMe_3)Ir(SH)_2$ (**5**) (~10%), $Cp^*(PMe_3)Ir(S\text{-}tBu)_2$ (**3**) (~5%), $Cp^*(PMe_3)Ir(S\text{-}tBu)H$ (**2**) (~30%), and $Cp^*(PMe_3)IrH_2$ (**1**) (~20%), respectively. The identity of these materials was determined by independent syntheses, as described below.

Photolysis of the Dihydride 1 in Di-*tert*-butyldisulfide. This experiment was run similar to the photolysis of **1** in t-BuSH, except that di-*tert*-butyldisulfide was quickly pipetted onto the dihydride in the drybox. The tube was frozen, evacuated on a vacuum line, and sealed. After thawing, the tube was placed in a photolysis set-up held at 5 °C. The solution was irradiated for approximately 4 h. The same mixture of products described above for the photolysis of **1** in t-BuSH was observed. $Cp^*(PMe_3)Ir(S\text{-}tBu)(SH)$ (**4**) (~45%), $Cp^*(PMe_3)Ir(SH)_2$ (**5**) (~5%), $Cp^*(PMe_3)Ir(S\text{-}tBu)_2$ (**3**) (~20%), $Cp^*(PMe_3)Ir(S\text{-}tBu)H$ (**2**) (~25%), and $Cp^*(PMe_3)IrH_2$ (**1**) (~5%).

$Cp^*(PMe_3)Ir(OEt)H$ (6). The (ethoxy)hydride **6** was synthesized using a modification of the procedure described for the PPh_3-substituted analogue $Cp^*(PPh_3)Ir(OEt)H$.[13] In the drybox, 200 mg (0.42 mmol) $Cp^*(PMe_3)IrCl_2$ (**7**) and 115 mg (1.69 mmol) NaOEt were placed in a 250 ml round bottom flask equipped with a magnetic stirbar and a vacuum stopcock. The reaction flask was evacuated on a vacuum line, and approximately 100 ml of EtOH was transferred onto the solids under vacuum at -196 °C. After allowing the ethanol to thaw, the flask was held at 0°C and protected from light. After stirring for 3 hours, ethanol was removed under vacuum. The residue was returned to the drybox and extracted with 50 ml pentane. Removal of pentane gave **6** as a yellow oil, contaminated with ca. 2% $Cp^*(PMe_3)Ir(H)Cl$.[14] Spectroscopic data for **6**: ^{1}H NMR (d^6-benzene) δ 3.92 (m, 2H), 1.78 (dd, J = 2.2, 0.7 Hz, 15H), 1.36 (t, J = 6.8 Hz, 3H), 1.30 (d, J = 10.4 Hz, 9H), -14.02 (d, J = 39.0 Hz, 1H); $^{13}C\{^{1}H\}$ NMR (d^6-benzene) δ 90.0 (d, J = 3.9 Hz), 77.2(s), 24.0 (s), 16.9 (d, J = 37.0 Hz), 10.5 (s); $^{31}P\{^{1}H\}$ NMR (d^6-benzene) δ -33.1 (s); IR (d^6-benzene) : 2956, 2908, 2062, 954 cm^{-1}.

$Cp^*(PMe_3)Ir(SH)H$ (8). In the drybox, 120 mg of crude **6** (approx. 0.27 mmol) was dissolved in 10 ml of benzene and placed in a bomb. The solution was degassed with a freeze-pump-thaw cycle. From a known-volume bulb, 1.5 equiv H_2S (110 torr, 66.34 ml at 298K, 0.40 mmol) was condensed into the solution at -196 °C. The solution was thawed and allowed to stand at room temperature for 2 h. Lyophilization of benzene gave **8** as a yellow, extremely air-sensitive powder. Crystallization from saturated pentane solution at -40 °C in the drybox afforded 87.2 mg (0.20 mmol, 73.8%) of pure **8** as a yellow powder. ^1H NMR (d^6-benzene) δ 1.80 (d, J = 1.7 Hz, 15H),1.60 (s, 9H), 1.35 (d, J = 10.3 Hz, 9H),-16.47 (d, J = 35.1 Hz, 1H); ^{13}C {^1H} NMR (d^6-benzene) δ 93.0 (d, J = 3.4 Hz), 38.1 (s), 35.2 (s), 18.7 (d, J = 40.6 Hz), 10.3 (s); ^{31}P {^1H} NMR (d^6-benzene) δ -38.2 (s); MS (EI) : m/e 494/492 (M^+, $^{193}Ir/^{191}Ir$); IR (KBr pellet) : 2959, 2907, 2096, 958 cm^{-1}; Anal. Calcd. for $C_{17}H_{34}IrPS$: C, 41.36%; H, 6.94%. Found: C, 41.24%; H, 6.96%; mp, 67-77 °C (dec).

$Cp^*(PMe_3)Ir(SMe)H$ (9). The reaction was run using the same procedure as described for compound **8**, starting with 125 mg (approx. 0.28 mmol) of crude **6** and 4.5 equiv MeSH (150 torr, 139.22 ml at 298K, 1.29 mmol). The crude product was crystallized in the drybox from a concentrated pentane solution at -40 °C, giving 77.4 mg (0.17 mmol, 61.2%) of **9** as yellow crystals. ^1H NMR (d^6-benzene) δ 2.53 (s, 3H), 1.86 (d, J = 2.5 Hz, 15H), 1.40 (d, J = 10.2 Hz, 9H), -16.58 (d, J = 36.4 Hz, 1H); ^{13}C {^1H} NMR (d^6-benzene) δ 92.8 (d, J = 3.3 Hz), 20.9 (d, J = 2.1 Hz), 18.8 (d, J = 40.1 Hz), 10.1 (s); ^{31}P {^1H} NMR (d^6-benzene) δ -38.9 (s); IR (KBr pellet) : 2958, 2847, 2114, 953 cm^{-1}; MS (EI) : m/e 452/450 (M^+, $^{193}Ir/^{191}Ir$); Anal. Calcd. for $C_{14}H_{28}IrPS$: C, 37.23%; H, 6.25%. Found: C, 37.22%; H, 6.31%.

$Cp^*(PMe_3)Ir(S\text{-}tBu)H$ (2). The reaction was run using the same procedure as described for compound **8**, starting with 160 mg (approx. 0.36 mmol) of crude **6** and 5 equiv t-BuSH (238 torr, 139.22 ml at 298K, 1.78 mmol). The crude product was crystallized in the drybox from a concentrated pentane solution at -40 °C, giving 154.7 mg (0.31 mmol, 87.0%) of **2** as yellow crystals. ^1H NMR (d^6-benzene) δ 1.80 (d, J = 1.7Hz, 15H), 1.60 (s, 9H), 1.35 (d, J = 10.3 Hz, 9H), -16.47 (d, J = 35.1 Hz, 1H); ^{13}C {^1H} NMR (d^6-benzene) δ 93.0 (d, J = 3.4 Hz), 38.1 (s), 35.2 (s),

18.7 (d, J = 40.6 Hz), 10.3 (s); $^{31}P\{^{1}H\}$ NMR (d^6-benzene) δ -38.2 (s); MS (EI) : m/e 494/492 (M^+, $^{193}Ir/^{191}Ir$); IR (KBr pellet) : 2959, 2907, 2096, 958 cm^{-1}; Anal. Calcd. for $C_{17}H_{34}IrPS$: C, 41.36%; H, 6.94%. Found: C, 41.24%; H, 6.96%; mp, 105-105.5 °C.

X-ray Crystal Structure Determination of Complex 2. Large yellow-brown octahedral crystals of complex 2 were obtained by slow crystallization from pentane at -40 °C. Fragments cleaved from some of these crystals were mounted on glass fibers using polycyanoacrylate cement. Preliminary precession photographs indicated orthorhombic Laue symmetry and yielded approximate cell dimensions.

The crystal used for data collection was then transferred to our Enraf-Nonius CAD-4 diffractometer and centered in the beam. Automatic peak search and indexing procedures yielded the orthorhombic reduced primitive cell. The final cell parameters and specific data collection parameters for this data set are given in Table VI.

The 3003 unique raw intensity data were converted to structure factor amplitudes and their esd's by correction for scan speed, background, and Lorentz and polarization effects. No correction for crystal decomposition was necessary. Inspection of the azimuthal scan data showed a variation I_{min}/I_{max} = 0.78 for the average curve. An empirical correction based on the observed variation was applied to the data. Inspection of the systematic absences indicated uniquely space group Pbca. Removal of systematically absent data left 2646 unique data in the final data set.

The structure was solved by Patterson methods and refined via standard least-squares and Fourier techniques. In a difference Fourier map calculated following the refinement of all non-hydrogen atoms with anisotropic thermal parameters, peaks were found corresponding to the positions of many of the hydrogen atoms on the ligands. These hydrogen atoms were assigned idealized locations and values of B_{iso} approximately 1.3 times the B_{eqv} of the atoms to which they were attached. They were included in structure factor calculations, but not refined. In a subsequent difference Fourier, a peak was found in a position consistent with a hydride ligand. A hydrogen atom was placed there and its position and thermal parameters were refined.

Table VI. Crystal and data collection parameters for complex 2.

Empirical formula: Ir S P C_{17} H_{34}

A)Crystal Parameters at T = 25°C[a,b]

a = 15.5586(15) Å — Space Group: Pbca
b = 15.6966(16) Å — Formula weight = 493.7 amu
c = 16.6142(20) Å — Z = 8
α = 90.0° — d(calc) = 1.62 g cm^{-3}
β = 90.0°
γ = 90.0° — μ(calc) = 67.3 cm^{-1}
V = 4057.5(12) $Å^3$
Size: 0.22x0.37x0.40 mm

B) Data Measurement Parameters
Radiation : Mo Kα (λ = 0.71073 Å)
Monochromator : Highly-oriented graphite (2θ = 12.2)
Detector : Crystal scintillation counter, with PHA.
Reflections measured : + H, + K, + L
2θ range: 3 -> 45 deg — Scan Type: θ-2θ
Scan width: Δθ = 0.60 + 0.35 tanθ
Scan speed: 0.72 -> 6.70 (θ, deg/min)
Background: Measured over 0.25*(Δθ) added to each end of the scan.
Vert. aperture = 3.0 mm — Horiz. aperture = 2.0 + 1.0 tanθ mm
No. of reflections collected: 3003
No. of unique reflections: 2646

Intensity standards: Over the data collection period no decrease in intensity was observed.
Orientation: Reorientation was not needed times during data collection.

a. Unit cell parameters and their esd's were derived by a least-squares fit to the setting angles of the unresolved Mo Kα components of 24 reflections with 2θ between 27° and 29°.
b. In this and all subsequent tables the esd's of all parameters are given in parentheses, right-justified to the least significant digit(s) of the reported value.

Table VII. Positional parameters and their estimated standard deviations for complex **2**.

Atom	x	y	z	B(Å²) [a]
IR	0.07913(1)	0.10413(1)	0.14823(1)	2.897(4)
S	0.22031(8)	0.05123(9)	0.13096(7)	4.11(3)
P	0.0418(1)	-0.02657(8)	0.18717(9)	4.36(3)
C1	0.1214(3)	0.2404(3)	0.1720(3)	3.9(1)
C2	0.0503(3)	0.2415(3)	0.1217(3)	4.0(1)
C3	-0.0196(3)	0.2024(3)	0.1638(3)	4.7(1)
C4	0.0109(3)	0.1813(3)	0.2408(3)	4.4(1)
C5	0.0981(3)	0.2025(3)	0.2459(3)	3.9(1)
C6	0.2098(4)	0.2778(4)	0.1551(4)	7.7(2)
C7	0.0455(5)	0.2828(4)	0.0396(4)	8.2(2)
C8	-0.1117(4)	0.1999(4)	0.1335(5)	9.7(2)
C9	-0.0442(5)	0.1499(4)	0.3098(4)	9.0(2)
C10	0.1541(5)	0.1948(4)	0.3195(4)	8.3(2)
C11	0.0941(5)	-0.0639(4)	0.2779(4)	8.1(2)
C12	0.0620(5)	-0.1127(3)	0.1173(5)	7.2(2)
C13	-0.0710(4)	-0.0445(4)	0.2095(4)	6.8(2)
C14	0.2542(3)	0.0470(3)	0.0241(3)	4.7(1)
C15	0.2357(4)	0.1290(4)	-0.0193(4)	7.2(2)
C16	0.2119(4)	-0.0264(4)	-0.0202(3)	6.2(1)
C17	0.3513(4)	0.0318(5)	0.0273(4)	7.6(2)
N1	0.054(3)	0.060(3)	0.059(3)	3(1)*

[a] Starred atoms were included with isotropic thermal parameters.

Hydrogen Atoms Included but not refined.

Atom	x	y	z	B(Å²) [a]
H6B	0.2519	0.2472	0.1847	9.9*
H6C	0.2221	0.2729	0.0990	9.9*
H6A	0.2108	0.3359	0.1702	9.9*
H7B	0.0992	0.2767	0.0129	10.6*
H7C	0.0018	0.2557	0.0085	10.6*
H7A	0.0322	0.3414	0.0453	10.6*
H8B	-0.1114	0.1952	0.0763	12.4*
H8C	-0.1405	0.1523	0.1558	12.4*
H8A	-0.1403	0.2508	0.1486	12.4*
H9B	-0.0915	0.1185	0.2889	11.7*
H9C	-0.0110	0.1144	0.3439	11.7*
H9A	-0.0651	0.1973	0.3395	11.7*
H10B	0.1354	0.1477	0.3511	10.7*
H10C	0.2120	0.1861	0.3036	10.7*
H10A	0.1500	0.2454	0.3505	10.7*
H11B	0.1545	-0.0647	0.2698	10.4*
H11C	0.0806	-0.0267	0.3211	10.4*
H11A	0.0746	-0.1197	0.2900	10.4*
H12B	0.0312	-0.1028	0.0687	9.3*
H12C	0.1217	-0.1158	0.1059	9.3*
H12A	0.0434	-0.1650	0.1403	9.3*
H13B	-0.0885	-0.0078	0.2517	8.8*
H13C	-0.1043	-0.0330	0.1627	8.8*
H13A	-0.0791	-0.1021	0.2252	8.8*
H15B	0.1758	0.1403	-0.0178	9.4*
H15C	0.2660	0.1742	0.0059	9.4*
H15A	0.2540	0.1242	-0.0738	9.4*
H16B	0.2272	-0.0786	0.0049	7.9*
H16C	0.1510	-0.0197	-0.0182	7.9*
H16A	0.2303	-0.0268	-0.0745	7.9*
H17B	0.3779	0.0775	0.0554	9.9*
H17C	0.3625	-0.0200	0.0545	9.9*
H17A	0.3734	0.0290	-0.0258	9.9*

[a] Starred atoms were included with isotropic thermal parameters.

Table VIII. Anisotropic thermal parameters for complex **2**.

Name	B(1,1)	B(2,2)	B(3,3)	B(1,2)	B(1,3)	B(2,3)	Beqv
IR	3.151(7)	2.464(7)	3.076(7)	-0.120(7)	-0.139(7)	0.017(7)	2.897(4)
S	3.77(5)	4.64(6)	3.93(6)	0.65(5)	-0.22(5)	-0.56(5)	4.11(3)
P	5.60(7)	2.86(5)	4.63(6)	-0.44(6)	-0.29(6)	0.67(5)	4.36(3)
C1	3.7(2)	2.6(2)	5.5(3)	-0.5(2)	0.5(2)	-1.1(2)	3.9(1)
C2	5.7(2)	2.1(2)	4.2(2)	0.4(2)	-0.4(2)	0.0(2)	4.0(1)
C3	3.5(2)	3.3(2)	7.3(3)	0.7(2)	-0.8(2)	-1.8(2)	4.7(1)
C4	5.1(2)	3.1(2)	4.9(2)	-0.2(2)	1.9(2)	-0.9(2)	4.4(1)
C5	4.7(2)	3.3(2)	3.8(2)	0.3(2)	-0.7(2)	-1.0(2)	3.9(1)
C6	5.4(3)	5.2(3)	12.4(5)	-2.1(2)	2.8(3)	-2.0(3)	7.7(2)
C7	15.0(5)	4.0(3)	5.6(3)	2.0(3)	-2.1(4)	1.1(2)	8.2(2)
C8	4.4(3)	6.2(3)	18.4(6)	1.0(3)	-4.0(3)	-3.9(4)	9.7(2)
C9	12.4(4)	5.2(3)	9.4(4)	-1.5(3)	6.8(3)	-1.3(3)	9.0(2)
C10	10.6(4)	7.2(3)	7.0(3)	0.9(4)	-4.3(3)	-2.0(3)	8.3(2)
C11	11.0(4)	6.3(3)	6.9(3)	-0.2(3)	-2.7(3)	2.9(3)	8.1(2)
C12	10.3(4)	3.2(2)	8.0(4)	-1.0(3)	1.3(3)	-0.5(3)	7.2(2)
C13	6.6(3)	5.3(3)	8.5(4)	-2.2(3)	0.9(3)	0.7(3)	6.8(2)
C14	4.5(2)	5.2(3)	4.3(2)	0.1(2)	0.3(2)	-1.2(2)	4.7(1)
C15	10.2(4)	5.5(3)	5.9(3)	-0.3(3)	1.7(3)	0.6(3)	7.2(2)
C16	7.7(3)	6.1(3)	4.6(3)	-0.1(3)	-0.3(3)	-1.1(3)	6.2(1)
C17	4.4(3)	11.5(4)	7.0(3)	0.5(3)	0.7(3)	-2.7(3)	7.6(2)

The final residuals for 186 variables refined against the 2016 data for which $F^2 > 3\sigma(F^2)$ were R = 1.78 %, wR = 2.18 % and GOF = 1.351. The R value for all 2646 data was 5.15 %. In the final cycles of refinement a secondary extinction parameter was included (maximum correction 4% on F).

The quantity minimized by the least squares program was $\Sigma\, w(|F_o|-|F_c|)^2$, where w is the weight of a given observation. The p-factor, used to reduce the weight of intense reflections, was set to 0.02 in the last cycles of refinement due to possible effects of multiple diffraction. The analytical forms of the scattering factor tables for the neutral atoms were used and all scattering factors were corrected for both the real and imaginary components of anomalous dispersion.

Inspection of the residuals ordered in ranges of $\sin(\theta/\lambda)$, $|F_o|$, and parity and value of the individual indexes showed no unusual features or trends. The largest peak in the final difference Fourier map had an electron density of 0.42 $e^-/Å^3$, and the lowest excursion -0.30 $e^-/Å^3$.

The positional and thermal parameters of all atoms are given in Table VII with anisotropic thermal parameters (B's) given in Table VIII.

$Cp^*(PMe_3)Ir(SMe)_2$ (10). In the drybox, 242 mg (0.51 mmol) of $Cp^*(PMe_3)IrCl_2$ (7) and 107 mg (1.53 mmol) NaSMe were placed into a 100 ml Schlenk flask equipped with a stirbar. The flask was sealed with a rubber septum and removed from the drybox. Using standard Schlenk techniques, approximately 30 ml of dry ethanol was cannulated onto the mixture, which was then allowed to stir. The mixture quickly became a yellow, homogeneous solution. After stirring overnight, the rubber septum was replaced with a vacuum stopcock and the ethanol was stripped on the vacuum line. The resulting yellow solid was returned to the drybox, extracted with pentane, and filtered through celite. After concentration, the yellow solution was cooled to -40 °C in the drybox freezer to give 122 mg (0.25 mmol, 48.1%) of **10** as orange needles. ^1H NMR (d^6-benzene) δ 2.09 (s, 6H), 1.58 (d, J = 2.0 Hz, 15H), 1.41 (d, J = 10.3 Hz, 9H); $^{13}C\{^1H\}$ NMR (d^6-benzene) δ 94.2 (d, J = 3.8 Hz),14.6 (d, J = 41.0 Hz), 11.9 (d, J = 3.7 Hz), 8.6 (s); $^{31}P\{^1H\}$ NMR (d^6-benzene) δ - 33.4 (s); IR (KBr pellet) : 2968, 2902, 953 cm^{-1}; MS (EI) : m/e 498/496 (M^+, $^{193}Ir/^{191}Ir$); Anal. Calcd. for $C_{15}H_{30}IrPS_2$: C, 36.20%; H, 6.08%. Found: C, 36.36%; H, 5.95%.

$Cp^*(PMe_3)Ir(S\text{-}tBu)_2$ (3). In the drybox, 180 mg (0.38 mmol) $Cp^*(PMe_3)IrCl_2$ (7) and 95 mg (0.85 mmol) NaS-tBu were placed in a 250 ml round bottom flask equipped with a magnetic stirbar and a vacuum stopcock. The reaction flask was evacuated on a vacuum line, and approximately 100 ml of EtOH was transferred onto the solids under vacuum. The reaction mixture, initially a slurry, was stirred at room temperature for 2 h, giving a yellow, homogeneous solution. The volatile materials were removed under vacuum and the residue returned to the drybox. The residue was extracted with pentane, filtered through celite and concentrated. The concentrated extract was cooled in the drybox freezer (-40 °C) to give 97 mg (0.17 mmol, 43.9%) of **3** as an orange powder. Concentration of the mother liquor and cooling to -40 °C gave a second crop of 22 mg (0.04 mmol, 9.9%) of **3**. ^1H NMR (d^6-benzene, 60°C) δ 1.65 (s, 18H), 1.58 (d, J = 10.2 Hz, 9H), 1.55 (d, J = 2.0 Hz, 15H); $^{13}C\{^1H\}$ NMR (d^6-benzene, 40°C) δ 95.0 (d, J = 3.3 Hz), 40.4 (s), 37.4 (s), 16.7 (d, J = 42.6 Hz), 9.7 (s); $^{31}P\{^1H\}$ NMR (d^6-benzene) δ -35.4 (s); IR (KBr pellet) : 2964, 2910, 952 cm^{-1}; MS (EI) : m/e 720/718/716 ($Cp^*_2Ir_2S_2$), 582/580 (M^+, $^{193}Ir/^{191}Ir$); mp, 128-129°C; Anal. Calcd. for $C_{21}H_{42}IrPS_2$: C, 43.35%; H, 7.28%. Found: C, 43.56%; H, 7.37%; mp, 125-135 °C (dec).

$Cp^*(PMe_3)Rh(S\text{-}tBu)_2$ (14). The reaction was run using the procedure described for compound **3**, starting with 320 mg (0.83 mmol) $Cp^*(PMe_3)RhCl_2$ (**11**) and 112.2 mg (2.08 mmol) NaS-tBu. Crystallization from concentrated pentane solution at -40 °C gave 281 mg (0.57 mmol, 68.7%) of **14** as a red powder. ^1H NMR (d^6-benzene, 60°C) δ 1.65 (s, 18H), 1.54 (d, J = 2.9 Hz, 15H), 1.48 (d, J = 10.2 Hz, 9H); $^{13}C\{^1H\}$ NMR (d^6-benzene, 40°C) δ 99.8 (d, J = 4.0 Hz), 41.9 (d, J = 1.6 Hz), 37.4 (s), 17.7 (d, J = 36.1 Hz), 10.3 (s); $^{31}P\{^1H\}$ NMR (d^6-benzene) δ 5.0 (d, J = 157.2 Hz); MS (FAB, sulfolane) : m/e 523 (M^+ - S-tBu + sulfolane), 492 (M^+); Anal. Calcd. for $C_{21}H_{42}RhPS_2$: C, 51.21%; H, 8.59%. Found: C, 51.31%; H, 8.68%; mp, 120-140 °C (dec).

Reaction of $Cp^*(PMe_3)IrCl_2$ with NaSH. The reaction was run using the procedure described for compound **11**, starting with 684.2 mg (1.44 mmol) $Cp^*(PMe_3)IrCl_2$ (**7**) and 241.6 mg (4.31 mmol) NaSH. The resulting homogeneous solution was bright green. A ^1H NMR spectrum of the crude material showed the mixture to be approximately 85% of the desired

metalladithiol $Cp^*(PMe_3)Ir(SH)_2$ (**5**) and 15% of the green dimer $Cp^*(PMe_3)Ir(\mu\text{-}S)IrCp^*$ (**13**). The two materials were separated by chromatography on Alumina III in the drybox using 10% thf/hexanes as eluent.The band containing the green dimer **13** eluted first. Spectroscopic data for complex **13**: ^1H NMR (d^6-benzene) δ 1.72 (s), 1.72 (d, J = 2.0 Hz, 15H), 1.55 (d, J = 10.2 Hz, 9H); $^{13}C\{^1H\}$ NMR (d^6-benzene) δ 92.7 (d, J = 4.1 Hz), 85.8 (s), 14.6 (d, J = 39.3 Hz), 10.1 (s), 9.0 (d, J = 1.0 Hz); $^{31}P\{^1H\}$ NMR (d^6-benzene) δ -37.8 (s); IR (KBr pellet) : 2969, 2903, 950 cm^{-1}; U. V. (hexanes) λ_{max} 317 ($\varepsilon = 8.8 \times 10^3$), 400 ($\varepsilon = 5.4 \times 10^3$), 690 ($\varepsilon$ = 950).

$Cp^*(PMe_3)Ir(SH)_2$ (5). The reaction was run using a procedure similar to that described for compound **3**, starting with 522.6 mg (1.10 mmol) $Cp^*(PMe_3)IrCl_2$ (**7**) and 171.1 mg (3.05 mmol) NaSH. The solvent (EtOH), however, was charged with 12 equiv H_2S from a known-volume bulb (406 torr, 508.51 ml at 298K, 13.1 mmol) by vacuum transfer at -196 °C prior to addition to the reaction mixture. Within 30 min at room temperature, the solution became bright yellow and homogeneous. The volatile materials were removed under vacuum and the residue returned to the drybox. The residue was extracted with pentane, filtered through celite and the solvent removed under vacuum. This gave 477.4 mg (1.01 mmol, 91.6%) of pure **5**. ^1H NMR (d^6-benzene) δ 1.48 (d, J = 2.0 Hz, 15H), 1.32 (d, J = 10.5 Hz, 9H), -1.93 (d, J = 4.5 Hz, 2H); $^{13}C\{^1H\}$ NMR (d^6-benzene) δ 93.0 (d, J = 3.6 Hz), 14.3 (d, J = 41.8 Hz), 8.8 (s); $^{31}P\{^1H\}$ NMR (d^6-benzene) δ - 33.4 (s); IR (KBr pellet) : 2970, 2911, 2521, 2496, 955 cm^{-1}; MS (EI): m/e 720/718/716 ($Cp^*_2Ir_2S_2$), 470/468 (M^+, $^{193}Ir/^{191}Ir$); Anal. Calcd. for $C_{13}H_{26}IrPS_2$: C, 33.25%; H, 5.58%. Found: C, 33.14%; H, 5.62%; mp, 155-158 °C (dec).

X-ray Crystal Structure Determination of Complex 5. Orange-yellow tabular crystals of complex **5** were obtained by slow crystallization from toluene at -40 °C. Some of these crystals were mounted on glass fibers using polycyanoacrylate cement.

The crystal used for data collection was then transferred to our Enraf-Nonius CAD-4 diffractometer and centered in the beam. It was cooled to -85 °C by a nitrogen flow low-temperature apparatus which had been previously calibrated by a thermocouple placed at the sample position. Automatic peak search and indexing procedures yielded the orthorhombic

reduced primitive cell. Inspection of the Niggli values revealed no conventional cell of higher symmetry. The final cell parameters and specific data collection parameters for this data set are given in Table IX.

The 4357 raw intensity data were converted to structure factor amplitudes and their esd's by correction for scan speed, background, and Lorentz and polarization effects. No correction for crystal decomposition was necessary. Inspection of the azimuthal scan data showed a variation $I_{min}/I_{max} = 0.74$ for the average curve. An empirical correction based on the observed variation was applied to the data. Inspection of the systematic absences indicated uniquely space group Pbca. Removal of systematically absent data left 3851 unique data in the final data set.

The structure was solved by Patterson methods and refined via standard least-squares and Fourier techniques. In a difference Fourier map calculated following the refinement of all non-hydrogen atoms with anisotropic thermal parameters, peaks were found corresponding to the positions of most of the hydrogen atoms. Hydrogen atoms were predicted idealized locations, then refined with isotropic thermal parameters. Before the refinement, twelve data which were apparently due to multiple diffraction were removed from the data set. In the final cycles of refinement a secondary extinction parameter was included (maximum correction 24% on F).

The final residuals for 259 variables refined against the 2554 accepted data for which $F^2 > 3\sigma(F^2)$ were R = 3.14 %, wR = 3.46 % and GOF = 1.45. The R value for all 3851 data was 6.01 %.

The quantity minimized by the least squares program was $\Sigma\, w(|F_o|-|F_c|)^2$, where w is the weight of a given observation. The p-factor, used to reduce the weight of intense reflections, was set to 0.03 throughout the refinement. The analytical forms of the scattering factor tables for the neutral atoms were used and all scattering factors were corrected for both the real and imaginary components of anomalous dispersion.

Inspection of the residuals ordered in ranges of $\sin(\theta/\lambda)$, $|F_o|$, and parity and value of the individual indexes showed no unusual features or trends. The largest peak in the final difference Fourier map had an electron density of 2.09 $e^-/Å^3$, and the lowest excursion -1.53 $e^-/Å^3$. All large excursions were located near the iridium atom.

Table IX. Crystal and data collection parameters for complex **5**.

Empirical formula: $IrS_2PC_{13}H_{26}$

A) Crystal Parameters at T = -85°C [a,b]

a = 8.8211(14) Å
b = 14.848(3) Å
c = 25.648(6) Å
α = 90.0°
β = 90.0°
γ = 90.0°
V = 3359(2) Å^3
Size: 0.13x0.24x0.44 mm

Space Group: Pbca
Formula weight = 469.7 amu
Z = 8
d(calc) = 1.86 g cm^{-3}
μ(calc) = 82.3 cm^{-1}

B) Data Measurement Parameters
Radiation : Mo Kα (λ = 0.70926 Å)
Monochromator : Highly-oriented graphite (2θ = 12.2)
Detector : Crystal scintillation counter, with PHA.
Reflections measured : + H, + K, + L
2θ range: 3 -> 55 deg Scan Type: ω
Scan width: Δω = 0.70 + 0.35 tanθ
Scan speed: 7.87 -> 5.03 (ω, deg/min)
Background: Measured over 0.25*(Δω) added to each end of the scan.
Vert. aperture = 3.0 mm Horiz. aperture = 2.0 + 1.0 tanθ mm
No. of reflections collected: 4357
No. of unique reflections: 3851

Intensity standards: (294),(392),(2,7,12); measured every 1 hours of x-ray exposure time. Over the data collection period no decrease in intensity was observed.
Orientation: Three reflections were checked after every 200 measurements. Crystal orientation was redetermined if any of the reflections were offset by more than 0.10 degree from their predicted positions. Reorientation was not needed during data collection.

a Unit cell parameters and their esd's were derived by a least-squares fit to the setting angles of the unresolved Mo Kα components of 24 reflections with 2θ between 28° and 28°.

b In this and all subsequent tables the esd's of all parameters are given in parentheses, right-justified to the least significant digit(s) of the reported value.

The positional and thermal parameters of all atoms are given in Table X with anisotropic thermal parameters (B's) given in Table XI.

Reaction of $Cp^*(PMe_3)IrCl_2$ with Na_2S. In the drybox, 18.0 mg (0.04 mmol) $Cp^*(PMe_3)IrCl_2$ (7) and 5 mg (0.06 mmol) Na_2S were placed in a 50 ml round bottom flask equipped with a magnetic stirbar and a vacuum stopcock. The reaction flask was evacuated on a vacuum line, and approximately 25 ml of EtOH was transferred onto the solids under vacuum. Upon thawing, the resulting homogeneous solution turned bright green. After removal of ethanol, the resulting green residue was returned to the drybox and chromatographed on Alumina III using 10% thf/hexanes as eluent. The bright green band was collected, stripped under vacuum, and lyophilized from benzene. This gave 6.8 mg (0.009 mmol, 47.0%) of the dimer **13** as a green powder.

Reaction of $Cp^*(PMe_3)RhCl_2$ with NaSH: The reaction was run using the procedure for the reaction of the iridium dichloride **7** with NaSH described above, starting with 507 mg (1.32 mmol) $Cp^*(PMe_3)RhCl_2$ (**11**) and 150 mg (2.67 mmol) NaSH. The resulting homogeneous solution was dark magenta. A ^1H NMR spectrum of the crude material showed it to be a mixture of the desired metalladithiol $Cp^*(PMe_3)Rh(SH)_2$ (**14**) (~25%) and the magenta dimer $Cp^*(PMe_3)Rh(\mu\text{-}S)IrCp^*$ (**15**) (~75%). The two materials were separated by chromatography on Alumina III in the drybox using 10% thf/hexanes as eluent. The band containing the magenta dimer **15** eluted first. Spectroscopic data for complex **15**: ^1H NMR (d^6-benzene) δ 1.68 (d, J = 2.6 Hz, 15H), 1.60 (s, 15H), 1.41 (dd, J = 10.2, 0.7 Hz, 9H); $^{13}C\{^1H\}$ NMR (d^6-benzene) δ 97.4 (dd, J = 4.2, 4.0 Hz), 91.8 (d, J = 6.3 Hz), 16.4 (d, J = 33.3 Hz), 10.2 (s), 9.7 (s).

$Cp^*(PMe_3)Rh(SH)_2$ (14). The reaction was run using a procedure similar to that described for compound **5**, starting with 217 mg (0.56 mmol) $Cp^*(PMe_3)RhCl_2$ (**11**) and 84.0 mg (1.50 mmol) NaSH. The solvent (EtOH) was charged with 50 equiv H_2S from a known-volume bulb (2 x 400 then 1 x 200 torr, 508.51 ml at 298K, 27.8 mmol) prior to addition to the reaction mixture. Within 5 min at room temperature, the solution became bright orange and homogeneous. The volatile materials were removed under vacuum and the residue returned to

Table X. Positional parameters and their estimated standard deviations for complex **5**.

Atom	x	y	z	B(Å²)[a]
IR	0.13194(2)	0.03047(2)	0.12428(1)	1.431(4)
S1	0.3734(2)	-0.0308(1)	0.14573(8)	3.10(4)
S2	0.1281(2)	-0.0625(1)	0.04918(7)	2.51(3)
P	0.2561(2)	0.1361(1)	0.07756(7)	2.07(3)
C1	-0.0162(8)	0.1206(5)	0.1698(3)	2.1(1)
C2	-0.1054(8)	0.0653(5)	0.1359(2)	2.3(1)
C3	-0.0912(8)	-0.0254(5)	0.1535(3)	2.9(2)
C4	0.0153(9)	-0.0291(5)	0.1947(3)	2.6(1)
C5	0.0641(8)	0.0624(5)	0.2045(3)	2.3(1)
C6	-0.020(1)	0.2204(5)	0.1733(4)	3.7(2)
C7	-0.2217(8)	0.0980(7)	0.0977(3)	4.4(2)
C8	-0.1787(9)	-0.1016(6)	0.1301(4)	5.1(2)
C9	0.063(1)	-0.1100(6)	0.2244(3)	5.3(2)
C10	0.165(1)	0.0903(7)	0.2483(3)	4.5(2)
C11	0.1370(9)	0.2094(5)	0.0384(3)	3.2(2)
C12	0.3634(8)	0.2139(5)	0.1171(3)	3.0(2)
C13	0.3954(9)	0.0985(6)	0.0302(3)	3.6(2)
H6A	-0.109(7)	0.236(5)	0.191(3)	4(2)*
H6B	0.056(8)	0.245(5)	0.186(3)	6(2)*
H6C	-0.02(1)	0.255(9)	0.132(4)	14(5)*
H7A	-0.306(8)	0.098(5)	0.111(2)	3(2)*
H7B	-0.195(9)	0.159(5)	0.085(3)	6(2)*
H7C	-0.23(1)	0.055(6)	0.067(4)	9(3)*
H8A	-0.271(8)	-0.095(5)	0.133(2)	3(2)*
H8B	-0.14(1)	-0.108(7)	0.084(4)	12(4)*
H8C	-0.147(9)	-0.147(6)	0.147(4)	7(3)*
H9A	0.022(8)	-0.114(5)	0.263(3)	4(2)*
H9B	0.034(8)	-0.162(5)	0.210(3)	6(2)*
H9C	0.18(1)	-0.116(6)	0.225(4)	9(3)*
H10A	0.105(8)	0.088(5)	0.281(3)	5(2)*
H10B	0.24(1)	0.060(5)	0.254(3)	7(2)*
H10C	0.195(9)	0.159(5)	0.246(3)	6(2)*
H11A	0.202(9)	0.256(6)	0.027(3)	7(3)*
H11B	0.073(8)	0.172(5)	0.014(3)	5(2)*
H11C	0.064(7)	0.247(5)	0.062(3)	3(2)*
H12A	0.435(8)	0.254(5)	0.091(3)	5(2)*
H12B	0.269(9)	0.244(5)	0.143(3)	6(2)*
H12C	0.438(9)	0.184(6)	0.133(3)	5(2)*
H13A	0.454(8)	0.153(4)	0.018(3)	4(2)*
H13B	0.47(1)	0.057(6)	0.047(4)	8(3)*
H13C	0.342(7)	0.074(4)	0.006(2)	2(1)*
H1	0.43(2)	0.014(9)	0.168(6)	16(5)*
H2	0.26(2)	-0.09(1)	0.055(6)	24(7)*
CP	-0.0266	0.0387	0.1716	

[a] Starred atoms were included with isotropic thermal parameters.

Table XI. Anisotropic thermal parameters for complex **5**.

Name	B(1,1)	B(2,2)	B(3,3)	B(1,2)	B(1,3)	B(2,3)	Beqv
IR	1.492(8)	1.600(8)	1.200(7)	0.11(1)	-0.041(9)	0.028(9)	1.431(4)
S1	2.06(7)	4.37(9)	2.87(7)	1.00(9)	-0.20(6)	0.85(7)	3.10(4)
S2	3.21(8)	2.53(7)	1.79(6)	-0.04(7)	0.18(7)	-0.52(6)	2.51(3)
P	2.06(7)	2.26(7)	1.90(6)	-0.50(7)	-0.13(7)	0.27(6)	2.07(3)
C1	2.1(3)	2.3(3)	1.9(3)	0.4(2)	1.0(2)	-0.0(2)	2.1(1)
C2	1.9(3)	3.5(3)	1.6(3)	0.2(3)	-0.1(2)	-1.2(2)	2.3(1)
C3	2.6(3)	3.0(3)	3.3(3)	-0.8(3)	1.4(3)	-0.7(3)	2.9(2)
C4	3.5(3)	2.1(3)	2.4(3)	0.7(3)	1.4(3)	0.5(3)	2.6(1)
C5	2.2(3)	3.6(3)	1.2(2)	0.5(3)	-0.2(2)	0.2(2)	2.3(1)
C6	4.1(4)	2.2(3)	4.8(4)	0.5(3)	1.4(4)	-0.9(3)	3.7(2)
C7	1.5(3)	8.4(6)	3.4(4)	1.4(4)	-0.6(3)	-0.6(4)	4.4(2)
C8	2.7(3)	5.1(4)	7.6(5)	-1.8(3)	2.2(4)	-3.5(4)	5.1(2)
C9	8.3(5)	3.6(4)	4.0(4)	2.5(4)	3.5(4)	2.1(3)	5.3(2)
C10	4.0(4)	7.7(5)	1.6(3)	1.3(4)	-0.6(3)	-1.1(4)	4.5(2)
C11	3.4(3)	2.9(3)	3.5(3)	-0.3(3)	-0.4(3)	0.8(3)	3.2(2)
C12	2.7(3)	3.4(3)	3.1(3)	-1.1(3)	-1.0(3)	-0.0(3)	3.0(2)
C13	3.1(3)	4.9(4)	2.7(3)	-1.1(4)	0.7(3)	-0.3(3)	3.6(2)

the drybox. The residue was extracted with pentane, filtered through celite and concentrated under vacuum. Crystallization at -40 °C in the drybox gave 85.4 mg (0.22 mmol, 40.1%) of pure **14**. ^{1}H NMR (d^6-benzene) δ 1.45 (d, J = 3.0 Hz, 15H), 1.22 (d, J = 10.4 Hz, 9H), -2.07 (dd, J = 3.9, 0.6 Hz, 2H); $^{13}C\{^{1}H\}$ NMR (d^6-benzene) δ 98.6 (dd, J = 4.8, 3.2 Hz), 15.7 (d, J = 36.0 Hz), 9.3 (s); $^{31}P\{^{1}H\}$ NMR (d^6-benzene) δ 8.2 (d, J = 144.4 Hz); MS (EI): m/e 380 (M^+); mp, 144-158 °C (dec).

Reaction of $Cp^*(PMe_3)RhCl_2$ with Na_2S. In the drybox, 24.7 mg (0.06 mmol) $Cp^*(PMe_3)RhCl_2$ (**11**) and 5 mg (0.06 mmol) Na_2S were placed in a 50 ml round bottom flask equipped with a magnetic stirbar and a vacuum stopcock. The reaction flask was evacuated on a vacuum line, and approximately 25 ml of EtOH was transferred onto the solids under vacuum. Upon thawing, the resulting homogeneous solution turned bright magenta. After removal of ethanol, the resulting purple/red residue was returned to the drybox and chromatographed on Alumina III using 10% thf/hexanes as eluent. The magenta band was collected, stripped under vacuum, and lyophilized from benzene. This gave 11.6 mg (0.04 mmol, 62.0%) of the dimer **15** as a magenta powder.

$Cp^*(PMe_3)Ir(S\text{-}tBu)Cl$ (16). In the drybox, 35.0 mg (0.06 mmol) of the bis-(*tert*-butyl) thiolate **3** was dissolved in 2 ml acetone and placed in a vial equipped with a magnetic stirbar. To the stirring solution was added an acetone slurry of 7.8 mg (0.06 mmol) aniline hydrochloride. After stirring 8 hours, the acetone was removed under vacuum. The residue was extracted with pentane, concentrated, and cooled to -40 °C in the drybox freezer to give 23.7 mg (0.04 mmol, 74.7%) of **16** as an orange powder. ^{1}H NMR (d^6-benzene) δ 1.80(s, 9H),1.41 (d, J = 2.3 Hz, 15H), 1.40 (d, J = 10.7 Hz, 9H); $^{13}C\{^{1}H\}$ NMR (d^6-benzene) δ 93.0 (d, J = 3.0 Hz), 42.0 (s), 36.6 (s), 13.7 (d, J = 41.6 Hz), 8.6 (s); $^{31}P\{^{1}H\}$ NMR (d^6-benzene) δ -28.8 (s); MS (EI) : m/e 528/526 (M^+, $^{193}Ir/^{191}Ir$); IR (KBr pellet) : 2956, 2912, 953 cm^{-1}; Anal. Calcd. for $C_{17}H_{33}ClIrPS$: C, 38.66%; H, 6.31%. Found: C, 39.05%; H, 6.33%.

$Cp^*(PMe_3)Rh(S\text{-}tBu)Cl$ (17): The reaction was run using the procedure described for compound **16**, starting with 26.0 mg (0.05 mmol) $Cp^*(PMe_3)Rh(S\text{-}tBu)_2$ (**12**) and 6.9 mg (4.31

mmol) aniline hydrochloride. The crude product was crystallized from pentane at -40 °C to give 17.8 mg (0.04 mmol, 76.8%) of **17** as red microcrystals. ^{1}H NMR (d^6-benzene) δ 1.79(s, 9H),1.38 (d, J = 3.1 Hz, 15H), 1.32 (d, J = 11.2 Hz, 9H); ^{13}C {^{1}H} NMR (d^6-benzene) δ 99.0 (dd, J = 5.1, 3.7 Hz), 43.1 (d, J = 2.2 Hz), 36.4 (s), 14.9 (d, J = 35.7 Hz), 9.1 (s); ^{31}P {^{1}H} NMR (d^6-benzene) δ 11.0 (d, J = 142.6 Hz); IR (KBr pellet) : 2964, 2911, 947 cm^{-1}.

Reaction of $Cp^*(PMe_3)Ir(S\text{-}tBu)Cl$ (16) with NaOEt. In the drybox, 2.0 mg (0.0038 mmol) of **16** and 0.5 mg (0.007 mmol) NaOEt were loaded into a 50 ml round bottom flask equipped with a magnetic stirbar and vacuum stopcock. The reaction flask was evacuated on a vacuum line, and approximately 25 ml of EtOH was transferred onto the solids under vacuum. The initially bright yellow solution paled considerably over 1 h. Removal of ethanol under vacuum left 1.64 mg (0.0033 mmol, 88%) of a pale yellow residue. The residue was extracted into d^6-benzene and filtered to afford an NMR sample. The material produced in the reaction was identical to **2** and found to be at least 95% pure by ^{1}H NMR spectroscopy.

Reaction of $Cp^*(PMe_3)Rh(S\text{-}tBu)Cl$ (17) with NaOEt. A sample 23.3 mg of a mixture of **17** and residual bis-thiolate **12** along with 4 mg (0.06 mmol) NaOEt were placed into a 50 ml Schlenk flask equipped with a magnetic stirbar and vacuum stopcock. The flask was evacuated on the vacuum line and approximately 20 ml EtOH was condensed in at -78 °C. The mixture was moved to a constant temperature bath held at -40 °C and stirred for 48 h. The ethanol was then removed under vacuum at -20 °C. Approximately 1 ml of d^8-toluene, pre-cooled to -30 °C was cannulated onto the sample to afford an NMR sample. Analysis of the mixture by ^{1}H NMR spectroscopy showed approximately 50% conversion to the thiolate hydride **18**. Spectroscopic data for **18**: ^{1}H NMR (d^8-toluene) δ 1.76 (d, J = 1.8 Hz, 15H), 1.55 (s, 9H), 1.18 (d, J = 10.3 Hz, 9H), -13.01 (dd, J = 45.8, 24.4 Hz, 1H).

$Cp^*(PMe_3)Ir(SH)Me$ (20), Method A: In the drybox, 60.5 mg (0.14 mmol) of $Cp^*(PMe_3)IrMe_2$ (**19**) was loaded into a bomb and dissolved in 5 ml of benzene. The solution was degassed with a freeze-pump-thaw cycle. From a known-volume bulb, 2 equiv H_2S (78.5 torr, 66.34 ml at 298K, 0.28 mmol) was condensed into the solution at -196 °C. The bomb was placed

in a bath at 65 °C for 6 weeks. Removal of solvent in the drybox gave 42.2 mg (0.09 mmol, 66.7%) of **20** as a yellow powder, pure by ^{1}H NMR spectroscopy. ^{1}H NMR (d^6-benzene) δ 1.55 (d, J = 1.9 Hz, 15H), 1.17 (d, J = 10.0 Hz, 9H), 0.66 (d, J = 6.3 Hz, 3H), -2.57 (d, J = 4.4 Hz, 1H); ^{13}C {^{1}H} NMR (d^6-benzene) δ 91.9 (d, J = 3.8 Hz), 14.1 (d, J = 38.6 Hz), 8.8 (s), -23.4 (d, J = 9.7 Hz); ^{31}P {^{1}H} NMR (d^6-benzene) δ -37.8 (s).

$Cp^*(PMe_3)Ir(SH)Me$ (20), Method B: In the drybox, 9.0 mg (0.02 mmol) $Cp^*(PMe_3)Ir(Cl)Me$ (**21**) and 10.0 mg (0.18 mmol) NaOEt were placed in a 50 ml round bottom flask equipped with a magnetic stirbar and a vacuum stopcock. The reaction flask was evacuated on a vacuum line, and approximately 15 ml of EtOH was transferred onto the solids under vacuum. After stirring for 2 h, the volatile materials were removed under vacuum and the residue returned to the drybox. The residue was extracted with pentane, filtered through celite and stripped. This gave 8.7 mg (0.02 mmol, 96.3%) of **20** as a yellow powder. The product was dissolved in d^6-benzene to afford an NMR sample, which showed the product to be pure by ^{1}H NMR spectroscopy.

$Cp^*(PMe_3)Ir(SCMe_2S)$ (22): In the drybox, 174 mg (0.37 mmol) of the metalladithiol **5** was placed in a 100 ml round bottom flask equipped with a magnetic stirbar and dissolved in 50 ml acetone. To the stirring solution was added an acetone slurry of 60.9 mg (0.47 mmol) aniline hydrochloride. After stirring 3 hours, the acetone was removed under vacuum. The residue was extracted with hexanes and chromatographed on Alumina III. The product was stripped and redissolved in a minimum amount of toluene. The toluene solution was layered with pentane and cooled to -40 °C in the drybox freezer to give 122 mg (0.24 mmol, 64.7%) of **22** as yellow crystals. ^{1}H NMR (d^6-benzene) δ 2.02 (s, 3H), 1.81 (s, 3H),1.59 (d, J = 2.0Hz, 15H), 1.51 (d, J = 10.3 Hz, 9H); ^{13}C {^{1}H} NMR (d^6-benzene) δ 93.7 (d, J = 3.5 Hz), 68.1 (s), 44.8 (s), 43.4 (s), 15.6 (d, J = 42.0 Hz), 9.4 (s); ^{31}P {^{1}H} NMR (d^6-benzene) δ -29.6 (s); MS (FAB) : m/e 510/508 (M^+, ^{193}Ir/^{191}Ir); IR (KBr pellet) : 2975, 2911, 2902, 954 cm^{-1}; Anal. Calcd. for $C_{16}H_{30}IrPS_2$: C, 37.70%; H, 5.93%. Found: C, 37.58%; H, 5.93%.

X-ray Crystal Structure Determination of Complex 22. Yellow crystals of complex **22** were obtained by slow crystallization from toluene/heptane at -40 °C. Fragments cleaved from some of these crystals were mounted on glass fibers using polycyanoacrylate cement.

The crystal used for data collection was then transferred to our Enraf-Nonius CAD-4 diffractometer and centered in the beam. Automatic peak search and indexing procedures yielded the reduced monoclinic primitive cell. The final cell parameters and specific data collection parameters for this data set are given in Table XII.

The 2830 unique raw intensity data were converted to structure factor amplitudes and their esd's by correction for scan speed, background, and Lorentz and polarization effects. No correction for crystal decomposition was necessary. Inspection of the azimuthal scan data showed a variation $I_{min}/I_{max} = 0.42$ for the average curve. An empirical correction based on the observed variation was applied to the data. Inspection of the systematic absences indicated uniquely space group P21/c. Removal of systematically absent data left 2501 unique data in the final data set. The structure was solved by Patterson methods and refined via standard least-squares and Fourier techniques.

The final residuals for 101 variables refined against the 2257 data for which $F^2 > 3\sigma(F^2)$ were R = 3.8 %, wR = 5.2 % and GOF = 2.73. The R value for all 2501 data was 4.3%.

The quantity minimized by the least squares program was $\Sigma\, w(|F_o|-|F_c|)^2$, where w is the weight of a given observation. The p-factor, used to reduce the weight of intense reflections, was set to 0.03 in the last cycles of refinement due to possible effects of multiple diffraction. The analytical forms of the scattering factor tables for the neutral atoms were used and all scattering factors were corrected for both the real and imaginary components of anomalous dispersion.

The positional and thermal parameters of the non-hydrogen atoms are given in the Table XIII.

$Cp^*(PMe_3)Ir(SC(S)H)(SH)$ (23). In the drybox, 67.6 mg (0.16 mmol) $Cp^*(PMe_3)Ir(SH)H$ **8** was dissolved in 10 ml benzene and loaded into a bomb. The solution was degassed with a freeze-pump-thaw cycle. From a known-volume bulb, CS_2 (55.0 torr, 66.34 ml at 298K, 0.19 mmol) was condensed into the solution at -196 °C. The solution was thawed, protected from light,

Table XII. Crystal and data collection parameters for complex 22.

Empirical formula: $IrS_2PC_{16}H_{30}$

A)Crystal Parameters at T = -85 C [a,b]

a = 10.1610(20) A
b = 10.2040(20) A
c = 19.127(2) A
alpha = 90.0 deg
beta = 104.28(2) deg
gamma = 90.0 deg
V = 1921.9(12) A3
Size: 0.20x0.45x0.50 mm

Space Group: P21/c
Formula weight = 589.7 amu
Z = 4
d(calc) = 1.76 g cm-3

μ(calc) = 72.0 cm-1

B) Data Measurement Parameters

Radiation : Mo Kalpha (lambda = 0.71073 A)
Monochromator : Highly-oriented graphite (2theta = 12.2)
Diffractometer : Enraf-Nonius CAD-4
Reflections measured : + H, + K, +/-L
2theta range: 3 -> 45 deg
Scan Type: theta-2theta
Scan width: delta theta = 0.70 + 0.35 tan theta
Scan speed: 5.03 (theta, deg/min)
Background: Measured over 0.25*(delta theta) added to each end of the scan.
Vert. aperture = 3.0 mm
Horiz. aperture = 2.0 + 1.0 tan theta mm
No. of reflections collected: 2830

C) Data reduction and refinement

Intensity standards were measured every 1 hours of x-ray exposure time.
No correction for crystal decay was necessary.
Empirical absorption correction based on azimuthal scan data:
Tmax= 0.997, Tmin= 0.422
No. of atoms in least-squares: 20
No. of unique reflections: 2501
No. of reflections with Fsq>3*sigma(Fsq) : 2257

Final residuals:
R = 3.8%
Rall = 4.3%
wR = 5.2%
p-factor = 0.03
G.O.F. = 2.73
No. parameters = 181

a. Unit cell parameters and their esd's were derived by a least-squares fit to the setting angles of the unresolved Mo Kalpha components of 24 reflections with 2theta between 22 deg and 30 deg.
b. In this table the esd's of all parameters are given in parentheses, right-justified to the least significant digit(s) of the reported value.

Table XIII. Positional parameters and their estimated standard deviations for complex 22.

Atom	x	y	z	B(A2)[a]
IR	0.21025(3)	0.16930(3)	0.38818(2)	1.445(8)
S1	0.4068(2)	0.2957(3)	0.4343(1)	2.16(5)
S2	0.1715(3)	0.3745(3)	0.3303(1)	2.29(5)
P	0.2972(3)	0.0982(3)	0.2980(1)	2.07(5)
C1	0.0034(9)	0.104(1)	0.3893(5)	1.8(2)*
C2	0.0917(9)	-0.008(1)	0.4006(4)	2.0(2)*
C3	0.1993(9)	0.014(1)	0.4673(5)	2.2(2)*
C4	0.167(1)	0.135(1)	0.4979(5)	2.1(2)*
C5	0.047(1)	0.191(1)	0.4500(5)	2.2(2)*
C6	-0.120(1)	0.123(1)	0.3312(6)	3.1(2)*
C7	0.071(1)	-0.134(1)	0.3586(5)	2.6(2)*
C8	0.300(1)	-0.000(1)	0.5021(5)	3.0(2)*
C9	0.245(1)	0.193(1)	0.5673(5)	2.8(2)*
C10	-0.025(1)	0.316(1)	0.4603(6)	3.4(2)*
C11	0.3176(9)	0.448(1)	0.3956(5)	2.2(2)*
C12	0.404(1)	0.532(1)	0.3596(5)	3.2(2)*
C13	0.271(1)	0.526(1)	0.4537(5)	3.1(2)*
C14	0.401(1)	-0.051(1)	0.3176(6)	4.0(3)*
C15	0.172(1)	0.059(1)	0.2151(5)	3.3(2)*
C16	0.413(1)	0.206(1)	0.2662(6)	3.5(2)*

[a] Starred atoms were included with isotropic thermal parameters.

and left at room temperature for 18 h. Removal of solvent left a yellow oil. The crude product was returned to the drybox and dissolved in d^6-benzene. Analysis by ^1H NMR spectroscopy showed **23** to be the only product. Attempts to isolate the material as a solid failed due to slow decomposition in solution. ^1H NMR (d^6-benzene) δ 11.97 (s, 1H), 1.46 (d, J = 1.6 Hz, 15H), 1.33 (d, J = 10.8 Hz, 9H), -2.01 (d, J = 4.8 Hz, 1H); ^{13}C {^1H} NMR (d^6-benzene) δ 230.8 (s), 94.4 (d, J = 3.2 Hz), 15.2 (d, J = 40.5 Hz), 8.8 (s); ^{31}P {^1H} NMR (d^6-benzene) δ -37.7 (s); IR (d^6-benzene) : 2977, 2910, 2530, 1016, 954, 680 cm^{-1}.

Reaction of $Cp^*(PMe_3)Ir(SCMe_2S)$ (22) with H_2S. In the drybox, 23.0 mg (0.045 mmol) of the metallacycle **22** was dissolved in 1 ml d^6-benzene and placed in a Wilmad 505-PS 8" NMR tube fitted with a Cajon adaptor. The solution was frozen and the tube evacuated on a vacuum line. From a known-volume bulb, 7.5 equiv H_2S (95 torr, 66.34 ml at 298K, 0.34 mmol) was condensed into the solution at -196 °C. The solution was thawed and placed in a bath held at 80 °C for 24 h. The tube was then placed in an NMR tube cracker and the volatile materials removed to another NMR tube, leaving 20.6 mg (0.044 mmol, 97.8%) of the metalladithiol **5**. Analysis of the volatile materials by ^1H NMR spectroscopy showed one product, presumably 2,2-propanedithiol. ^1H NMR (d^6-benzene) δ 2.44 (septet, J = 0.6 Hz, 2H), 1.51 ppm (t, J = 0.6 Hz). [Lit.[21c] ^1H NMR (CCl_4) δ 2.63 (m), 1.86 (t)].

References

1. (a) Gates, B. C.; Katzer, J. R.;Schuit, G. C. A. In *Chemistry of Catalytic Processes*; McGraw Hill: New York, 1979; Chapter 5. (b) Masoth, F. E. *Adv. Catal.* **1978**, *27*, 265. (c) Chianelli, R. R.; Pecoraro, T. A. *J. Catal.* **1981**, *67*, 430. (d) Chianelli, R. R. *Catal. Rev.-Sci. Eng.* **1984**, *26*, 361. (e) Chianelli, R. R.; Pecoraro, T. A.; Halbert, T. R.; Pan, W. H. Stiefel, E. I. *J. Catal.* **1984**, *86*, 226. (f) Chianelli, R. R.; Harris, S. *J. Catal.* **1984**, *86*, 400. (g) Angelici, R. J. *Acc. Chem. Res.* **1988**, *21*, 387.

2. (a) Spies, G. H.; Angelici, R. J. *J. Am. Chem. Soc.* **1985**, *107*, 5569. (b) Sanchez-Delgado, R. A.; Marquez-Silva, R. L.; Puga, J.; Tiripicchio, A.; Camellini, M. T. *J. Organomet. Chem.* **1986**, *316*, C35. (c) Spies, G. H.; Angelici, R. J. *Organometallics* **1987**, *6*, 1897. (d) Chen, J.; Angelici, R. J. *Organometallics* **1989**, *8*, 2277.

3. See: (a) Kuehn, C. G.; Isied, S. S. *Prog. Inorg. Chem.*, **1980**, *27*, 153, and references therein. (b) Kopf, H.; Schmidt, M. *Angew. Chem. Int. Ed. Engl.*, **1965**, *4*, 953.(c) Green, M. L. H.; Lindsell, W. E. *J. Chem. Soc. A*, **1967**, 1455. (d) Kirillova, N. I.; Gusev, A. I.; Pasynskii, A. A.; Struchkov, Y. T. *J. Struct. Chem.*, **1973**, *14*, 812. (e) Briant, C. E.; Hughes, G. R.; Minshall, P. C.; Mingos, D. M. P. *J Organomet. Chem.* **1980**, *202*, C18. (f) Gaffney, T. R.; Ibers, J. A. *Inorg. Chem.*, **1982**, *21*, 2857. (g) Rauchfuss, T. B.; Ruffig, C. J. *Organometallics*, **1982**, *1*, 400. (h) Ghilardi, C. A.; Midollini, S.; Nuzzi, F.; Orlandini, A. *Transition Met. Chem.* **1983**, *8*, 73. (i) Mueting, A. M.; Boyle, P.; Pignolet, L. H. *Inorg. Chem.*, **1984**, *23*, 44. (j) Rauchfuss, T. B.; Ruffing, C. J. *Organometallics*, **1985**, *4*, 524. (k) Bottomley, F.; Drummond, D. F.; Egharevba, G. O.; White, P. S. *Organometallics*, **1986**, *5*, 1620.

4. (a) Kopf, H.; Schmidt, M. *J. Organomet. Chem.*, **1965**, *4*, 426. (b) Kopf, H.; Schmidt, M. *Z. Anorg. Chem.*, **1965**, *340*, 139. (c) Giddings, S. A. *Inorg. Chem.*, **1967**, *6*, 849. (d) Harris, M. G.; Green, M. L. H.; Lindsell, W. E. *J. Chem. Soc. A*, **1969**, 1453. (e) Dias, A. R.; Green, M. L. H. *J. Chem. Soc. A*, **1971**, 2807. (f) Sato, M.; Yoshida, T. *J. Organomet. Chem.*, **1972**, *39*,

389. (g) Davidson, J. L.; Shiralian, M.; Manojlovic-Muir, L.; Muir, K. W. *J. Chem. Soc., Dalton Trans.*, **1984**, 2167.

5. Liaw, W.; Kim, C.; Darensbourg, M. Y.; Rheingold, A. L. *J. Am. Chem. Soc.* **1989**, *111*, 3591.
6. (a) Davidson, J. L.; Sharp, D. W. A. *J. Chem. Soc., Dalton Trans.*, **1975**, 2283. (b) Kubicki, M. M.; Kergoat, R.; Scordia, H.; Gomes de Lima, L. C.; Guerchais, J. E.; L'Haridon, P. *J. Organomet. Chem.*, **1988**, *340*, 41.
7. Janowicz, A. H.; Bergman, R. G. *J. Am. Chem. Soc.* **1983**, *105*, 3929.
8. Janousek, B. K.; Reed, K. J.; Brauman, J. I. *J. Am. Chem. Soc.* **1980**, *102*, 3125.
9. Dickerson, R. G.; Gray, H. B.; Haight, G. P. In *Chemical Principles*, Third Edition; Benjamin/Cummings, Inc.: Menlo Park, 1979; Chapter 15.
10. Hydrogen abstraction from *t*-BuSH is known to produce the *tert*-butylthiyl radical. See, Campredon, M.; Kanabus-Kaminska, J. M.; Griller, D. *J. Org. Chem.* **1988**, *53*, 5393, and references therein.
11. Dr. Christian Schade, unpublished results.
12. Ito, O.; Matsuda, M. *Bull. Chem. Soc. Jpn.* **1978**, *51*, 427.
13. Newman, L. J.; Bergman, R. G. *J. Am. Chem. Soc.* **1985**, *107*, 5314.
14. Isobe, K.; Bailey, P. M.; Maitlis, P. M. *J. Chem. Soc., Dalton Trans.*, **1981**, 2003.
15. Newman, L. J. *Ph.D. Thesis*, University of California, Berkeley, 1986.
16. McGhee, W. D.; Foo, T.; Hollander, F. J.; Bergman, R. G. *J. Am. Chem. Soc.* **1988**, *110*, 8543.
17. For other examples see, (a) Chatt, J.; Shaw, B. L. *Chem. and Ind.* **1960**, 931. (b) Vaska, L. *J. Am. Chem. Soc.* **1961**, *83*, 756. (c) Vaska, L.; DiLuzio, J. W. *J. Am. Chem. Soc.* **1962**, *84*, 756. (d) Foo, T. *Ph.D. Thesis*, University of California, Berkeley, 1989.
18. Buchanan, J. M.; Stryker, J. M.; Bergman, R. G. *J. Am. Chem. Soc.* **1986**, *108*, 1537.

19. (a) Jones, W. D.; Feher, F. J. *Organometallics*, **1983**, *2*, 562.Periana, R. A.; Bergman, R. G. *Organometallics*, **1984**, *3*, 508.

20. (a) Klein, D. P.; Bergman, R. G. *J. Am. Chem. Soc.* **1989**, *111*, 3079. (b) Dr. Jeffrey C. Hayes, unpublished results.

21. The first synthesis of 2,2-propanedithiol was accomplished by treating acetone with H_2S at 7500-8500 atm. (a) Cairns, T. L.; Evans, G. L.; Larchar, A. W.; McKusick, B. C. *J. Am. Chem. Soc.* **1953**, *74*, 3982. Other routes have since been developed. See: (b) Demuynck, M.; Vialle, *J. Bull. Soc. Chim. Fr.*, **1967**, 1213. (c) Adolfsson, L.; Andersson, R.; Olsson, K. Chemica Scripta, **1980**, *16*, 122.

22. (a) Wilkinson, G.; Singer, H. *J. Chem. Soc. A* **1968**, 2156. (b) Senoff, C. V. *Can. J. Chem.* **1970**, *48*, 2444. (c) Stiddard, M. H.; Townsend, R. E. *J. Chem. Soc. A* **1970**, 2719. (d) Gaylor, J. R.; Senoff, C. V. *Can. J. Chem.* **1970**, *48*, 2444. (e) Mueting, A. M.; Boyle, P.; Pignolet, L. H. *Inorg. Chem.* **1984**, *23*, 44.

23. Milstein, D.; Calabrese, J. C.; Williams, I. D. *J. Am. Chem. Soc.* **1986**, *108*, 6387.

24. Chaudret, B. P.; Poilblanc, R. *Inorg. Chim. Acta* **1979**, *34*, L209.

25. Henderson, R. A.; Hughes, D. L.; Richards, R. L.; Shortman, C. *J. Chem. Soc. Dalton Trans.* **1987**, 1115.

26. Friend, C. M.; Roberts, J. T. *Acc. Chem. Res.* **1988**, *21*, 394.

27. Dr J. H. Freudenberger, unpublished results.

28. Angelici, R. J.; Gingerich, R. G. W. *Organometallics* **1983**, *2*, 89.

29. Mueting, A. M.; Boyle, P. D.; Wagner, R.; Pignolet, L. H. *Inorg. Chem.* **1988**, *27*, 271.

30. See: (a) Butler, I. S.; Fenster, A. E. *J. Organomet. Chem.*, **1974**, *66*, 161, and references therein. (b) Yaneff, P. V. *Coord. Chem. Rev.* **1977**, *23*, 183, and references therein. More recent examples include: (c) Werner, H.; Bertleff, W. *Chem. Ber.*, **1980**, *113*, 267. (d) Darensbourg, D. J.; Rokicki, A.; Darensbourg, M. Y. *J. Am. Chem. Soc.* **1981**, *113*, 3223. (e)

Darensbourg, D. J.; Rokicki, A. *Organometallics*, **1982**, *1*, 1685. (f) Bianchini, C.; Ghilardi, C. A.; Meli, A.; Midollini, S.; Orlandini, A. *J. Organomet. Chem.*, **1983**, *248*, C13. (g) Bruce, M. I.; Humphrey, M. G.; Swincer, A. G.; Wallis, R. C. *Aust. J. Chem.*, **1984**, *37*, 1747. (h) Leboeuf, J.-F.; Leblanc, J.-C.; Moise, C. *J. Organomet. Chem.*, **1987**, *335*, 331. (i) Mishra, A.; Agarwala, U. C. *Inorg. Chim. Acta*, **1988**, *145*, 191.

LAWRENCE BERKELEY LABORATORY
TECHNICAL INFORMATION DEPARTMENT
1 CYCLOTRON ROAD
BERKELEY, CALIFORNIA 94720